

---

# Characterization of H3K56me3, a novel histone core modification

Antonia Jack

---



**Dissertation**

München, 29. April 2014

---

# **Characterization of H3K56me<sub>3</sub>, a novel histone core modification**

**Antonia Jack**

---

**Dissertation**

der Fakultät für Biologie der Ludwig-Maximilians-Universität

München

zur Erlangung des akademischen Grades Doctor rerum  
naturalium (Dr. rer. nat.)

von Antonia Jack aus Glasgow (Schottland)

München, den 29. April 2014

Eingereicht am 29. April 2014

Mündliche Prüfung am 29. Juli 2014

1. Gutachter: Prof. Dr. Peter Becker
2. Gutachter: Prof. Dr. Heinrich Leonhardt
3. Gutachter: Prof. Dr. Kirsten Jung
4. Gutachter: Prof. Dr. Dirk Eick

**Eidesstattliche Erklärung**

Ich versichere hiermit an Eides statt, dass die vorgelegte Dissertation von mir selbständig und ohne unerlaubte Hilfe angefertigt ist.

München, den .....

.....

(Antonia Jack)

---

Preface.....	I
Summary.....	II
1 Introduction.....	1
1.1 Chromatin structure and assembly.....	1
Mechanisms for regulating chromatin structure .....	4
1.2 Histone modifications.....	4
1.2.1 Acetylation (ac).....	5
1.2.2 Lysine Methylation (me).....	8
1.2.3 Phosphorylation (ph).....	13
1.3 Modification of histone H3 core residues and their implications on nucleosome structure .....	14
1.3.1 H3K56 at the DNA entry/exit site .....	14
1.3.2 H3 PTMs at the dyad.....	17
1.3.3 H3K79 on the solvent-exposed nucleosome surface .....	17
1.3.4 H3K64 on the lateral surface.....	18
1.4 Histone variants .....	19
2 Discussion.....	20
2.1 Identification of H3K56 as a site of trimethylation .....	20
2.1.1 Evolutionary conservation and heterochromatin .....	20
2.1.2 Identification of SUV39H1/H2 as potential writers of H3K56me3.....	20
2.1.3 Identification of JMJD2D and JMJD2E as potential erasers of H3K56me3 .....	22
2.1.4 H3K56me3 cell cycle appearance.....	24
2.1.5 H3K56me3 in <i>C. elegans</i> .....	26
2.2 Genome-wide localization of H3 core modifications and their functional implications	27
2.2.1 Core modifications at promoter and enhancer regions .....	28
2.2.2 Core modifications in the gene body.....	31
2.2.3 Core modifications at repeat elements: Telomeres and centromeres .....	34
2.3 Mislocalization of core modifications and disease.....	37
2.4 Concluding remarks.....	38
References.....	39
3 Results.....	53
3.1 H3K56me3 is a novel, conserved heterochromatic mark that largely but not completely overlaps with H3K9me3 in both regulation and localization. ....	53
3.2 Versatile toolbox for high throughput biochemical and functional studies with fluorescent fusion proteins .....	66

## Table of contents

---

Appendix.....	79
Contributions .....	79
Curriculum Vitae .....	80
Acknowledgements .....	82

## Preface

During my doctoral studies a large portion of my research focused on the covalent post-translational modification of histones, from which I published one first author paper “H3K56me3 is a novel, conserved heterochromatic mark that largely but not completely overlaps with H3K9me3 in both regulation and localization.” and one second author publication “Versatile toolbox for high throughput biochemical and functional studies with fluorescent fusion proteins.”. Both manuscripts are included in this cumulative thesis and appear in place of the “Materials and methods” and “Results” sections. Additional information on “Materials and methods” such as working protocols, further plasmid information and primers are all stored in the lab of Priv.-Doz. Dr. Sandra Hake and are available upon request. During my work on trimethylation of H3K56, I came across several comprehensive reviews on histone core modifications, most of which focussed on the impact such marks have on nucleosome structure. I, therefore, decided to write a review myself in which I aimed to provide an extra layer of information by relating structural findings to possible *in vivo* functions of core modifications, through evaluation of their genomic distribution. As such, much of what I discuss in the review relates to possible roles in transcription, however many of the principles can be applied to other cellular functions in which individual modifications have been implicated. I enjoyed writing the review article, titled “Getting down to the CORE of HISTONE MODIFICATIONS”, shortly before writing my PhD thesis and have since heard that it has been accepted for publication in *Chromosoma*. Considering the primary manuscript of my thesis focuses on trimethylation of H3K56, which is found in the histone core domain, I felt including slightly modified parts of the review would facilitate the readers understanding of how modifications in such regions might function, given their restricted accessibility. In doing so, I hope that readers will be able to view H3K56me3 in the context of other histone H3 core modifications and that this will allow them to postulate, as I have, about the functional roles of this novel mark. These parts include section 1.4 “Modification of histone H3 core residues and their implications on nucleosome structure” in my thesis introduction and section 2.2 “Genome-wide localization of H3 core modifications and their functional implications” in my discussion.

To increase the readability of the thesis, the “Introduction” is directly followed by the “Discussion” plus a joint reference list for both parts. Subsequent to these sections come the two research papers, which constitute the “Results” part of the thesis. This layout is in accordance with the university guidelines for preparing a cumulative thesis.

## SUMMARY

The compaction of DNA into chromatin is a phylogenetically conserved process, which is not only important in terms of organizing the genetic code into the confines of the cell nucleus, but also provides a means of regulating access to the underlying sequence during processes such as transcription, replication and repair. One of the major mechanisms for manipulating DNA accessibility is post-translational modification (PTM) of histone proteins. Although originally regarded as being limited to the more accessible histone N-terminal tails, technological advances in the last decade have provided evidence that PTMs can also occur within the histone core domains. Given the extensive histone-histone and histone-DNA interactions with which the latter regions are associated, it was postulated that modifications within these domains could directly alter nucleosome structure and stability - a hypothesis which has since been supported by accumulating experimental data.

The primary manuscript in this cumulative thesis describes the identification and characterization of H3K56me3, a novel histone H3 core modification. In this paper, we identify both enzymes responsible for setting the mark (writers) and those responsible for regulating its removal (erasers). Interestingly, these enzymes are also known to regulate H3K9me3, a well characterized histone tail modification, famous for its role in heterochromatin formation. In addition, we show that H3K56me3 distribution overlaps with H3K9me3, localizing to silenced regions including the centromeres, but not telomeres, of mitotic cells and the chromocentres of interphase cells. Given the similarity in sequence surrounding both H3 residues, we performed extensive specificity studies to ensure our observations were not a result of antibody cross-reactivity. In this regard our antibody performed well and we can therefore conclude that H3K56me3 is a novel histone core modification associated with heterochromatin. Finally, we show that this modification is conserved, at least within metazoans, and that it shows some interesting differences compared to H3K9me3 in the *C. elegans* germline. Together with the finding that unlike H3K9me3, H3K56me3 is not present at the telomeres of mitotic chromosomes, this highlights possible functional differences between the two modifications, at least within certain processes, which will be interesting to pursue in future studies.

Changes in local PTM patterns can be brought about by histone variants, the incorporation of which lead to potential alterations in the physiochemical properties of a nucleosome. Indeed there is evidence that certain histone variants are more commonly associated with a certain repertoire of modifications, which likely reinforce any structural changes the variant may impart. For example, a variant which has the potential to destabilize a nucleosome, is more likely to harbour “activating” PTMs, together contributing to a more open chromatin conformation and recruitment of factors for which such an environment is necessary. In the second paper of this thesis, through the testing of a novel GFP-multiTrap binder tool, we were able to confirm previously published data that showed the histone



variant H2A.Z is enriched for H3K4me2 relative to its canonical counterpart, H2A. Although highly controversial, H2A.Z has been reported to destabilize nucleosomes, which would fit with the enrichment of a modification associated with transcriptional activation. Contained within this paper are also further, more extensive tests, performed by our collaborators, which show the GFP-multiTrap binder plate to be a highly useful tool for quantitative measurement studies with fluorescent fusion proteins, with many applications in chromatin biology.

# 1 INTRODUCTION

## 1.1 Chromatin structure and assembly

“Simplicity is the ultimate sophistication”- Leonardo da Vinci

The simplicity of DNA makes it remarkable that what lies within it is the heritable genetic blueprint required to sustain any particular life-form. Inscribed with such valuable information, its protection, regulation and propagation to the next generation are paramount to the success and survival of the organism carrying it. To fulfil these requirements, eukaryotes organize their DNA into a compact structure, known as chromatin, which not only allows the storage of vast amounts of genetic information within the confines of the cell nucleus, but also provides a means of regulating all processes based on the underlying code.

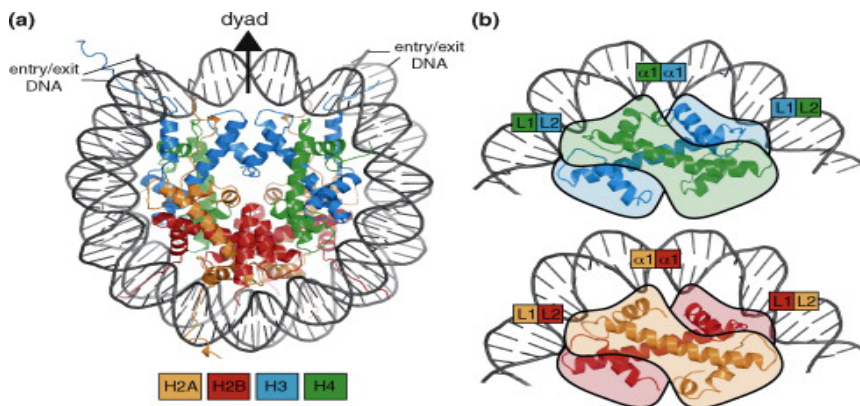


**Figure 1. Basic architecture of the nucleosome core particle.** (a) The crystal structure of the first nucleosome core particle (NCP) revealed 146 base pairs (bp) of duplex DNA wrapped around a central histone core in a left-handed superhelix ((1) ; pdb code 1AOI). The eight histone proteins (two each of H2A, H2B, H3, and H4) form two types of similarly organized heterodimers: H2A–H2B and H3–H4. In the octamer, these four dimers are arranged about a two-fold symmetry axis, called the dyad, which also intersects with the middle of the DNA fragment. Two symmetry-related H3–H4 dimers define the center of the octamer, and contact the DNA around the dyad. (b) In the nucleosome, each histone dimer grips three consecutive minor grooves of DNA in a similar fashion, with the central contact primarily made by the N-terminal side chains and backbone of the  $\alpha 1$  helix for each histone in the dimer ( $\alpha 1$ - $\alpha 1$ ), and the two outer contacts made by the loops preceding the second helix of one histone and the third helix of the other (L1–L2). The four histone dimers thus use just two basic motifs ( $\alpha 1$ - $\alpha 1$  and L1–L2) to coordinate 12 minor grooves of DNA. Taken from (2), with permission from Elsevier.

The basic unit of chromatin is the nucleosome in which 1.65 left-handed superhelical turns ( $\sim 146$ bp) of DNA are wrapped around a protein octamer containing two of each of the canonical histones: H2A, H2B, H3 and H4 (Figure 1a) (1). Histones are small, basic proteins, which are amongst the most abundant in any eukaryote’s proteome. Although there is little similarity between the primary sequences of the four canonical histones, each contains a highly conserved structural motif, known as the histone fold domain. This domain is formed by the association of three alpha-helices ( $\alpha 1$ -3), which are connected by two loop regions (L1 and L2). The histone fold domains interact to form the core of

the nucleosome and are therefore under considerable structural constraint, limiting their divergence across the phylogenetic tree. In addition, all histones have an intrinsically disordered N-terminal tail region. The clustering of cationic residues, within these regions, leads to their protrusion away from the nucleosome core and, together with the flexibility endowed by their unstructured organization, facilitates their proposed primary function, as recruitment platforms. Although dispensable for the organization of the histones into a nucleosome (3), the histone tails appear to be important in mediating inter-nucleosomal interactions and higher-order structures (3). Histone H2A is unique in that it also has a long C terminal tail, which interfaces with the H3-H4 core domains and is important for binding of the linker histone, H1 (4,5). *In vivo*, assembly of the nucleosomes occurs in a sequential manner in which an H3-H4 tetramer is first deposited onto the DNA, followed by binding of two H2A-H2B dimers. Within both the H3-H4 dimers and the H2A-H2B dimers, the histone fold domains are arranged antiparallel to one another, which facilitates hydrogen bonding between the L1 loop of one histone and the L2 loop of the other (Figure 1b) (1). Additional contact occurs between the  $\alpha 1$  helices of opposite histones. The H3-H4 tetramer is assembled by the association of two H3-H4 dimers, which interact via a 4-helix bundle formed between the two H3 histones. Upon addition of the H2A-H2B dimers, a similar bundle forms between H4 and H2B, allowing the assembly of the full octamer. In this process, the presence of DNA is required for the association of the tetramer with the dimers, *in vivo*, and the use of highly-charged histone chaperones prevents the occurrence of non-specific interactions (6). This association forms the first level of compaction and functions, in part, by alleviating the repulsive forces that prevent a naked DNA strand from folding alone. Within each nucleosome, major interactions, between the DNA and histones, occur at 14 different locations via  $\alpha 1\alpha 1$  DNA binding motifs or by using the L1 and L2 loops (Figure 1b) (7). These interactions are facilitated by a combination of hydrogen bonding, between the phosphate oxygen of the DNA and the amide group of the histone residue, and electrostatic associations with the basic side chains. At the nucleosomal DNA entry/exit point, the penultimate 13bps of DNA interact with the H3 $\alpha$ N helices, which do not form an integral part of the (H3-H4)<sub>2</sub> tetramer (7). These interactions are weaker than those occurring within the nucleosome dyad and it is thought that this allows DNA breathing to occur, facilitating binding of, for example, transcription factors, to underlying *cis*-regulatory sites (8).

Early studies, in which chromatin was partially digested using nucleases and analyzed by electron microscopy, famously depicted the repeating units along the length of DNA as “beads on a string” (Figure 2) (9). In this conformation chromatin is described as accessible and has a diameter of approximately 10nm. Binding of the additional linker histone, H1, wraps a further 20bps of DNA and compacts this structure into a chromatosome (10), an important step in the establishment of what has been traditionally termed the 30nm fibre (Figure 2). In recent years, the identification of several distinct 30nm fibre structures (reviewed in (11)), along with the use of new *in situ* techniques, which bring into question its presence *in vivo* (12), have led to controversial views surrounding the exact nature of this structure.

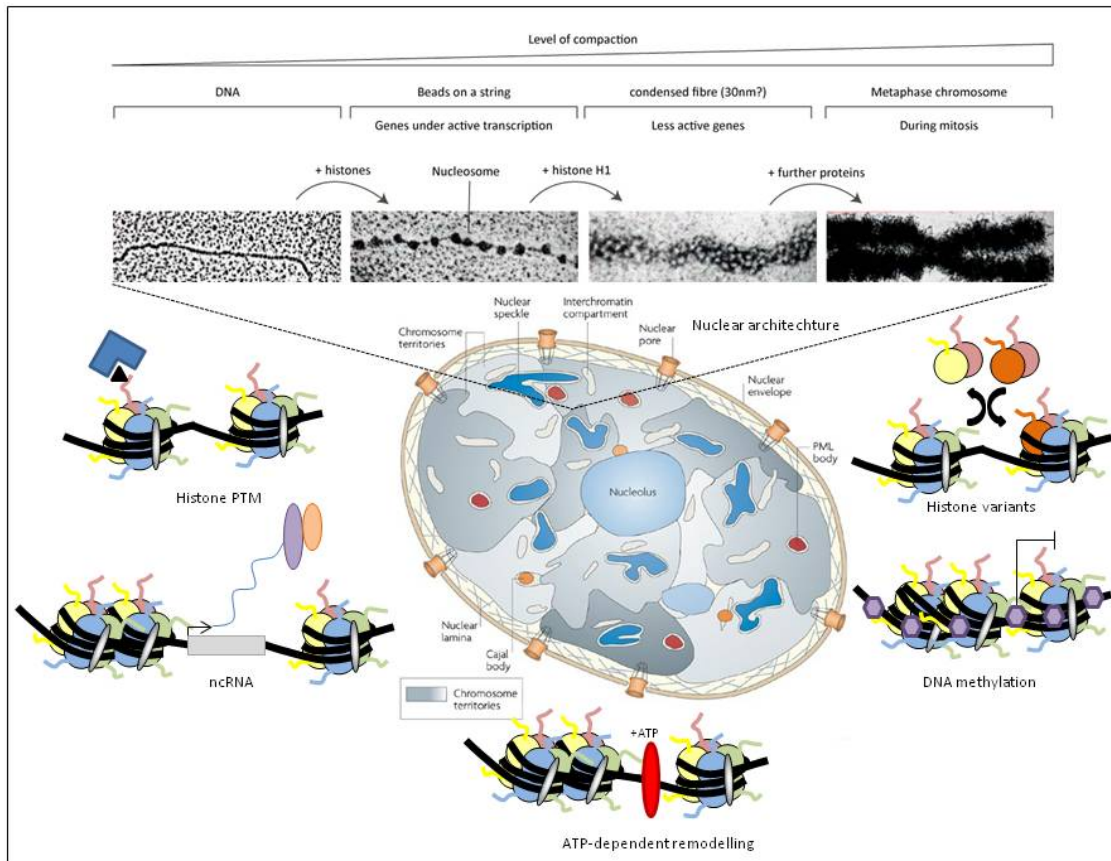


**Figure 2. Chromatin structure and the mechanisms by which it is regulated.** Assembly of chromatin is depicted in the electron micrographs (EM) at the top of the diagram with increasing compaction from left to right. Below are the major mechanisms used to regulate chromatin structure. Adapted from (13) and adapted by permission from Macmillan Publishers Ltd: Nature Reviews Genetics (14), copyright 2007.

Irrespective of the precise conformation, the organization of chromatin into higher-order structures seems refractory to the requirement that the genetic information be accessible for DNA-based processes, such as transcription, replication and repair, to occur. However, chromatin is a highly dynamic and malleable structure and only with the development and application of techniques such as genome-wide analyses (and chromatin capture), are we beginning to fully appreciate the extent of this lability. While chromatin has traditionally been split into two main types: euchromatin, which is gene rich, adopts a more ‘open’ conformation and is conducive to transcription; and heterochromatin, which is gene poor, densely packed and refractory to transcription, our increased understanding of how DNA accessibility is regulated has led to the formulation of more complex categorizations based, for example, on associated protein complexes (15). These categorizations often comprise, at least in part, histone modification signatures (16,17). A more recent proposal, however, highlights some of the problems with this approach and the need to take into account the structural features of chromatin, by incorporating data from techniques such as chromosomal capture techniques to fully understand chromatin function in three dimensions (18).

## **Mechanisms for regulating chromatin structure**

Broadly speaking there are six, highly interconnected mechanisms for regulating chromatin structure (Figure 2): 1. ATP-dependent remodelling, which uses the energy from ATP hydrolysis to evict or move nucleosomes along the DNA; 2. DNA methylation, which is thought to induce tighter wrapping of the DNA around the nucleosome, as well as serving a recruitment function and is associated with transcriptionally silenced regions; 3. Non-coding RNAs (ncRNAs), which are involved in a number of processes, including protein recruitment, RNAi-mediated silencing, higher-order structure and nuclear organization; 4. Nuclear organization, which contributes to the formation of ‘inactive’ and ‘active’ domains; 5. Covalent post-translational modifications (PTMs) of histones, which can act directly, by altering nucleosomal interactions, or indirectly, through recruitment of protein complexes; and 6. Incorporation of histone variants, which can alter the physiochemical properties of the nucleosome as well as the PTM pattern. Given that this thesis focuses primarily on histone PTMs, including in the context of histone variants, the latter two mechanisms will be reviewed in more detail, while the others will be largely omitted.

### **1.2 Histone modifications**

Post-translational histone modification is most well known for its occurrence on the N-terminal tails, however in the last decade an increasing number of core residues have also been identified as target sites. Enzymes that regulate the addition of chemical groups are termed writers and those that catalyze their removal are known as erasers. The covalent addition of specific groups onto targeted residues can alter their size, charge density and hydrophobicity (19). Such changes have been proposed to mediate chromatin structure in two ways: Firstly, by facilitating the recruitment of protein complexes, a process mostly associated with the N-terminal tail regions; and secondly, by directly altering histone-histone and histone-DNA interactions, a process primarily associated with modifications of the histone core domains. When looked at as individual modifications, PTMs can appear to have seemingly opposing roles in the different cell processes in which they are involved. For example H3 serine 10 phosphorylation (H3S10ph) has been implicated in both transcriptional activation during heat shock (20) and chromatin condensation during mitosis (21). However such differences can, in part, be explained by an extended view of the “Histone Code” hypothesis, which states that PTMs function in a interdependent, combinatorial manner (in both *cis* and *trans*), to modulate the interactions of multivalent chromatin-associated proteins/complexes (22,23). As such, specific combinations of modifications, rather than individual marks, in conjunction with the proteins they recruit lead to the establishment and overall function of different chromatin domains e.g. heterochromatin and euchromatin (22,24). Indeed, the identification of conserved protein motifs, capable of recognizing and binding specific modifications adds weight to this prediction. Proteins harbouring one or more of these domains, known as readers, are usually found in multi-subunit, enzyme-containing complexes,

the composition and balance of which determines the structure and function of chromatin regions (15,24). With the discovery of an increasing number histone modification types and locations, the complexity of this code is increasing. The list of modifications now includes acetylation, methylation, phosphorylation (discussed in more detail below), ubiquitination, sumoylation, poly-ADP-ribosylation, citrullination, biotinylation, glycosylation, glutathionylation and isomerization, the latter of which is the only non-covalent one. Several of these PTMs can occur on the same type of residues suggesting a degree of competition occurs, the outcome of which is likely determined by the local levels of writers and erasers, as well as other chromatin-associated proteins. As genome-wide analyses tools improve, so we can better appreciate the complexity in the interplay between not just PTMs but also factors such as DNA methylation patterns, histone variant incorporation and nucleosome occupancy, in establishing chromatin domains.

### 1.2.1 Acetylation (ac)

Acetylation is regulated by histone acetyltransferases (HATs), which transfer an acetyl group from acetyl Coenzyme A (acetyl-CoA) onto the positively charged  $\epsilon$ -amino group of lysine residues (Table 1). This results in charge neutralization and an increase in hydrophobicity. Consequently, this type of modification favours the formation of secondary structures and has been suggested to increase the  $\alpha$ -helical content of the N-terminal tails (25,26). In addition, loss of the lysine positive charge alters electrostatic interactions between the residue and negatively charged DNA or histone groups, resulting in a reduced affinity. Along these lines, H4K16ac has been shown to negatively influence higher-order chromatin structures (27) by weakening interactions between H4 and H2A-H2B in neighbouring nucleosomes (28). In line with these biophysical alterations, histone acetylation has traditionally been associated with the promotion of a more 'open', transcriptionally-permissive chromatin state, where as deacetylation, by histone deacetylases (HDACs) (Table 1), favours a more 'closed', transcriptionally-silent state (29). In addition to reinstating the positive charge, the latter reaction also makes the lysine residue available for other modifications, such as methylation (discussed later in this section), providing a means of regulating competition between modifications at a specific site.

HATs can be split into two major groups: type-A and type-B. While type-A HATs are typically found in the nucleus, act on nucleosomal histones and are associated with transcription, type-B HATs are found in the cytoplasm, acetylate soluble histones and are associated with DNA replication (30,31). Type-A HATs can be further classified into three sub-groups based on conserved sequence motifs and structures: p300/CREB binding protein (CBP), which act as global transcriptional coactivators, GCN5 related N-Acetyltransferases (GNAT), which play a role in Epidermal Growth Factor (EGF) signalling and cell cycle progression and MYST (Moz, Ybf2 (Sas3), Sas2, Tip60), which are involved in DNA damage repair (32).

## Introduction

PTM	Position	Writer				Eraser				Reader
		S.c	C.e	D.m	Mammals	S.c	C.e	D.m	Mammals	
<b>Acetylation</b>	H2AK4 H2AK5	Esa1	mys-1? cbp-1?	Tip60	TIP60,P300/CBP HAT1	Rpd3	hda-1? hda-2?		HDAC3	
	H2AK7	Esa1								
	H2AK9	Elp3, Gcn5							HDAC5	
	H2BK11 H2BK12	Gcn5	cbp-1?		P300/CBP, ATF2	Rpd3, Hda1, Hos3	hda-1? hda-2? hda-4?			
	H2BK16 H2BK15	Gcn5	cbp-1?		P300/CBP, ATF2					
	H3K9	Gcn5, Rtt109		dGcn5		Rpd3, Set3, Hda1, Hos2, Hst1	hda-1? hda-2? hda-3? hda-4?	dHDAC1	SIRT1/6	
	H3K14	Gcn5, Hpa2, Esa1, Elp3, Sas2, Sas3	mys-4? mys-1? cbp-1?	dGcn5, Taf1, dCBP	P300/CBP, TAF1, hGCN5, PCAF, MOZ, MORF, TIP60, SRC1, HBO1				HDAC5	Bromo, PHD
	H3K18	Gcn5	cbp-1?	dCBP	P300/CBP					
	H3K23	Gcn5, Sas3	mys-4? cbp-1?		P300/CBP					
	H3K27	Gcn5, Rtt109		dCBP						
	H3K36	Gcn5								
	H3K56	Rtt109	cbp-1?	dCBP	P300/CBP	Hst3/4		Sir2	SIRT1/2/6	
	H3K122		cbp-1?		P300/CBP					
	H4K5	Esa1, Gcn5	mys-1? cbp-1?	Hat1, dCBP	HAT1, TIP60, P300, HBO1	Rpd3, Set3, Hos2, Hst1	hda-1? hda-2?		HDAC3	Bromo
H4K8	Esa1, Elp3, Gcn5	mys-1?	dCBP	TIP60, P300, HBO1					Bromo	
H4K12	Hat1, Esa1, Hpa2, Gcn5	mys-1? cbp-1?		TIP60, P300, HBO1				HDAC3		
H4K16	Sas2, Esa1, Gcn5	mys-1? mys-2?	dMof, Atac2	hMOF, TIP60, ATF2	Sir2		Sir2	SIRT1/2	Bromo	
<b>Methylation</b>	H3K4	Set1	set-1, set-2, (set-12, set-16?), ash-2, lin-59?	Trx, Trr, Ash1, Set1	SET1, NSD2-3, SET7/9, MLL1-4, SMYD3, ASH1L	Jhd2		Lid, Suv33	LSD1/KDM1A, AOF1, JARID1A- D/KDM5A-D	PHD, CHROMO, WD40, ADD, Tudor, MBT, Zf-CW
	H3K9		met-1 met-2	Suv39, G9a Ash1,	SUV39H1/H2, G9a, GLP, SETDB1, RIZ1, ASH1L	Rph1	Jmjd2a	dKDM4B	LSD1, JHDM2A/B, JMJD2A- D/KDM4A-D, PHF8, KDM7A	PHD, CHROMO, WD40, Ankyrin
	H3K14									
	H3K23									CHROMO
	H3K27		mes-2, mes-3, mes-6	Ez	EZH1/2, NSD2-3, G9a					CHROMO, WD40
	H3K36	Set2	mes-4, met-1, met-2	Set2, Mes4, Ash1	SETD2, SETD3 NSD1-3, SMYD2, ASH1L, SETMAR	Jhd1, Rph1, Gis1	Jmjd2a	dKDM4A/B	JHDM1A/B, JMJD2A- C/KDM4A-C	CHROMO, PHD, PWWP
	H3K56				G9a, SUV39H1/H2				JMJD2D/KDM4D, JMJD2E/KDM4E	
	H3K64				SUV39H1/H2 (indirect)					
	H3K79	Dot1		Grappa	DOT1L					
	H4K12									
H4K20			Pr-set7, Suv4-20, Ash1	ASH1L, NSD1/2, PR-SET7, SUV4- 20H,				KDM7A, PHF8		
<b>Phosphorylation</b>	H2AS1	Sps1			MSK1					
	H2AT119 H2AT120			NHK-1, AuroraB	BUB1					
	H2AS129 H2A.XS139	Tel1, Mek1			ATM, ATR	Pph3			PP2A, Wip1, PP6, PP4	
	H2BS10 H2BS14	Ste20			MST1, HIPK2					
	H2BS33 H2BS32			TAF1	RSK2					
	H2BS36				AMPK					
	H2BY37				WEE1					
	H3T3				HASPIN				PP1	BIR
	H3T6				PKCβ					
	H3S10	Snf1, Ipl1	Aurora B	Jil-1, Aurora B	TG2, Aurora B, MSK1/2, JNK, IKKα, PKB, RSK2, ERK, p38, Fyn, Act, COT, PIM1, CDK8	Glc7	PP1	PP2A	PP1, DUSP1	14-3-3
	H3T11				DLK/ZIP, PRK1, PKM2, CHK1				PP1, PPP1CC	
	H3T45				PKCδ					
	H3S28				MSK1/2, ERK1/2, p38, Fyn, MLTKα, Aurora B, RPSK6a4	Glc7			PP1	
H3Y41				JAK2						
H4S1	CkII			CKII						
H4S47				PAK2						

**Table 1. Major histone modifications.** Alternative residue numbers that refer to mammalian histones are shown in red. Writers, erasers and reader domains are shown for *Saccharomyces cerevisiae* (*S.c.*), *Caenorhabditis elegans* (*C.e.*), *Drosophila melanogaster* (*D.m.*) and mammalian modifications. Question marks represent predictions based on structural homology to proteins from the other organisms. Adapted from (33). For references see text.

In higher eukaryotes, HDACs can be divided into four main groups: Class I HDACs, which are related to yeast RPD3 and comprise HDAC 1, 2, 3 and 8; Class II HDACs, which are related to yeast Histone Deacetylase-A 1 (HDA1) and include HDAC 4, 5, 6, 7, 9 and 10; Class III, which is made up of the SIRTuins (SIRTs); and Class IV, consisting of just one member, HDAC 11 (34). Unlike class I, II and IV enzymes, which are all zinc-dependent, the SIRTs require the co-factor nicotinamide adenine dinucleotide (NAD<sup>+</sup>) for their function. In general the HATs and HDACs are rather promiscuous in their specificity and a certain amount of compensation can occur. Moreover, an increasing number of non-histone proteins, including key regulators such as p53, are being found to be targeted by the same enzymes, highlighting the problems in defining the cause of cellular changes upon manipulation of enzyme levels.

While HATs are often found as components of multi-subunit complexes involved in transcriptional activation, HDACs form part of those involved in transcriptional repression, supporting the early idea that histone acetylation plays a role in transcriptional regulation (35). Histone acetylation is not only implicated in transcriptional control, but also in processes such as DNA replication (36) and repair (37), differentiation (38) and apoptosis (39). Like transcription, these processes are mediated through the interaction of acetylation regulators with DNA binding proteins that allow the integration and transduction of many cellular signals (40). In addition to the enzymes that regulate them, acetylated lysine residues can be recognized by other proteins containing the same conserved domains capable of binding the added moiety. These domains include: the Bromodomain (41) and the Plant Homeo Domain (PHD) (42) (Table 1). The bromodomain, contains a structural fold called the ‘BRD fold’, which consists of two helical loops that form a hydrophobic pocket that selects for acetylated, rather than unacetylated lysine residues (43). The PHD domain is a zinc finger-like domain, which is found on many chromatin associated proteins, but only recently implicated in histone acetyl binding (42).

Interestingly, proteins which utilize these domains for acetyl-recognition commonly use a tandem set-up in which one PHD domain recognizes a certain sequence while the other binds an acetylated lysine via a hydrophobic pocket (42,44). Furthermore, it was recently shown that binding of the double PHD domain of the HAT, MOZ/MYST3, induces  $\alpha$ -helical turns in the H3 tail, which consequently promote further post-translational modification (44). This indicates that once a specific protein binds a modification it may initiate a cascade of further modifications to enforce a particular outcome.



### 1.2.2 Lysine Methylation (me)

Methylation occurs in three forms, mono-, di- or tri-methylation (me1, me2, me3), on lysine residues (Table 1) and two forms, mono- and di-methylation, on arginine (R) residues. Due to the presence of two terminal nitrogens on arginine, di-methylation of these residues can occur either symmetrically, where each receives one methyl group or asymmetrically, where both groups are added onto the same nitrogen. Although progress has been made in the arginine methylation field, much more is known about lysine methylation and, due to its relevance to my project, I will focus on this for the remainder of this section. Unlike acetylation of lysine residues, methylation does not result in charge alteration. Instead, addition of methyl groups causes the loss of polar amino (NH) groups and a decrease in hydrogen bonding capacity (45). Furthermore, alterations in the conformation of the side chain may also occur. Compared to HATs and HDACs, the lysine methyltransferases (KMTs) and demethylases (KDMs) are relatively specific for both the residue they target and the number of methyl groups they add or remove, respectively (Table 1). The H3K79 KMT, Dot1, appears to be quite unique in that it is the only enzyme which regulates methylation at this residue and works in a distributive manner to facilitate addition of one, two or three methyl groups (46). This has led to the controversial debate over the functional redundancy of the different H3K79 methylation states. All KMTs use S-adenosyl-L-methionine (SAM) as their methyl donor (47) (Figure 3) and with the exception of Dot1, all contain a conserved SET domain (Suppressor of Variegation, Enhancer of Zeste and Trithorax). This domain is evolutionarily conserved and was first identified in the three *Drosophila melanogaster* proteins that give it its acronym (48-50). SET-domain containing proteins can be further divided based on sequence motifs surrounding the domain and similarities within the domain itself (51) (Figure 3a). These families include Suppressor of Variegation 39 (SUV39), Suppressor of Variegation 4-20 (SUV4-20), SET domain containing protein 1 (SET1), SET domain containing protein 2 (SET2), Enhancer of Zeste (EZ), RIZ, and Set and MYND containing protein (SMYD). Additionally, SET7/9 and SET8, also known as PR-SET7 exist, but do not fall into any of the aforementioned groups.

Although KDMs evaded detection for a long time, the identification of Lysine Specific Demethylase 1 (LSD1 /KDM1A) in 2004, challenged the idea that methylation is a one-way process. Since then a multitude of KDMs have been discovered (Table 1), which, like the KMTs, are residue and methyl-state specific. LSD1 and mammalian-specific LSD2/KDM1B (52) both contain a flavin adenine dinucleotide (FAD)-dependent amine oxidase domain, which is responsible for the demethylation of H3K4me1 and me2 (Figure 3b). In addition, a much larger group of KDMs exists, which all contain a Jumonji C (JmjC) domain that uses  $\text{Fe}^{2+}$ ,  $\text{O}_2$  and  $\alpha$ -ketoglutarate to hydroxylate the methyl group (53) (Figure 3b). The reaction then proceeds in much the same way as that of LSD1 (54). Importantly, the LSD proteins require a protonated nitrogen as a hydrogen donor and therefore cannot target trimethylated residues. JmjC KDMs, on the other hand, can target all three states of methylation.



proliferation, DNA repair as well as on the KMTs and KDMs. G9a/EHMT2 and G9a-like protein (GLP)/EHMT1, catalyze both H3K9me1 and H3K9me2. They can, in addition, bind their products using ankyrin repeats (57). These repeats form a hydrophobic pocket, which is characteristic to methyl-binding modules. While the cage formed by G9a and GLP can accommodate H3K9me1/2, it is too narrow to fit three methyl groups. SUV39 homolog 1 (SUV39H1) and 2 (SUV39H2), both responsible for H3K9me2 and me3 catalysis, contain a chromodomain, which forms a hydrophobic pocket that can accommodate H3K9me3. The H3K9me2/3 reader, heterochromatin protein 1 (HP1), also interacts via a chromodomain (58). Interestingly, it has recently been proposed that slight differences in binding affinities between the pockets of SUV39H and HP1 help reduce competition for residue interaction (59). While HP1 has a minor preference for H3K9me2, SUV39 favours the trimethyl state and it is thought these propensities facilitate the spread of heterochromatin (see next section). In a similar manner to the binding of acetylated peptides to their readers, when in complex with methyl-binding domains, the H3 tail adopts an extended conformation that is thought to facilitate further interactions between it and the protein (19). This achieves a degree of specificity that, for example, allows the chromodomain of Polycomb to distinguish a different target to the chromodomain of HP1 (60). Along these lines, a certain amount of specificity is therefore conferred by the sequence surrounding the target residue (60).

#### **1.2.2.1 Lysine methylation and constitutive heterochromatin formation**

Lysine methylation is rather ambiguous in terms of function and as such has been linked to both euchromatic and heterochromatic regions. While higher states of methylation at H3K9, H3K27 and H4K20 are generally regarded as indicators of transcriptional silencing, H3K4, H3K36 and H3K79 methylation are associated with activation (61). In reality these correlations are not so black and white, however the role of histone methylation in heterochromatin formation has been extensively studied and provides a good example of how modifications function in assembling a specific chromatin domain.

Broadly speaking heterochromatin is densely packed making it refractory to transcription, however defined features and differences in packaging dynamics has led to its classification into two, further sub-groups: constitutive and facultative (62). The genome-wide distribution of facultative heterochromatin is cell-type dependent and is often associated with differentiation, development and stress. This type of heterochromatin retains the capacity to adopt a more open conformation in response to specific cellular or environmental cues, allowing regulated access to any genes and regulatory elements with which they are associated (62). Constitutive heterochromatin is different in that it contains a high density of DNA repeat elements most commonly associated with the telomeres and centromeres. These features and their functions are conserved between different cell types and therefore the same regions of DNA are tightly packaged into this type of chromatin. It is thought that

the repressive structure of constitutive heterochromatin is conducive to the maintenance of genomic stability, preventing re-arrangements, which might otherwise occur between the highly similar sequences, and facilitating correct chromosome segregation. Any genes within regions of constitutive heterochromatin will be poorly expressed and the spreading of this form of chromatin, into adjacent, non-repetitive regions can lead to the silencing of neighbouring genes - a phenomenon known as Position Effect Variegation (PEV).

Centromeres are specialized regions of chromatin, identifiable by their incorporation of the histone H3 variant CENtromeric Protein A (CENP-A). These regions are responsible for assembly of the kinetochore, which serves as the attachment point for the mitotic spindle and is required for proper sister chromatid segregation during mitosis (63). CENP-A is uniquely incorporated into these regions and is essential for their function with deletion of this histone variant causing severe defects in cell division (64). While the functionality and the presence of CENP-A are conserved between centromeres of different species the overall architecture is rather different (65). In *S. cerevisiae*, three DNA elements, CDEI, CDEII and CDEIII are responsible for the functionality of this region and span a total of approx. 125bp. A 15bp stretch of CDEIII serves to recruit a complex of proteins necessary for the assembly of a single nucleosome, containing CENP-A, over the middle AT-rich CDEII element (65). In contrast, centromere assembly in higher eukaryotes is not strictly DNA sequence dependent and is governed by large arrays of repetitive DNA, known as satellite repeats. During interphase, these repeats cluster together to form chromocenters that can be microscopically visualized as DAPI-dense regions in the nucleus. Blocks of CENP-A-containing nucleosomes are assembled onto these repeats and are interspersed with H3-containing nucleosomes, encompassing anywhere from 500-1500bp in humans (65). Interestingly, while the flanking pericentromeric heterochromatin is associated with expected, repressive modifications, such as DNA methylation, H3K9me<sub>3</sub>, H3K27me<sub>3</sub> and H4K20me<sub>3</sub>, the canonical H3 found at the centromeres is enriched for H3K4me<sub>2</sub>, a mark normally correlated with euchromatin, but not other hallmarks of open chromatin such as hyperacetylation (66). In addition, studies in mouse also revealed the presence of H2A.Z in these regions and it is conceivable that these latter features facilitate transcription of ncRNAs within these regions (67).

In mammals, the establishment of pericentric heterochromatin occurs in a sequential manner (68,69) (Figure 4). Recent evidence suggests that the binding of transcription factors to sites within the repeats, may serve as an early step in establishing this form of chromatin, working together with ncRNAs to facilitate the recruitment of G9a/GLP and SUV39H1/H2 (70,71). In addition, H3K9me is monomethylated outside of chromatin and subsequently incorporated into the repeat units, where it acts as a substrate for SUV39H1/H2 (72,73). H3K9me<sub>3</sub> has been shown to act as a high-affinity binding site for HP1 (74), which is subsequently recruited to these regions. While the HP1 chromodomain (CD) has been shown to be important for H3K9me<sub>3</sub> recognition, the chromoshadow domain (CSD) functions in HP1 dimerization and interacts with the  $\alpha$ N region of nucleosomal histone

H3 (75,76). This latter interaction is thought to require some loosening of the DNA at the entry/exit site. HP1 binding has been shown to compact chromatin by interacting with nucleosomal DNA, histones and other chromatin associated factors. For example, it recruits DNA methyltransferases (DNMTs) (77) and synergistically stabilizes SUV4-20H2, thereby promoting H4K20me3 and recruitment of the cohesin complex (78).

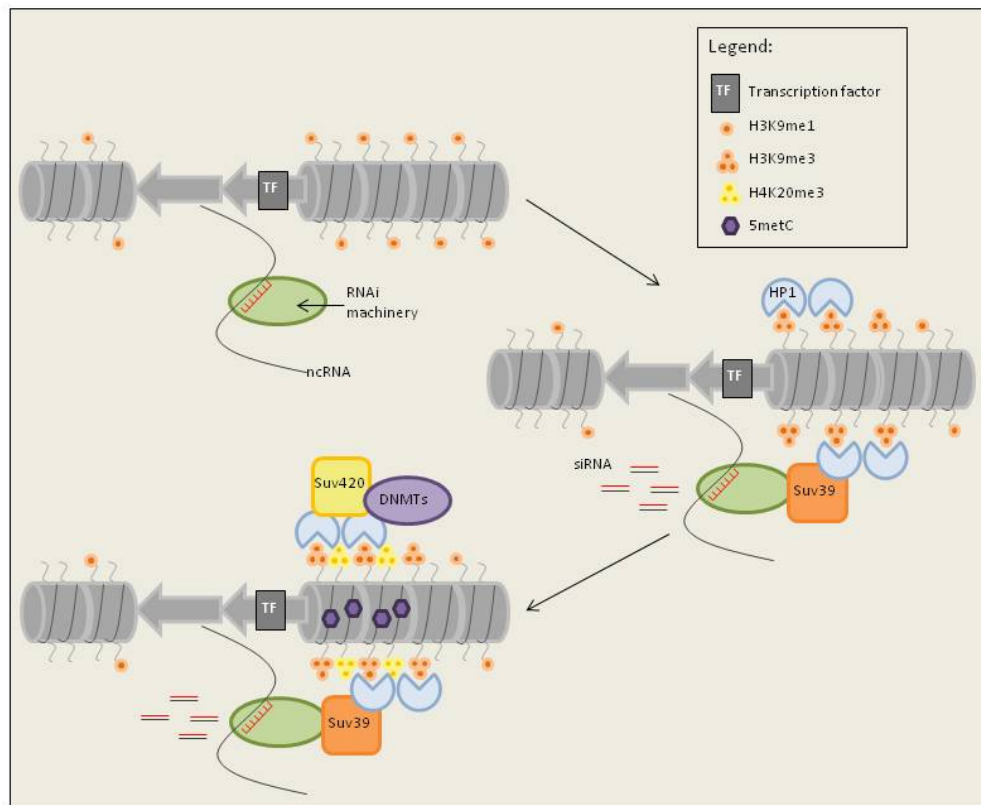


**Figure 4. Establishment of pericentric heterochromatin.** Establishment occurs in a stepwise manner beginning with recruitment of transcription factors and the RNAi machinery, followed by deposition of H3K9me3 by Suv39 and subsequent binding of HP1. Finally accumulation of Suv4-20 and DNMTs leads to H4K20me3 and DNA methylation (5metC), respectively.

Cohesion is established between sister chromatids during S-phase, linking them together until their separation during anaphase. The cohesin complex is initially distributed along the length of sister chromatids and remains as such until mitosis. In metazoans, removal of the complex begins in prophase (79). After this phase, it is only present at the centromeres, where it facilitates the alignment of chromosomes on the spindle (80). It is thought that centromere-specific recruitment of the phosphatase PP2A is important in counteracting cohesin-targeted kinase activity, thereby preserving the complex at these regions, while removal in the chromosome arms takes place (79). A second round of dissociation then occurs during anaphase when the enzyme separase cleaves Scc1, a subunit which stabilizes the cohesin ring structure. Interestingly in yeast, all cohesin removal occurs during the metaphase to anaphase transition via the separase pathway (79). Misregulated cohesin recruitment

leads to chromosome segregation defects (78), indicating the importance of this process in maintaining genomic stability.

### 1.2.3 Phosphorylation (ph)

Phosphorylation is catalyzed by kinases and removed by phosphatases (Table 1). Like acetylation, the addition of a phosphate group onto serine, threonine or tyrosine residues results in a charge alteration. In this case, however, the residues gain a negative charge. As with acetylation, this alteration disfavours certain electrostatic interactions, for instance with DNA, and it has been shown that these two types of modifications are often linked (81,82). It is not surprising, therefore, that phosphorylation has been implicated in gene activation (83,84). This type of modification has been shown, in some cases, to antagonize repressive methylation marks at nearby residues or prevent the removal of activating methylation marks. For example, H3T11ph accelerates H3K9 demethylation by JMJD2C to regulate androgen receptor targeted transcription (85), while H3T6ph prevents H3K4 demethylation during the same process (86). Intriguingly and seemingly contradictory, some phosphorylation marks including H3S10ph and H3S28ph are found on both open and closed chromatin regions (87,88). Despite roles in processes such as transcription, histone phosphorylation is perhaps most famous for its role in mediating mitotic and meiotic chromosome condensation (21,89). H3S10ph accumulates at the centromeres during mitosis, where it is sufficient to displace HP1 binding at the neighbouring H3K9 residue (90), a process that is thought to be necessary for proper chromatin condensation and segregation. H3T3ph is also associated with mitosis, during which it becomes enriched at the centromeres. This regional accumulation is important for the recruitment of the Chromosomal Passenger Complex (CPC) and therefore the regulation of chromosome separation rather than condensation (91). It was recently shown that this forms the start of a cascade in which the presence of CPC results in H3S10ph and subsequent recruitment of the HDAC Hst2p (SIRT2 homolog), which targets H4K16ac (28). As mentioned earlier, loss of this modification facilitates the formation of higher-order structures (27), and Wilkins et al., could show that this favours interactions between H4 and the H2A-H2B dimer in adjacent nucleosomes thereby promoting mitotic chromosome condensation.

Phosphorylation marks are recognized by a number of well characterized domains including the 14-3-3 family (92), BRCT, SH2, WW, FHA, WD-40, LRR and BIR (56) (Table 1). The CPC subunit, Survivin, contains a BIR domain and the structural basis for its recognition of H3T3ph was recently resolved (93). Although surrounded by negatively charged residues of the BIR domain, H3T3ph docks onto a small patch of positive charge found between the side chains of the Survivin K62 and H80 residues. Further interactions between the other peptide residues and negative regions of the BIR domain further stabilize the conformation. Interestingly, similarities can be drawn in the way the BIR domain of Survivin and the PHD finger domains, which are often recruited to methylatable residues,

bind the main chain of the H3 peptide. This shows that both types of domain use a common mode of recognizing a peptide sequence, but achieve specificity for PTM recognition via variations in their binding pockets. For example, the PHD fingers of the INhibitor of Growth (ING) factors form a hydrophobic pocket that recognizes H3K4me3, whereas the Survivin BIR domain binds H3T3ph via a small positively charged region (93).

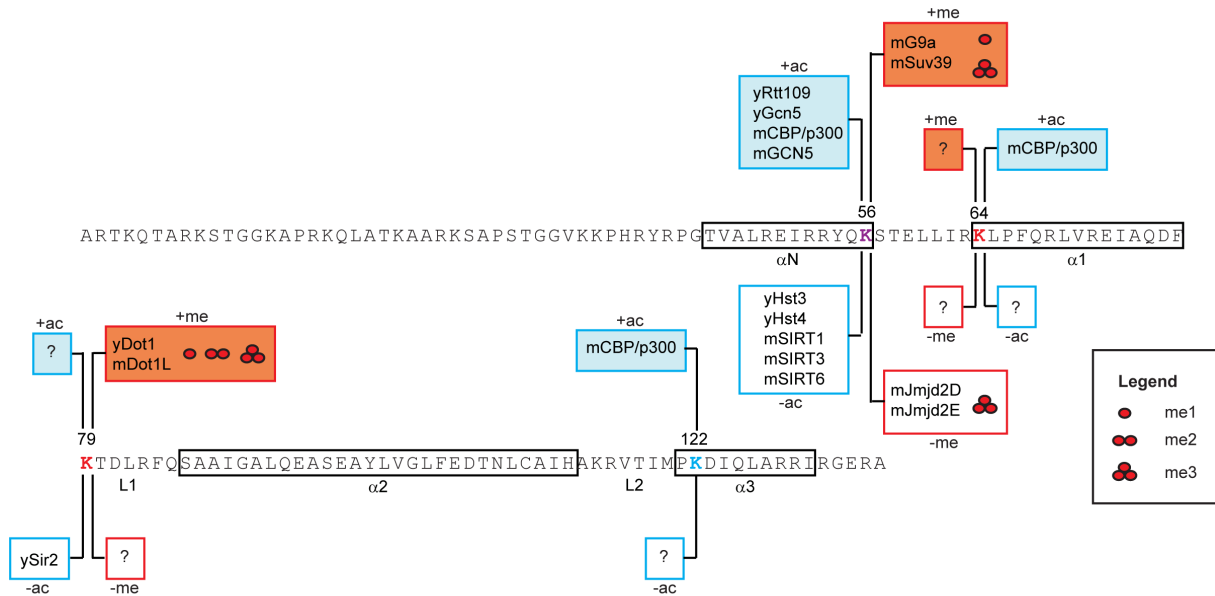
### **1.3 Modification of histone H3 core residues and their implications on nucleosome structure**

The modified residues discussed so far are all found within the accessible histone N-terminal tail regions. Although PTMs in the histone tails have been shown to be important for higher-order chromatin assembly, affecting inter-nucleosomal interactions (94), their protrusion away from the nucleosome limits their participation in intra-nucleosomal interactions that occur at the heart of the nucleosome. Although once thought to be inaccessible to histone modifying enzymes, technological advances have led to the discovery that an increasing number of residues within the histone core regions can in fact be covalently modified and that these residues occupy functionally significant positions within the nucleosome (95).

#### **1.3.1 H3K56 at the DNA entry/exit site**

Although part of the core globular histone domain, lysine 56 of histone H3 (H3K56) lies in the amino-terminal alpha helix (H3 $\alpha$ N) (Figure 5a), which is significantly less structured than the histone fold. Nevertheless, this region has been shown to be important for stabilization of the nucleosome and is positioned by the H2A docking domain, to interact with the penultimate 10 bp of DNA, at the DNA entry /exit site (1) (Figure 5b, top left). In addition, in yeast, it has been shown that ~ 30% of transcription factor binding sites reside within this region (96). H3K56 is well documented as a site of acetylation (ac), occurring on ~ 30% of yeast histone H3 (97) and is predominantly associated with the incorporation of H3 during DNA replication and repair (37,98). In higher eukaryotes H3K56ac is far less abundant appearing on less than 1% of mammalian H3 (99). However, unlike in yeast, H3K56 can also be methylated in these organisms, with monomethylation playing a key role in DNA replication (100) and trimethylation likely having a role in heterochromatin formation (101). Acetylation of H3K56, disrupts the normal water-mediated interaction between it and the DNA entry gyre (102) and has been shown, by single-molecule fluorescence resonance energy transfer (FRET), to increase the rate of DNA unwrapping by 7-fold as compared to the unmodified residue (103). Although X-ray crystallography suggests there is no change in the nucleosome structure or DNA conformation (104), this is compatible with the FRET data given that crystallization stabilizes the DNA in a 'closed' conformation (105).

a



b

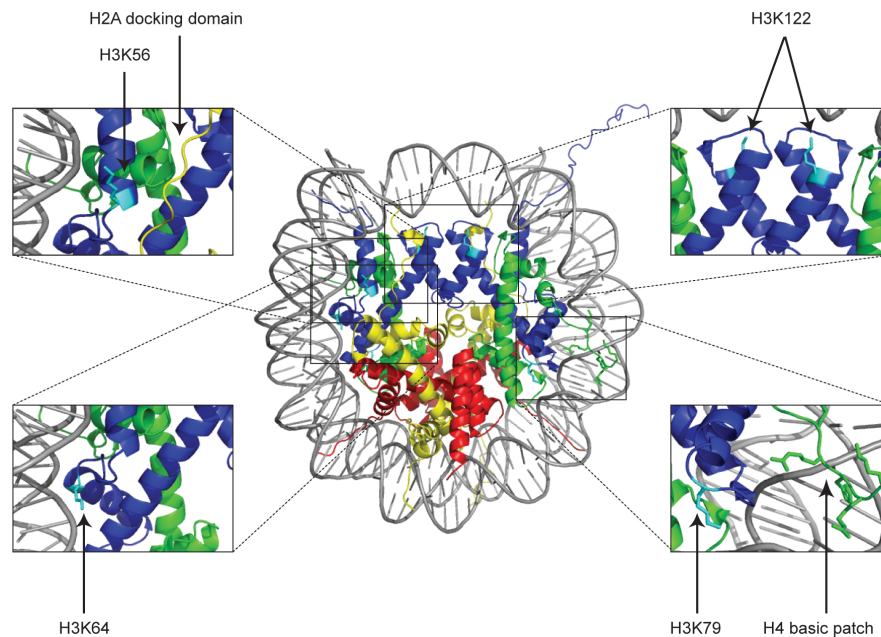


**Figure 5. Position and regulation of histone H3 core modifications.** a) Sequence (NCBI Reference Sequence NP\_002098.1) and secondary structure of human histone H3.3 with core modified residues, for which there is more than just mass spectrometry data, highlighted in purple (methylated and acetylated), blue (acetylated) and red (methylated). Writers and erasers are displayed above and below the sequence, respectively and the colouring of the surrounding box matches the modification colour-coding used for the residues. (y) and (m) denote yeast and mammalian, respectively. (b) The crystal structure of the nucleosome (PDB ID: 1Aol) (1). H3 is shown in blue, H4 in green, H2A in yellow, H2B in red and DNA in grey. Discussed H3 core modifications (H3K56, H3K64, H3K79 and H3K122) are highlighted in cyan. Zoomed images show H3K56 and the H2A docking domain (top left), H3K122 (top right), H3K64 (bottom left) and H3K79 and the H4 basic patch (bottom right).



It has been shown that although there is extensive histone-DNA interaction at the entry/exit site, these contacts are relatively weak, compared to those at the nucleosome dyad (106). Loosening of the DNA, therefore, facilitates the binding of proteins to the chromatin fibre by promoting a more accessible nucleosomal environment (107). It is conceivable that these proteins include chromatin remodelers (97) and it was previously reported that a H3K56Q mutation, chemically mimicking acetylation of this residue, thereby contributes modestly to nucleosome repositioning (103). Additionally, it had been proposed that given the pivotal location of H3K56, its acetylation might lead to destabilization of the nucleosome. Recently, however, these findings have been disputed (107,108).

There is also some controversy over the exact effect H3K56ac has on chromatin compaction *in vitro*. While it is generally accepted that H3K56ac has no effect on *cis* acting interactions within individual nucleosomal arrays, discrepancies lie in the effects it has on *trans* array-array interactions (103,104). One postulated reason for this is that H3K56 acetylation may only disrupt oligomerization of sub-saturated arrays, which may better reflect the *in vivo* local chromatin environment in which H3K56ac is found, but such arrays were not tested in all studies. The use of H3K56ac to decrease interactions between multiple arrays may be a means of maintaining nucleosome-depleted regions (NDRs) of chromatin permissible for such functions as DNA replication and repair (104).

Recently, using pulsed electron-electron double resonance spectroscopy coupled with site-directed spin labelling, the structure of the (H3-H4)<sub>2</sub> histone tetramer was investigated and revealed that, while the H3-H3 interface retains a similar structure as observed in a nucleosomal context, the H3 $\alpha$ N extension is more heterogeneous, so that in this conformation additional flexibility may enhance the likelihood of post-translational modifications and further interactions with chromatin-associated proteins (109). In yeast, H3K56 is primarily acetylated by the HAT, Rtt109 (110), which requires the presence of the histone chaperone Asf1 and therefore occurs on (H3-H4)<sub>2</sub> tetramers before incorporation into chromatin. In mammals and flies, H3K56ac is mediated by the HATs, CBP/p300 (111) and GCN5 (112).

In higher eukaryotes, H3K56 has also been identified, by mass spectrometry (MS), as a site of methylation (113,114) and further *in vivo* data demonstrated the presence of me1 (100) and me3 (101). Recent crystal structures, reconstituted with methylated histones, show that although this type of modification is thought to induce less severe structural changes compared to charge-altering modifications, it can still alter the capacity of a residue to hydrogen bond and can change the conformation of the side chain (45). In this respect, methylation of this residue may alter the water-mediated hydrogen bond between H3K56 and the DNA backbone, although to date there is no available experimental data to confirm this.

Adjacent to H3K56 is serine 57, which has been identified by MS as a site of phosphorylation (115). Although there is currently no further evidence for this mark *in vivo*, it is imaginable that the presence

of this mark could affect the binding of proteins at H3K56, acting as a phospho-methyl binary switch (116).

### 1.3.2 H3 PTMs at the dyad

H3K122 acetylation is the most recent core modification to be characterized and is found at the nucleosome dyad axis (Figure 5b, top right), where the contact between histone and DNA is at its strongest (106). So far this modification has only been characterized in higher eukaryotes where, like H3K56ac, it is deposited by CBP/p300 (Figure 5a) (117). Similar to H3K56, addition of an acetyl group at H3K122 is likely to disrupt a water-mediated contact between it and the nucleosomal DNA (118). Interestingly, recent *in vitro* studies showed that unlike PTMs at the DNA entry/exit site, those at the dyad do not affect DNA unwrapping, but rather function by facilitating nucleosome disassembly (108,119) and sliding (120,121). Given that salt-dependent nucleosome disassembly has recently been shown to begin with the ‘loosening’ of the (H3-H4)<sub>2</sub> tetramer and the (H2A-H2B) dimer interface, before (H2A-H2B) dissociation from the DNA (122), one could speculate that H3K122ac and other modifications within the dyad axis facilitate this process. H3T118 can be phosphorylated and sits between, although not directly adjacent to, H3K122 and H3K115, the latter of which has also been identified, by MS, as a site of acetylation. Mutations of H3T118 fall into the class of SWI/SNF (SWItching and Sucrose Non Fermentation) INdependence (SIN) histone mutations, which in yeast, can functionally compensate for loss of the ATP-dependent chromatin remodeller SWI/SNF and are either found near the dyad-DNA contact points or the tetramer-dimer packing interface (123). Like the other two dyad modifications, H3T118ph facilitates nucleosome disassembly and does not appear to affect DNA unwrapping *in vitro* (108). Interestingly, a recent study, in which the binding of nucleosome assembly proteins (NAPs) was assessed in the presence of different modifications, showed that H3T118ph enhanced NAP-peptide interactions, while H3K122ac diminished them (124). Engineered histone H3, containing site-specific genetically incorporated acetyl-lysine (103) was, however, successfully assembled into chromatin, *in vitro*, using a combination of NAP1 and ATP-dependent chromatin assembly factor (ACF) (117). This suggests further studies will be needed to delineate the *in vivo* functions and relationship of these modifications.

### 1.3.3 H3K79 on the solvent-exposed nucleosome surface

H3K79 is found on the first loop of the histone H3 globular domain (Figure 5a) and is exposed on the solvent accessible surface of the nucleosome (Figure 5b, bottom right). Unlike the DNA entry/exit point this region does not contact the DNA, however mutational analysis has shown that residues surrounding H3K79 are important for heterochromatic silencing in yeast (125,126). H3K79 can be mono-, di- and tri-methylated by the enzyme Disruptor of Telomeric Silencing (Dot1) (Figure 5a) (127-129). This enzyme is conserved and in most organisms analyzed to date and with the exception

of trypanosomes (130), is the only enzyme identified as able to mediate this modification. In the case of H3K79, addition of methyl groups has been shown to disrupt a weak hydrogen bond between it and the L2 loop of histone H4 and it has been demonstrated that the induced side chain rearrangement causes the partial uncovering of a hydrophobic pocket lined by H3L82 and H4V70 (45). While such changes are small, alterations of the electrostatic potential and nucleosomal surface may lead to a more cumulative effect. In addition, the nucleosomal position of H3K79, in close proximity to the histone H4 N-terminal tail (Figure 5b, bottom right), is likely to facilitate its methylation by Dot1, given that this H4 region contains a stretch of basic residues necessary for Dot1 methyltransferase activity (131,132). Furthermore, higher levels of H3K79 methylation are dependent on another *trans*-mediated interaction, yH2BK123/hH2BK120 ubiquitination (H2Bub). This modification is a pre-requisite for Dot1-mediated H3K79me<sub>2</sub> and me<sub>3</sub>, as well as H3K4 methylation by COMPASS (133-135). Indeed, *in vitro* studies showed that H2Bub could actually stimulate H3K79me (136). The position of H2BK123, on the same solvent-exposed surface and in close proximity to H3K79, is likely to facilitate such cross-talk between the two modifications (137).

H3K79 has also been shown, by MS, to be acetylated in both humans (114) and yeast (138). In both organisms H3K79ac occurs in low abundance and the only regulatory data that exists is in yeast, where Sir2 has been shown to catalyze its removal (Figure 5a).

#### **1.3.4 H3K64 on the lateral surface**

H3K64 is located at the beginning of the  $\alpha$ 1-helix (Figure 5a) and tri-methylation of this residue is indirectly mediated, by the known H3K9 methyltransferases, SUV39H1 and SUV39H2 (139). This residue is located on the lateral surface of the nucleosome (Figure 5b, bottom left) and the crystal structure of the nucleosome core particle (NCP) shows that it contacts the nucleosomal DNA via hydrogen bonds between the main-chain amide nitrogen of H3K64 and the phosphates of the DNA backbone (118). In addition, the amino group of H3K64 may participate in stabilizing the H3  $\alpha$ 1 and  $\alpha$ 2 helices, via water-mediated hydrogen bonds. Considering the addition of methyl groups can alter hydrogen bonding, the aforementioned interactions may be disrupted, although modeling shows steric complementarity between the methyl group and the nucleosomal DNA (139). Both MS data (114) and antibody detection (140) show this residue can be acetylated in mammals. Like H3K56ac and H3K122ac, H3K64ac is catalyzed by CBP/p300 (140) (Figure 5a). Crystal structures of the NCP containing H3K64Q, show that while the presence of acetylation is not likely to affect hydrogen bonding to the DNA backbone, it may alter the interactions with the H3  $\alpha$ 1 and  $\alpha$ 2 helices as a result of a significant change in side-chain orientation (118). These findings are somewhat contradicted by recent FRET studies, which were used to analyze the stability of nucleosomal DNA interactions in nucleosomes containing chemically incorporated acetyl lysine at K64 (140). Using this second technique, it appears that H3K64ac does in fact negatively impact the stability of DNA-histone

interactions, reflecting possible limitations of using K to Q substitutions in some assays. Interestingly, the latter study also showed that this modification facilitates ATP-dependent chromatin remodeling in an enzyme specific manner, behaving, in this respect, differently from H3K56ac.

#### **1.4 Histone variants**

The major histones are transcribed from multiple, intron-less genes, in a replication-dependent manner, to cope with the increased genetic material during DNA synthesis. However, nucleosome assembly and disassembly are also essential in replication-independent processes, such as transcription and DNA repair. Many organisms have evolved nonallelic histone variants, which, although derived from their canonical counterparts, have altered amino acid sequences and are transcribed from a single, intron-containing gene, in a replication-independent manner. Many of the sequence changes lie in functionally significant regions and consequently, their incorporation into nucleosomes can alter the physiochemical properties of the chromatin building blocks, as well as their PTM pattern. Although it is highly debated, incorporation of one of the most conserved histone variants, H2A.Z, is thought to destabilize the nucleosome, facilitating its disassembly. This variant is often associated with regions such as the promoters, transcription start sites (TSS) and enhancers of active or poised genes (141), where nucleosome disassembly is crucial for allowing access to underlying *cis*-regulatory elements, binding of protein complexes and progression of the transcriptional machinery. In agreement with this, the presence of H2A.Z correlates with H3K4me2 (141), a modification associated with ‘active’ chromatin and nucleosomes containing H2A.Z are enriched for this modification, relative to H2A. In my contribution to the second paper of this thesis, I was able to verify the latter finding (142). The presence of H2A.Z at poised genes, which are often in a repressed state, insinuates that while H2A.Z may facilitate activation, other factors are required to trigger nucleosome disassembly or repositioning. In this regard, it has been suggested that the presence of modifications such as acetylation or monoubiquitination may influence the overall outcome (143). H3K56ac, for example, was recently shown to alter the substrate specificity of the yeast chromatin remodeler SWR-C, favouring the deposition of H2A rather than H2A.Z (144). The combined use of histone variants and PTMs provides a large number of possibilities to fine-tune the structure and accessibility of chromatin at targeted regions and as such, increasing our understanding of how they work is invaluable.

## 2 DISCUSSION

### 2.1 Identification of H3K56 as a site of trimethylation

Although previously detected by MS, a more stringent characterization of the histone core modification, H3K56me3 has never been carried out. Given the pivotal location of H3K56 at the nucleosome DNA entry/exit site and the wealth of literature implicating acetylation of this residue in an increasing number of cell processes, we sought to understand how trimethylation impacts chromatin-based functions. To this end, we developed a specific antibody and used it to identify potential regulators of H3K56me3 as well as the evolutionary conservation and cell cycle appearance of this modification. These results are presented in the first paper of this thesis, titled “H3K56me3 is a novel, conserved heterochromatic mark that largely but not completely overlaps with H3K9me3 in both regulation and localization”.

#### 2.1.1 Evolutionary conservation and heterochromatin

In order to assess the conservation of H3K56me3 in metazoans we used our antibody to probe acid extracted histones from cell lines of different organisms and could show that this modification is present in human, mouse, fly and worms. Although we did not test yeast histones, it was recently published that, like H3K9me, H3K56me1 is not detectable in *S.cerevisiae* (100). Of course this does not rule out that H3K56me3 does not exist in this organism, however it seems unlikely given that, unlike fission yeast, budding yeast do not have a SUV39 homolog, which we identified as a regulator of H3K56me3 deposition in mammals.

#### 2.1.2 Identification of SUV39H1/H2 as potential writers of H3K56me3

The characterization of H3K56me1 was recently published and included the identification of G9a as the KMT responsible for the deposition of this modification, both *in vivo* and *in vitro* (100). G9a is a member of the SUV39 family of KMTs, which, in addition to a SET domain, share common Pre-SET (9 Cys, 3 Zn) and Post-SET (CXCX<sub>4</sub>C) domains and all target H3K9 (51). Combining this information with our antibody staining data showing that H3K56me3 localizes to heterochromatic regions, overlapping significantly with H3K9me3, we asked whether the KMTs responsible for trimethylation of H3K9 were also involved in H3K56me3. In cells lacking SUV39H1/H2, H3K56me3 signal was severely diminished, indicating that these enzymes target H3K56 either directly or indirectly. G9a substrate specificity has been studied in detail and it has been shown that the sequence surrounding the residues it targets may play a role in its selectivity (145,146), a feature that also affects SUV39H recruitment. As well as targeting H3K9, which lies in the sequence TARKKST, G9a also methylates

H3K27 (147), H3K56 (100), H1.4K26 (148) and H1.2K187 (149), the surrounding sequences of which are AARKSA, RYQKST, KARKSA and KAAKSA, respectively. Looking at these sequences it would appear that the neighbouring serine is important for lysine selectivity although substrate specificity studies indicate that for G9a this is not the case (146). However, in these studies it was also concluded that substitution of threonine 6 (T6) within the H3K9 sequence significantly reduced G9a KMT activity and that the RK motif was of importance for methylation. These statements do not fit with all sequences surrounding G9a-methylatable residues and likely reflect some limitations in the experimental set-up. Interestingly, when comparing the conformation of H3S10 when H3 peptides are bound by either the G9a ternary complex or DIM-5, the *Neurospora crassa* homolog of SUV39H1, it is possible to see that in the case of G9a, H3S10 forms hydrogen bonds with water, where as with DIM-5 the main chain N-H and side chain hydroxyl group of H3S10 form hydrogen bonds with the catalytic side residues Y283 and D209 in the enzyme (150). In addition, H3T11 also hydrogen bonds to Q285, in the catalytic region of DIM-5, highlighting the likely importance of these peptide residues in guiding SUV39H1/H2, but not G9a, and substantiating our finding that H3K56 can also be trimethylated by SUV39H1/H2. If SUV39H1/H2 are able to trimethylate H3K56 directly, then phosphorylation of H3S57 and/or H3T58 could disrupt this activity by altering the enzyme binding affinity. With the exception of H3K56 and H3K9, SUV39H1/H2 does not methylate any of the other sites targeted by G9a, none of which contain the KST motif reiterating the importance of these residues. In addition, site selection is likely to require other residues both up- and downstream of the lysine target and also be dependent on their modification status (151,152). For example, *in silico* studies, predict that an H3K4me3K14ac-containing peptide would cause torsion of H3K9 into a limited region that would not allow enzyme binding (152). Interestingly, H3K14ac stimulates binding of the yeast 14-3-3 proteins Bmh1 and Bmh2, to H3S10ph peptides, suggesting that combinations of modifications enforce a particular readout (56). Structural studies combined with such computational methods could be used as another means of predicting combinatorial patterns of histone modifications and it would be interesting to see if differences arise between the modifications with which H3K9me3 and H3K56me3, co-occur.

As briefly mentioned, using IF, we saw that H3K56me3 largely overlapped with H3K9me3 localization patterns and in WT interphase cells was concentrated in the DAPI-dense chromocenters, suggesting a role in heterochromatin formation. In mice, disruption of the SUV39H1/H2 genes, leads to impaired pericentric heterochromatin formation and subsequent genomic instability thereby decreasing viability (153). The absence of SUV39H1/H2 results in H3K9me1 relocalization (accumulation) to the chromocenters, in interphase cells and a similar redistribution is seen for H3K56me1. H3K9me1 accumulation at these regions, likely arises because H3K9, which has been monomethylated outside of chromatin, by the KMTs, Prdm3 and Prdm16 (73), is deposited into pericentric heterochromatin by a HP1  $\alpha$ -CAF1-SETDB1 complex (72). However in the absence of SUV39H1/H2 subsequent trimethylation cannot take place. Although SETDB1 has the capacity to

trimethylate H3K9, this process requires the cofactor ATF  $\alpha$ -associated factor (AM) (154), which may not be present or sufficient enough to compensate for SUV39H absence. Given the accumulation of H3K56me1 at the chromocenters upon SUV39H1/H2 disruption, it is plausible that a similar mechanism exists for deposition of this modification within pericentric heterochromatin and that both marks are deposited at the same time. Alternatively, it could be that H3K9me precedes H3K56me and could even be a pre-requisite for the latter modification. Indeed, in the case of H3K64me3, another core modification which is reduced upon SUV39H1/H2 knockout, it was shown that loss of this mark did not result from lack of the KMTs but occurred rather as an indirect result of depleted H3K9me3 (155). The sequence surrounding H3K64 (LIRKL<sub>P</sub>), however, does not resemble those of H3K9 and H3K56, which are both followed by ST, and provides a likely reason that this modification is not a direct target of the SUV39Hs, where as H3K56 could be. Interestingly, a sub-set of the H3K9 KMTs, including G9a, GLP, SUV39H1, and SETDB1, have recently been shown to co-exist in a megacomplex that is recruited to both major satellite repeats and G9a target genes (156). Although G9a and GLP-mediated H3K9 methylation has traditionally been associated with euchromatin (157), more recent publications also suggest a role in pericentric heterochromatin maintenance (158), chromosome segregation and telomere length regulation (159). Recruitment of a complex containing both KMTs for lower and higher methylation states provides another means of initiating pericentric H3K9 and H3K56 methylation, perhaps in a simultaneous fashion. In future studies, it will be interesting to see whether G9a and GLP monomethylate H3K56 in these regions, thereby providing a substrate for SUV39H-mediated trimethylation, or whether, like in ES cells, they function simply to recruit DNMTs to these regions.

### 2.1.3 Identification of JMJD2D and JMJD2E as potential erasers of H3K56me3

In order to identify the enzyme responsible for removing H3K56me3, we overexpressed GFP-tagged Jmjc-demethylases and looked for any changes in the abundance of this modification, using our antibody. Both JMJD2D (KDM4D) and JMJD2E (KDM4E) caused a decrease in H3K56me3 and concurrent increase in H3K56me1. These two enzymes are highly related in sequence showing approximately 70% similarity. Although we could not prove that these enzymes targeted H3K56me3 directly, the results suggest that they remove two methyl groups, in one step, at this residue, since H3K56me2 levels remained unchanged. Like the writers regulating H3K56me, both demethylases also target H3K9me and it is plausible that these interactions are mediated by similarities in the sequences surrounding the target residues. Indeed, recent structural data provides insight into JMJD2D selectivity for H3K9me3.(160). When complexed with an H3K9me3-containing peptide, they could show that both JMJD2A/KDM4A and JMJD2D form contacts with R8, S10, T11 and G12, located at positions -1, +1, +2, and +3, respectively, relative to H3K9. Although the H3K56 sequence does not have the same residues in the -1 and +3 positions, the respective +1 and +2, S and T, are the same. The latter

three residues adopt a bent conformation that allows them to interact with a hydrophobic pocket that lies adjacent to the active site of the enzyme. Interestingly, for JMJD2D the peptide residues maintain a bent conformation via hydrogen bonds between 1) H3S10 and either the G12 amide nitrogen and carbonyl oxygen or the R8 carbonyl oxygen and 2) H3T11 and D139 in JMJD2D. Considering the H3K56 sequence has residues with charged side chains at both positions equivalent to G12 and R8, it would be useful to compute the effects this might have on the adopted peptide conformation. In the case of JMJD2A the bent conformation is stabilized only by intrapeptide bonds and H3T11 does not interact with D135 of the enzyme due to a rotated conformation. This indicates that while the two enzymes are structurally similar and both induce a similar peptide bending, their interactions with the surrounding sequence are different. Interestingly, the sequence surrounding the JMJD2E equivalent D139 is highly similar to that of JMJD2D but not JMJD2A. This suggests that like JMJD2D, JMJD2E likely positions the H3 tail such that it hydrogen bonds with H3T11. Further experiments showed that H3T11ph abrogates H3K9me3 demethylation by JMJD2 demethylases due to steric hinderance (160). This is contradictory to *in vivo* data showing that H3T11ph accelerates H3K9 demethylation by JMJD2C to regulate androgen receptor targeted transcription (85) and may reflect either the lack of other regulatory factors *in vitro*. Indeed, phosphorylation marks are very often associated with mitotic chromatin compaction, however, they are also implicated in transcriptional activation.

H3T11ph occurs in a centromere-specific manner during mitosis, where it could prevent H3K9me3 removal, thereby promoting regionalized maintenance of this mark. This localized accumulation of H3T11ph is due to its deposition by the Dlk/ Zip kinase and results in the replacement of H3S10ph exclusively at the centromeres during prophase (161). H3S10ph is deposited at the centromeres between late G2 and early prophase, following recruitment of the CPC by H3T3ph (28). H3S10ph then leads to the dissociation of HP1, although H3K9me3 levels remain unchanged (90). The appearance of H3T11ph at prophase and its persistence until early anaphase, may serve to preserve H3K9me3 by inhibiting the binding of JMJD2 demethylases (160). In addition, structural studies show that H3S10 and H3T11 have been shown to interact with DIM-5 (150), the *Neurospora* homolog of SUV39H1 and therefore phosphorylation of these residues would also fit with the loss of centromeric SUV39H at the metaphase to anaphase transition. Given the presence of serine and threonine residues in the same positions relative to H3K56 as those relative to H3K9, one could speculate that H3K56me3 is recognized and regulated by the same mechanism. Given the recent finding that the CSD of HP1  $\alpha$  interacts with the H3  $\alpha$ N region at the nucleosome DNA entry/exit site, it is plausible that this could be mediated by H3K56me3. Indeed, like the CD the CSD has a hydrophobic pocket, although so far there is no evidence that this can interact with histone modifications (162). One could imagine a scenario in which HP1 is first recruited, via its CD to the more abundant and accessible H3K9me3 and that subsequent binding is stabilized through interaction of the CSD with H3K56me3. Although we performed SILAC labelled comparative peptide pull-downs, to try and identify potential interactors for this modification, we were unsuccessful in finding anything that stood out. Since



histone core modifications are less accessible compared to tail modifications, it could be that proteins which interact with these residues require further interactions for recruitment or stabilization, which are not provided by the short peptides. It will therefore be important to repeat such experiments using mono- or poly-nucleosomes as the pull-down substrate, providing a more *in vivo* like situation. Considering that the CSD of HP1 interacts with the H3  $\alpha$  N, it would seem plausible that like H3S10, H3S57 is phosphorylated during mitosis, reinforcing the dissociation of HP1. Furthermore, in this scenario, H3T58ph could replace H3S57ph at mitotic centromeres, thereby preventing H3K56me3 removal, despite loss of SUV39H1/H2.

#### **2.1.4 H3K56me3 cell cycle appearance**

H3K56ac has been studied extensively in yeast, where it functions primarily in the deposition of histones during DNA replication and repair. As such the bulk appearance of this mark occurs during S-phase when it promotes the association of H3 with the histone chaperone CAF1 and its subsequent deposition into chromatin. Compared to yeast, H3K56ac is far less abundant in mammalian cells, occurring on 30% and 1% of H3 respectively. It therefore seems unlikely that this modification serves the same role in mammalian DNA replication as that in yeast. In addition, there is considerable debate and conflicting data over whether or not its appearance is cell cycle dependent in higher eukaryotes (111,163). Given that H3K56ac and H3K56me are mutually exclusive, we were interested in investigating whether H3K56me3 deposition showed any cell cycle dependence. Recent data on H3K56me1 showed that it is present at similar levels in all cell cycle stages and that in G1 it serves a functional role by recruiting PCNA, disruption of which impairs DNA replication (100). Using an EdU labelling approach to distinguish interphase from S-phase cells, we saw a decrease in H3K56me3 during DNA replication, which was not reflected by an increase of H3K56ac at this stage. One might speculate that this disappearance is mediated by other modifications and could be necessary in allowing replication of heterochromatic regions. Following replication, heterochromatin is rapidly re-established, a process that is facilitated through interactions between PCNA and enzymes such as deacetylases, DNMTs and the H4K20 KMT, SET8 (PR-Set7) (164). Indeed, mutation of PCNA interferes with heterochromatin silencing in yeast (165) and flies (166), indicating its importance in roles outside of DNA polymerase recruitment. PCNA has also been implicated in the establishment of sister-chromatid cohesion during S-phase by interacting with the HAT Eco1, thereby coupling acetylation of the multiprotein cohesin complex, to replication (167). This process is essential in ensuring the correct pairing of chromatids before their separation at the end of mitosis. In particular high levels of cohesin binding occurs at the centromeres and in yeast this is dependent on heterochromatin (168).

During prometaphase-to-metaphase transition SUV39H1/H2 have been shown to accumulate transiently at centromeres (169) and both gain- and loss-of-function studies indicate their importance

in proper chromosome segregation. Metaphase chromosome spread stains show that like SUV39H1/H2, H3K56me3 accumulates at the centromeric regions during this phase of mitosis and one could speculate that it plays a role in chromosome segregation. In mammals, the DNA-PK complex, containing the Ku heterodimer (Ku70/Ku80) and the catalytic sub-unit of DNA dependent protein kinase (DNA-PKcs), has recently been implicated in normal cell cycle progression through mitosis (170), where it is thought to modulate chromosome alignment and the meta-to-anaphase transition. This complex is more commonly known for its role in non-homologous end joining (NHEJ) repair, where Ku is responsible for guiding DNA-PKcs to DNA breaks and activating its kinase activity (171). In *S.pombe*, Ku has also been implicated in centromeric interactions, where it is important for loading of condensin onto retrotransposons, a process which is disrupted by H3K56ac (172). It would be interesting to see if, in mammalian systems, H3K56ac is also refractory to Ku binding. If this is the case then it may be that concentration of mammalian H3K56me3 at the mitotic centromeres serves to prevent acetylation within these regions, allowing recruitment of DNA-PK and successful alignment of chromosomes before segregation. Interestingly, in fission yeast, Clr4, the homolog of SUV39H, has been shown to interact with the APC/C-E3 ligase (173), which is necessary for the ubiquitination and subsequent degradation of cohesin complex subunits. Furthermore, SUV39H1/H2 dissociate from pericentric heterochromatin at the meta-to-anaphase transition, adding weight to the idea of a role in cohesion regulation. Although these ideas are plausible they are highly speculative and a lot more work will need to be done to investigate their true potential. If H3K56me3 does play a role in mediating mitosis, it is likely that its perturbation would result in chromosomal missegregation and genomic instability. Therefore, although this hypothesis is purely speculative, a more detailed analysis of H3K56me3 dynamics during mitosis could be performed to give beneficial insight into its role at the centromeres during this phase. Given that H3K56me3 appears to be regulated in similar ways to H3K9me3, it will be hard to use techniques such as enzyme inhibition or depletion to analyze functional effects of this mark in a specific manner. Although it is unlikely that H3K56me3 exists in *S. cerevisiae* there is a chance it exists in *S. pombe* given that this organism contains a homolog of SUV39 (Clr4) and this would provide an opportunity to perform mutational studies. In addition, since H3K56me3 appears to be present in *Drosophila*, mutational studies could also be performed in this organism using the recently developed “histone cassette replacement” technique (174). Although such studies have their limitations, they could at least be used as a means of distinguishing events involving H3K9 modification from those involving H3K56 modification.

The fact that little H3K56me3 is found at telomeres suggests that it plays a specialized role at centromeres, however considering that it appears to be regulated by the same enzymes as H3K9me3 it will be important to find out how these differential patterns are established. One hypothesis is that if H3S57ph or H3ST58ph exist *in vivo*, these modifications could influence H3K56me3 distribution. In particular, during mitosis tight spatial and temporal regulation of phosphorylation and dephosphorylation plays a key role in mediating events at the centromeres (28). Additionally, it has

recently been shown that within the histone tails it is not just modification of adjacent residues that can impart a physical effect on protein recruitment, but also those some distance away. For example, the binding of the tandem PHD domain of DPF3b to H3 is promoted by H3K14ac but inhibited by H3K4me, the latter of which interferes with two important interactions formed between the H3K4 side chain and two residues of the tandem domain (56). Therefore, other modifications, in either *cis* or *trans*, may affect H3K56me3 localization. Indeed, it is known that modifications are differentially regulated at the telomeres and centromeres. For example, in the absence of SUV39H1/H2, the levels of H3K27me3 are increased at pericentric heterochromatin, although undetectable at telomeres (175). This highlights the need to further understand the interplay between H3K56me3 and other chromatin regulators. In addition, since we have used antibody-based methods for all our analyses, it is possible that a nearby phosphorylation mark occludes the H3K56me3 antibody epitope and therefore some regions appear devoid of the methyl mark. H3K56me3 may also be regulated by other enzymes that have not yet been identified and which may act independently of H3K9me3, leading to differential patterning of the two modifications at specific loci. Indeed, although G9a has been shown to regulate H3K56me1, this modification is still detectable in *G9a*<sup>-/-</sup> cells, supporting the idea that other KMTs can regulate this modification *in vivo* (100). Despite efforts to perform *in vitro* methyltransferase assays using recombinant SUV39H, we were unable to detect neither H3K9me3 nor H3K56me3. This could have been due to loss of SUV39H enzymatic activity or due to insufficient interactions with the substrates used for the assay (H3 peptides or recombinant H3). It is feasible that SUV39H can only methylate H3K56 when it is presented in the nucleosomal context, perhaps requiring distant *cis* or *trans* interactions to target this site or additional factors to make the site accessible.

### 2.1.5 H3K56me3 in *C. elegans*

In addition to the aforementioned organisms, our collaborators performed a more comprehensive analysis of H3K56me3 in *C. elegans*. Substantiating what we saw in mammalian cells, this modification showed considerable overlap with H3K9me3 patterns in worms, likely playing a role in heterochromatin formation. Interestingly, the only major difference between H3K9me3 and H3K56me3 appeared in germline cells. In agreement with previously published data, our collaborators found that H3K9me3 was restricted to worm oocytes, whereas H3K56me3 was present in both oocytes and sperm. Interestingly, previous transcriptional analyses of mouse SUV39H1 and SUV39H2 showed that while their expression patterns overlap during embryogenesis, SUV39H2 mRNA is largely restricted to the testes in adult mice (176), suggesting a role in spermatogenesis. Indeed, SUV39 double-knock-out results in impaired meiotic chromosome pairing (153). Given the similarities between events during meiosis and mitosis, it would be interesting to further investigate H3K56me3 dynamics during germline establishment. It is worth mentioning that unlike in worms, H3K9me is present in mouse sperm highlighting that direct comparisons may not be valid. This is especially true

for the substrate specificities of worm KMTs, which do not always reflect the actions of their mammalian counterparts (Table 1).

In an RNAi screen of worm KMTs, our collaborators identified *met-2* and *set-25* as being important for H3K56me3 regulation, with reduction of either enzyme causing a decrease in this mark. Interestingly, these two enzymes both regulate H3K9 methylation and have recently been identified as being important for perinuclear sequestering of heterochromatin in worms (177). Tethering of constitutive heterochromatin at the nuclear periphery has been shown to be important for transcriptional repression (reviewed in (178)) and DNA damage repair (179). In yeast, H3K56ac has been shown to be important for disengaging Ku-mediated telomere sequestering at the nuclear periphery in order to allow its replication (172,180). Although it is unlikely that H3K56me3 exists in *S. cerevisiae* one could speculate that in worms this modification plays a role in mediating heterochromatin nuclear localization. It will be interesting to conduct further studies in higher eukaryotes to see if H3K56me3 is involved in antagonizing the effects of H3K56ac in other Ku-mediated processes, such as DNA damage repair.

Through IF studies, we were able to gain information about the localization of H3K56me3 allowing us to postulate about its possible functions. While it remains technically challenging to perform ChIP-chip or ChIP-seq for the analysis of repeat-dense genomic regions, Daujat et. al., were successful in using ChIP-qPCR to extrapolate information on H3K64me3 distribution in heterochromatin (139) (discussed in section 2.2.3 Core modifications at repeat elements: Telomeres and centromeres). Indeed analyzing the genome-wide localization of modifications has provided invaluable insight into not only their roles in cellular functions, in particular transcriptional regulation, but also how combinations of marks work together to promote a particular read-out. By considering the genomic distribution and roles of other well-studied core modifications, we may be able to identify links that help us to learn more about H3K56me regulation and functions.

## **2.2 Genome-wide localization of H3 core modifications and their functional implications**

As well as occupying important positions within a nucleosome and thereby possibly influencing its structural integrity, histone H3 core histone modifications are distributed in a non-random manner throughout the genome.

In this next section we integrate the *in vitro* data on H3 core modifications with information on their genomic distribution. Although we focus primarily on the impact of core modification localization on transcription, the principles of how they mediate this process can be extended to and are compatible with postulated roles in other important cellular functions.

### 2.2.1 Core modifications at promoter and enhancer regions

The chromatin organization within distinct regions associated with any particular gene is a key in defining its transcriptional plasticity and output. At gene promoters, for example, the density and positioning of nucleosomes determines the accessibility of essential *cis*-regulatory elements, which can either be exposed or occluded, facilitating or hindering, respectively, events such as transcription factor binding. Likewise, nucleosome arrangement around the transcriptional start site (TSS) and in the body of genes influences processes such as RNA polymerase II (RNAPII) recruitment and transcriptional initiation, elongation and termination (181,182).

Promoters of actively transcribed genes are associated with a high nucleosome turnover and are typically enriched in histone acetylation. Correlating this knowledge with the *in vitro* properties of H3K56ac, H3K122ac and H3K64ac, it is not surprising that these three core modifications are most abundant within these regions (Figure 6) (97,99,117,140). One could speculate that the increased DNA breathing H3K56ac confers at the DNA entry/exit site facilitates the preferred binding of transcription factors close to these regions or helps the invasion by RNAPs (183).

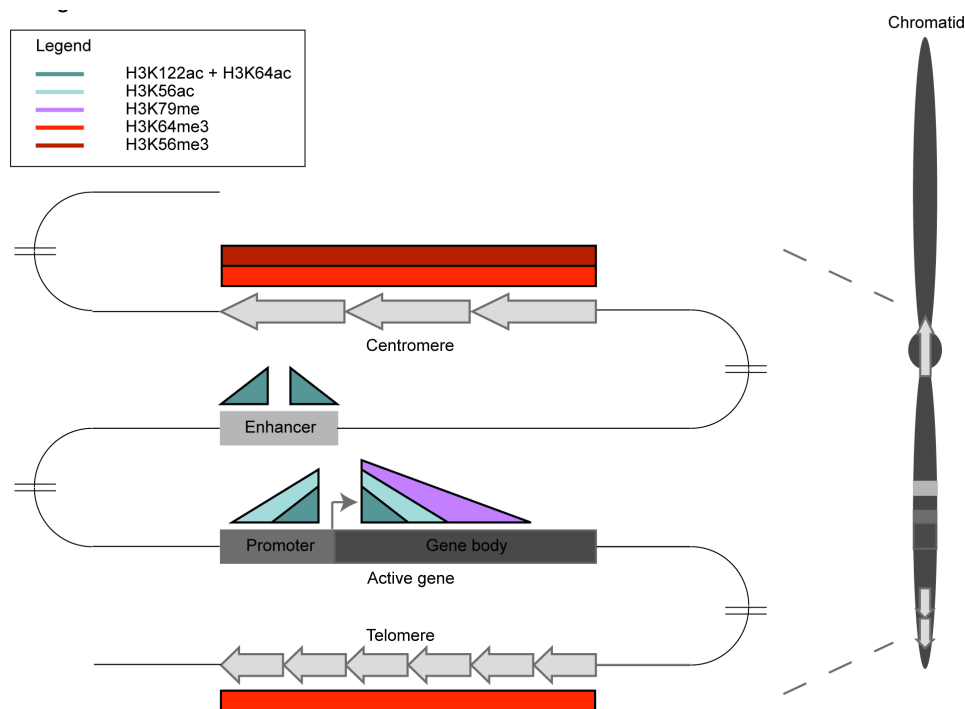


**Figure 6. Schematic depicting the major chromosomal distribution patterns of histone H3 core modifications.** The distribution patterns of H3K122ac and H3K64ac (blue), H3K56ac (cyan), H3K79me (purple), H3K64me3 (bright red), H3K56me3 (dark red) at common chromosomal features including the enhancer (light grey), promoter (mid-grey) and gene body (dark grey) of an active gene, telomeres (short, off-white arrows) and centromeres (long, off-white arrows). Distributions are generalized, based on genome-wide, single locus and immunofluorescence studies from different organisms and give a broad overview of histone H3 core modification genomic localization. Not depicted are more minor or species-specific distribution patterns, which are discussed in the main text. The general regions of a chromatid at which the chromosomal features are found, are shown on the right.

Profiling of H3K122ac-containing nucleosomes showed they are enriched for H3K56ac as well as other hallmarks of active transcription, but not H3K36me3 (117), which is typically found at the 3' end of actively transcribed genes and is associated with elongation (181). These findings substantiate genome-wide profiling data of H3K122ac, which showed that its distribution is limited to the flanking regions of the TSS (Figure 6), similar to H3K27ac and H2A.Zac. Likewise, H3K64ac is also enriched around the TSS (Figure 6) of active genes and is anti-correlated with repressive marks (140). H3K56ac has also been shown to overlap with H2A.Z at vertebrate promoters. Interestingly, recent findings show that H3K56Q-containing nucleosomes enhance the replacement of H2A.Z with H2A (144) indicating that H3K56ac may prepare H2A.Z nucleosomes for exchange. H3K122ac levels are proportional to the amount of mRNA expression (117), suggesting a role in transcriptional activation. The correlation to transcriptional activation is interesting, given the promotion of nucleosome disassembly when H3K122 is acetylated (108). One could speculate that H3K56ac allows limited access to a small region of nucleosome-obscured DNA, requiring relatively little energy, given the weaker DNA-histone contacts at these sites, and maintaining it in a poised state. Indeed, experimental evidence implicates H3K56ac in nucleosome disassembly during transcription (184). When the conditions favour transcriptional activation, acetylation at H3K122 could act as a switch to reinforce the signal and facilitate the more energy-demanding nucleosome disassembly or nucleosome sliding required for promoter clearance. The latter point is substantiated, by the confirmation of a direct function for H3K122ac in transcriptional activation, by the group of R. Schneider (117). Using an *in vitro* transcription assay, they showed that unlike the tail modification H3K18ac, H3K122ac alone could stimulate transcription from a chromatin template. Furthermore, histone eviction experiments demonstrated that nucleosomes displaying H3K122ac were more susceptible to displacement, reiterating the likely mechanism by which it functions. Given the negative effects H3K64ac has on nucleosome stability and its correlation with transcriptional activation (140), it will be interesting, in future studies, to assess any cross-talk that may occur between these modifications. The role of H3K56ac in the proposed hypothesis, as a mechanism of opening up chromatin but not activating transcription, is supported experimentally. In both yeast and humans, H3K56ac is found at some repressed genes and regions of DNA repair and therefore does not necessarily correlate with mRNA expression levels (37,99).

Genome-wide profiling in human embryonic stem (hES) cell lines showed that genes associated with the highest levels of H3K56 acetylation include almost all canonical histone genes, similar to a published study in yeast (97). Furthermore, in hES cells H3K56ac was also found to associate with many pluripotency regulators, such as Nanog, Sox2 and Oct4 (NSO) (99). The recent finding that H3K56ac and Oct4 interact directly, both *in vitro* and *in vivo* (185), suggests a direct mechanism by which these factors could be recruited to specific regions and also highlights the accessibility of H3K56 to binding proteins. The latter point is further substantiated by the finding that during G1 phase of the cell cycle, H3K56me1 acts as a chromatin docking site for PCNA, thereby facilitating

DNA replication (100). Interestingly, upon differentiation, H3K56ac is redistributed to the promoters of genes involved in development, such as the *HOX* genes, and those involved in somatic cell maintenance (99). In support of these findings, a study in mature adipocytes also found H3K56ac adjacent, but not overlapping, to some transcription factor binding sites, as well as hyperacetylation of this residue at developmental genes (186). Again this supports a role for H3K56ac in maintaining transcriptional plasticity rather than mRNA levels per se.

Findings by the group of B. Ren suggest that cell type-specific modification patterns at enhancer regions play a major role in driving differences in gene expression profiles associated with cell fate decisions (187). It has been postulated that the modification pattern of specifically placed nucleosomes may act to display transcription factor binding sites (188). H3K4me1/me2 enrichment is associated with enhancers and is often coupled with H3K27me3 if the gene that it is regulating is repressed or with H3K27ac when the gene is activated (189,190). In keeping with a similar distribution to H3K27ac, genome-wide analyses of H3K122ac and H3K64ac showed that both are also present at active enhancer regions (117,140). This is compatible with a role in transcriptional activation, whereby the presence of H3K64ac at enhancers likely decreases nucleosome stability and H3K122ac facilitates nucleosome disassembly, thereby permitting the binding of transcriptional activators to *cis*-regulatory sites.

Previous work in murine ES cells (mES) has shown that NSO co-occupancy at specific genomic regions is indicative of enhancer activity and that these factors are able to recruit p300, an acetyltransferase associated with H3K56ac, H3K122ac and H3K64ac (191). More recently super-enhancers have been discovered, which regulate the transcription of master regulator genes that control cell identity (192). In mES cells these super-enhancers consist of clusters of enhancers, which are densely occupied by NSO and have high levels of the Mediator co-activator complex (192). Given previous data showing co-localization of H3K56ac with NSO, the fact that p300 can catalyze addition of this modification and the established role of H3K56ac in ES cell identity, one might speculate that this modification could also be a mark of super-enhancers and that its misregulation could have deleterious effects on cell specification.

Taken together, the presence of acetylation within the histone H3 core at promoters and enhancers seems to function by promoting an 'open' and binding-permissive chromatin conformation. While the nucleosomal changes induced by H3K56ac do not seem to be strong enough to direct transcription alone, it appears that this modification may mark specific regions that respond to regulatory cues, for example during differentiation. In addition, it is directly involved in protein recruitment. The stronger effects of H3K64ac and H3K122ac, on the other hand, likely serve as a switch to commit to nucleosome disassembly and transcriptional activation. Given the long-range chromatin interactions between promoters and enhancers and the presence of these modifications on both elements (193), it

will be interesting to see if these three core marks have additional roles in facilitating chromatin looping and the selective association of specific regulatory regions.

### 2.2.2 Core modifications in the gene body

Unlike H3K122ac, H3K56ac is not only enriched at the promoters but also extends into the gene body of highly transcribed genes (Figure 6) (110), suggesting that while H3K122ac plays a role in transcriptional initiation, H3K56ac may also function in proximal promoter pause release. Although nucleosome occupancy in gene bodies is high compared to promoter regions, they must retain a level of dynamicity in order to allow chromatin disassembly at the transcriptional machinery and reassembly following its passage along the gene (194). Whereas H3K122ac appears to function solely in nucleosome disassembly, there is evidence that H3K56ac also functions in nucleosome assembly (37,98), providing a possible reason for the presence of this modification within the gene body of highly transcribed genes (195). Interestingly, neither recruitment of pre-initiation complex components to promoters of actively transcribed genes, nor the presence of RNAPII within the coding sequences, were affected in Asf1-mutant yeast strains, in which H3K56ac levels were diminished (110). Transcriptional repression of genes within heterochromatic loci, has been suggested to be regulated at the level of elongation rather than initiation considering the successful recruitment and binding of transcriptional activators, components of the pre-initiation complex and RNAPII to promoters within these regions (196,197). Rtt109 or Asf1 yeast mutant strains, as well as H3K56R substitution, inhibit transcription at a heterochromatinized locus. In contrast, the H3K56Q substitution is able to restore transcription in the Rtt109 mutant, reiterating that the presence of this mark is important in allowing RNAPII progression (198).

Although H3K56ac and RNAPII overlap (110), the finding that RNAPII is still present at coding sequences in Asf1 mutants (110) suggests that H3K56ac is not directly involved in its recruitment to transcribed regions. At these sites, it could therefore function by promoting the progression of RNAPII by loosening the nucleosomal DNA and/or by recruiting a factor that has not yet been identified.

*In vitro* data suggesting that H3K56ac can destabilize the (H3-H4)<sub>2</sub> tetramer, but not the nucleosome indicate that (H3K56ac-H4)<sub>2</sub> tetramers favour assembly with (H2A-H2B) dimers in order to form a more stable complex or they are otherwise disassembled (109). Considering both processes occur at transcriptionally active loci it is hard to decipher the exact role of H3K56ac within these regions. One could postulate that the presence of other histone modifications and different histone variants could favour the one or the other outcome.

H3K79 methylation is the core PTM most well known for its enrichment in the gene body (Figure 6). At these sites it is associated with the presence of RNAPII, suggesting a role in transcriptional elongation (199-201). In addition, within these regions H3K79me2 and me3 overlap with the presence



of Dot1 (202). This is not surprising given the requirement of several *trans*-histone interactions for Dot1-mediated H3K79 methylation and therefore the targeting of this enzyme to chromatin-incorporated, rather than soluble H3. Dot1 has been found as part of several elongating complexes (summarized in (137)), consistent with the overlap of H3K79me and RNAPII and a role in gene regulation. A recent study showed that Dot1-like methyltransferase (Dot1L), the mammalian homolog of Dot1, can directly bind the phosphorylated C-terminal domain (CTD) of RNAPII. Interestingly, this interaction occurs through a region on Dot1L that is unique to the multicellular eukaryotes (203), reflecting the possible evolution of a more streamlined process. In addition to its histone methylation roles, Dot1 has recently been proposed to function in other ways (204,205) and therefore correlations with this methyltransferase may not always serve as a means of analyzing H3K79me actions.

Given that all three H3K79me states share a common, nonprocessive methyltransferase, there has been some debate over the individuality of their functions. On the one hand it has been shown that Dot1 works in a distributive manner and that all states are functionally redundant (46), however the observation that H3K79me<sub>2</sub> and me<sub>3</sub> are differentially distributed in yeast (206), suggests otherwise. The latter finding is not only intriguing in terms of functional implications but also in terms of how the two modifications are independently regulated. Firstly, from the functional perspective, one could imagine that modified H3K79 behaves as a binding platform, given that *in vitro* data suggests methylation of this residue induces a more flexible side-chain conformation (45), likely facilitating association of this solvent exposed residue with potential binding partners. However, the accessibility of H3K79 within polynucleosomes is still unclear. Although, so far, there is little data on H3K79me binding partners, it is conceivable that such interactions are dependent on the extent of methylation, with H3K79me<sub>2</sub> recruiting a different repertoire of proteins compared to H3K79me<sub>3</sub>, thereby establishing different functional domains. Secondly, from the regulation perspective, the finding that Dot1 is present in multiple complexes makes it plausible that the differential distribution of H3K79me<sub>2</sub> and me<sub>3</sub> is established by the presence, or lack of, other complex components that may be involved in H3K79me. Furthermore, H3K79me<sub>3</sub> but not H3K79me<sub>2</sub> has been found to overlap with yH2BK123ub, suggesting the presence of the latter mark may influence localization. Interestingly, in *C.elegans*, Dot1 forms a negative feedback loop by opposing H2Bub, thereby reducing RNAPII transcription through polymerase pausing (207), indicating the need to better understand the molecular aspects of correlative studies.

Both yH2BK123ub and H3K79me<sub>3</sub>, but not H3K79me<sub>2</sub>, often associate with longer genes (208). Like the deposition of H3K36me<sub>3</sub> at the 3' end of genes, it could be that the presence of H3K79me<sub>3</sub> and yH2BK123ub prevent aberrant transcription in the wake of RNAPII. Indeed, there is already some evidence that H2Bub functions in this respect by promoting the assembly of nucleosomes (207,209). What is compelling is how these modifications could function in both transcriptional elongation,

where nucleosome turnover must take place, as well as cryptic transcription, where it must be prevented.

In yeast over 90% of total H3 is methylated at K79 with me<sub>3</sub> making up the majority (128). In mES cells this modification is far less abundant and the vast majority of the 11% of H3K79 that is methylated, harbours me<sub>3</sub> and to a lesser extent me<sub>2</sub> (114,210). This is interesting in light of recent ChIP-seq data from mouse adipocytes, which provides evidence that in mammals the conversion of H3K79me<sub>1</sub> to H3K79me<sub>2/3</sub> correlates with a transition from low to high level transcription (202). Considering, under normal growth conditions, most of the yeast genome is transcribed (211), differences in gene density and transcriptional activity could provide an explanation for the organismal differences with regards not only to the total levels of H3K79me, but also the abundance of the individual states.

Most of the data linking H3K79 methylation to transcriptional elongation come from correlative studies and it is hard to say whether it is cause or consequence. There is continual debate over whether this modification facilitates transcriptional activation or whether it plays a role in repression. While some of the earlier discrepancies have been accounted for by technical differences in ChIP protocols there remains considerable controversy (181,201,212-214). Although strong correlations between H3K79me and transcriptional activation fit with the finding that Dot1 is more abundant at the transcribed regions of active genes compared to inactive (202,215,216), H3K79me has also been found at some repressed regions (213,217,218). In addition, disruption of Dot1L in mice does not affect all transcriptional pathways (219) suggesting that if it does play a role in mediating gene expression, this occurs in a targeted manner. Unlike H3K79me<sub>2/3</sub>, which are found in proximity to the TSS, H3K79me<sub>1</sub> covers a broader gene-associated area extending both upstream and downstream of regions enriched for Dot1 (202), in mouse adipocytes. This suggests that while H3K79me<sub>2/3</sub> play a role in the early steps of elongation, H3K79me<sub>1</sub> has a different function. Although there is some overlap with H3K4me<sub>1</sub>, which has previously been shown to associate with enhancers, the presence of H3K79me<sub>1</sub> does not appear to be a general demarcation of these regulatory elements (201). However, its co-localization with some transcriptional activators at their binding sites has been shown, indicating that its targeted deposition within certain intergenic regions may play a gene-specific role (201,202).

H3K79me<sub>1</sub> has also been found at some poised genes (202) suggesting it may function to set the stage for gene activation in response to specific cues. Consistent with the presence of H3K79 methylation at these regions, RNAPII is also known to accumulate at some tightly regulated genes, such as human *c-myc* (220) and *Drosophila hsp70* (221), under repressive conditions. During the process of differentiation, dynamic changes in H3K79me<sub>2/3</sub> within transcribed regions have been shown, which parallel changes in mRNA levels (201,202), suggesting that together the three modification states may also serve specific functions in cell specification.

### 2.2.3 Core modifications at repeat elements: Telomeres and centromeres

The formation and confinement of genomic silencing at constitutive heterochromatin is crucial for the maintenance of genomic integrity and has been shown to be partly dependent on histone H3 core modifications.

Despite the high abundance of repeat sequences and low level of transcription within these regions, they are not functionally inert. Telomeres, for example, cap eukaryotic chromosome ends, preventing their recognition as sites of DNA damage and play an essential role in limiting the loss of protein-coding regions, which would otherwise occur as a result of the end replication problem (222). Although similar to telomeres in their dense nucleosomal packing and epigenetic features, centromeres serve a very different function and are responsible for assembly of the kinetochore, which serves as the attachment point for the mitotic spindle and is required for proper sister chromatid segregation during mitosis (223). In both mentioned structures, as well as other silenced genomic regions, the repressive, heterochromatic architecture is essential for the maintenance of genomic stability, preventing rearrangements, which might otherwise occur between the highly similar sequences (224). In higher eukaryotes this architecture is promoted by several epigenetic features including DNA methylation, which induces tighter wrapping of the DNA around the nucleosome (225) and H3K9me3, which recruits the chromo-domain protein, heterochromatic protein 1 (HP1) (224). As a result of its compact conformation any genes within constitutive heterochromatin will be poorly expressed, a trait which can spread into adjacent, non-repetitive regions through a phenomenon known as position effect variegation (PEV) (226).

H3K79 methylation has known functions in telomere silencing and in the yeast genome it is specifically excluded from these and other silenced regions (128,204). Indeed, mutation of Dot1 methyltransferase activity or substitution of H3K79 both lead to severe silencing defects (128,129,227). In several of the studies cited, these defects were measured by activation of a URA3 gene integrated in a region that is normally silenced, for example close to the telomere. This technique, however, has recently received some criticism since it was discovered that the silencing defects resulting from mutation of some proteins, including Dot1 and PCNA, are actually determined by uneven nucleotide metabolism at the URA3 promoter, rather than the effects of the tested proteins themselves (228). Despite these novel insights, a recent study monitoring changes at natural telomeric genes in H3K79-methylation defective mutants, showed that this modification is still important for the regulation of some coding sequences (229), although overall effects seem to be milder than formerly predicted. In addition, when other pathways are compromised the role of Dot1 in natural silencing may become more apparent (230), highlighting the need for further investigation.

In yeast, silencing is mediated by assembly of the Silencing Information Regulator (SIR) complex, consisting of the H4K16 deacetylase Sir2 together with Sir3 and Sir4 (231,232). Mutation of any of

these proteins leads to a complete loss of silencing (233). Several lines of evidence suggest H3K79me and Sir3 share an antagonistic relationship. Firstly, Sir3 and Dot1 both bind the same short basic patch of the histone H4 tail (131,132) and therefore compete for this site. Secondly, methylation at H3K79 disrupts contacts between the bromo-adjacent homology (BAH) and AAA+ domains of Sir3 and the lateral surface of the nucleosome (234,235). In this regard, H3K79me appears to function by altering the binding affinity of certain proteins rather than causing direct effects on the nucleosome structure. It was postulated that H3K79me distribution throughout most of the yeast genome, prevents Sir binding, causing its localization to discrete, silenced regions (128,236).

In higher eukaryotes there is very little mechanistic information on how H3K79me functions. However, H3K79me<sub>2</sub> marks a distinct set of replication origins in the human (237) and trypanosome genome (H3K76me<sub>2</sub>) and it has been shown that in *T. brucei* overexpression of Dot1A, one of two DOT1 homologs, causes continuous replication of nuclear DNA (238). In humans, these data favour the view that H3K79me<sub>2</sub>'s association with these origins and replicated chromatin during S-phase may play a role in preventing re-replication thereby preserving genome stability. In trypanosomes, however, H3K76me<sub>1/2</sub> occurs exclusively after replication and most likely initiates licensing, raising interesting questions regarding functional conservation. Several mammalian proteins contain a BAH domain similar to Sir3, raising the possibility that methylation of H3K79 may alter the binding of these proteins. In higher eukaryotes several of the proteins harboring the BAH module, including ORC1, are important for replicative events (239). In addition, the BAH domain is part of the mouse DNA methyltransferase 1 (DNMT1) enzyme and may be involved in its recruitment to the replication origins, suggesting a functional link between DNA methylation and replication (239). Finally MTA1, a subunit of the repressive, HDAC-containing NuRD complex, also contains a BAH domain and one could speculate that methylation of H3K79 could disrupt a nucleosomal interaction and hinder targeted chromatin remodeling and histone deacetylation within specific regions.

In mammals H3K79me<sub>2</sub> is present throughout heterochromatic regions (pericentric, centromeric, telomeric and sub-telomeric) (210), however its absence in Dot1L mutant cells leads to a general reduction in heterochromatic marks including H4K20me<sub>3</sub> and H3K9me<sub>2</sub> (but not H3K9me<sub>3</sub>) and an increase in H3K9ac. As a functional consequence, loss of Dot1L activity resulted in aberrant telomere elongation through activation of the Alternative Lengthening of Telomere (ALT) pathway (reviewed in (240)), a telomerase-independent mechanism of counteracting the end replication problem. The effects of dysfunctional Dot1L on telomere length appear to be conserved as similar alterations have been observed in yeast Dot1 mutant strains (129). As the authors point out this finding is intriguing given the presence of H3K79me-containing nucleosomes at mammalian telomeres and complete lack of nucleosomes at yeast telomeres. Moreover, the results in this study point to Dot1L playing a promotional role in heterochromatin maintenance, which seems counterintuitive to its link with transcriptional activation and the enrichment of H3K79me in euchromatin. Possible functions for

Dot1L in heterochromatin maintenance could be mediating the expression and/or distribution of heterochromatin-associated factors, or effects might result from changes to as yet unknown non-histone Dot1L targets.

In addition to alterations in H3K79me levels, H3K56 substitutions in yeast, also lead to silencing defects, especially at the telomeric regions (241,242). The silencing effects are, however, neither due to altered Sir protein recruitment or spreading, nor due to changes in other acetylated residues, such as H4K16 (242) although it may facilitate slight loosening of Sir binding (243). In yeast, H3K56 deacetylation is globally mediated by the HDACs Hst3 and Hst4 (244,245), mutation of which leads to defects in telomeric silencing as a result of hyperacetylation. This occurs despite recruitment of Sir2 (246). Although Sir2 itself has previously been implicated in H3K56 deacetylation, it is possible that alone it is not able to compensate for the loss of Hst3 and Hst4. In addition, its role in H3K56 deacetylation is controversial and there are several reports presenting conflicting data (242,243,246). It has recently been shown that HDACs mediate the stability of heterochromatin through the suppression of histone turnover (247) and given that H3K56ac is conducive to DNA unwrapping at the entry/exit site of the nucleosome, removal of this modification may facilitate this process by inducing a more closed conformation at these sites. A similar mechanism is likely to be used in higher eukaryotes, given that the HDACs SIRT1 and SIRT6, which can both deacetylate H3K56, have been shown to be associated with mammalian telomeres and to be important for their integrity (111,248-250).

H3K64me3 is found at constitutive heterochromatin, and ChIP-qPCR showed that it is enriched on repetitive DNA, including pericentromeric heterochromatin (Figure 6) (139). Interestingly, this localization does not require DNA methylation, consistent with other tail modifications in these regions, nor is it affected by HP1 localization (155). Instead, there appears to be cross-talk between H3K64me3 and H3K9me3. Indeed, knockout of SUV39H1/H2 causes not only a severe reduction in H3K9me3, but also H3K64me3. An elegant experiment by Lange et. al., in which H3K9me3 was artificially recruited to pericentromeric heterochromatin in *SUV39H1/H2* double knockout cells, showed restoration of H3K64me3 at these regions. This indicates a dependency of H3K64me3 on H3K9me3 rather than on the SUV39Hs (155). It is perhaps not surprising that H3K64 is not directly regulated by the Suv39Hs, considering the surrounding amino acids are different to those of H3K9. In this regard it would be interesting to carry out similar dependency-based experiments for H3K56me3 to decipher when in the heterochromatin formation chain of events it is deposited. One might predict that it occurs concomitantly, or just shortly after H3K9me3, but before H3K64me3. Given that it is found in organisms with little or no DNA methylation, it is also possible that H3K56me3 occurs independently of this process. Interestingly, in mouse NIH3T3 cells, overexpression of H3 in which K64 was substituted to arginine (R), resulted in a reduction of PTMs and factors representing hallmarks of constitutive heterochromatin, including H3K9me3, H4K20me3 and HP1, indicating an important role for H3K64me3 in heterochromatin maintenance. As a means to test our antibody, we

also made H3K56R mutants and could therefore easily perform similar assays to test global effects on other heterochromatic marks.

### 2.3 Mislocalization of core modifications and disease

Given the importance and implications of histone core modification genomic localization, it is not surprising that their mislocalization is implicated in several pathological processes. The occurrence of abnormal fusion proteins through genomic rearrangement is a common feature of many cancers. In over 70% of infant leukaemias, for example, the 5'-region of the *Mixed Lineage Leukemia (MLL)* gene is fused to various translocation partners, many of which are involved in transcriptional initiation and elongation (reviewed in (251)). In addition to other fundamental cellular processes, MLL is involved in transcriptional control of specific genes within the developmentally regulated *Hox* cluster (252). Amongst the MLL fusion partners are CBP/p300 and several elongating complex members which are capable of interacting with Dot1. Fusion-facilitated mistargeting of these histone modifying activities alters the pattern of PTMs at specific regions, such as the *Hox* genes, resulting in aberrant gene expression. In this regard, altered H3K79me patterns can contribute to the disruption of normal haematopoiesis and the progression of leukaemia (253,254) - a finding that has been substantiated using an inducible MLL fusion protein expression system. Indeed, Dot1 inhibitors are effective at reducing the growth of MLL leukaemias (255) and are currently in phase 1 clinical trials (ClinicalTrials.gov Identifier: NCT01684150, Drug: EPZ-5676).

A common fusion protein linked to prostate cancer is formed through the joining of the 5'-UTR region of the androgen-regulated *TMPRSS2* gene to the oncogenic transcription factor, *ERG* (256,257). It is thought that this fusion is brought about through the interaction of the androgen receptor (AR) at specific binding sites, which mediates chromatin looping, thereby inducing abnormal spatial proximity between the two gene partners (258). Recent studies have shown that AR-binding sites at *TMPRSS2* and *ERG* breakpoints are enriched in H3K79me and H4K16ac raising the possibility that histone modifications may play a novel role in chromatin looping (259,260) and promote the formation of fusion proteins. Finally, it has also been demonstrated that DNA tumor viruses encode oncoproteins, which amongst other regulatory proteins, target CBP/p300 (261-263). A recent publication showed that in cells expressing the Simian Virus 40 T antigen, higher levels of CBP/p300 resulted in an increase in H3K56ac and H4K12ac (264). In the case of adenovirus early region 1A, CBP/p300 is re-localized from the promoters of genes involved in differentiation and antiviral defense to those involved in cell proliferation, altering their histone acetylation patterns, including H3K56ac distribution (265).

Given the enrichment of H3K56me3 at metaphase centromeres it is likely that this modification plays a key role in ensuring equal partitioning of DNA to the two daughter cells during mitosis. If this is the

case then one could postulate that loss or reduction of H3K56me3 may impede proper chromosome segregation and lead to genomic instability.

Furthering our understanding of the effects of H3 core modifications on transcription and long-range interactions will be crucial in delineating their role in disease pathogenesis. In addition, identifying the enzymes that regulate them could enhance our array of potential drug targets.

## 2.4 Concluding remarks

The identification of histone core modifications and their genome-wide mapping gives us further insight into the regulation of DNA accessibility across the genome. While many functional conclusions have already been drawn about the role of these modifications at specific genomic loci, most of the data is based on correlative studies. In addition, the interpretation of mutational studies can be problematic. For example, the commonly used K to Q substitution to mimic acetylation behaves differently, in multiple assays, compared to acetylation itself. Such mutations also lead to 100% of histones being “acetylated” all the time, which does not reflect the *in vivo* situation. The finding that several lysine residues can be both methylated and acetylated also complicates such studies as replacement with a Q not only mimics acetylation but also prevents methylation. Deciphering whether histone PTMs take place as cause or consequence of the processes with which they are linked, also remains problematic (discussed in (266)). H3K56ac and H3K79me have both been implicated in cellular functions outside of transcription, for example mitotic and meiotic regulation and the DNA damage response. Such roles are consistent with their predicted mode of action in transcription.

With the development of more sensitive MS machines the repertoire of core histone PTMs is increasing (267,268). In addition, the explosion of data implicating core modifications in DNA damage repair, cell cycle regulation, cell fate determination and disease pathogenesis highlights the need to better understand the mechanisms underlying their functions and regulation. Finally, with the implementation of chromatin capture techniques our understanding of the importance of chromatin organization in the nucleus is growing and it is likely that, as in the case of H3K56ac and telomere localization, new functions for histone modifications in mediating processes such as long-range interactions will become apparent. Given the pivotal role of non-random nuclear organization in maintaining genomic stability, it will be intriguing to see how we can integrate this new knowledge with what we already know to further our understanding of cellular homeostasis and disease pathogenesis.

## REFERENCES

1. Luger, K., Mader, A.W., Richmond, R.K., Sargent, D.F. and Richmond, T.J. (1997) Crystal structure of the nucleosome core particle at 2.8 Å resolution. *Nature*, **389**, 251-260.
2. Bowman, G.D. (2010) Mechanisms of ATP-dependent nucleosome sliding. *Current opinion in structural biology*, **20**, 73-81.
3. Dorigo, B., Schalch, T., Bystricky, K. and Richmond, T.J. (2003) Chromatin fiber folding: requirement for the histone H4 N-terminal tail. *Journal of molecular biology*, **327**, 85-96.
4. Vogler, C., Huber, C., Waldmann, T., Ettig, R., Braun, L., Izzo, A., Daujat, S., Chassignet, I., Lopez-Contreras, A.J., Fernandez-Capetillo, O. *et al.* (2010) Histone H2A C-terminus regulates chromatin dynamics, remodeling, and histone H1 binding. *PLoS genetics*, **6**, e1001234.
5. Shukla, M.S., Syed, S.H., Goutte-Gattat, D., Richard, J.L., Montel, F., Hamiche, A., Travers, A., Faivre-Moskalenko, C., Bednar, J., Hayes, J.J. *et al.* (2011) The docking domain of histone H2A is required for H1 binding and RSC-mediated nucleosome remodeling. *Nucleic acids research*, **39**, 2559-2570.
6. Akey, C.W. and Luger, K. (2003) Histone chaperones and nucleosome assembly. *Current opinion in structural biology*, **13**, 6-14.
7. Luger, K. and Richmond, T.J. (1998) DNA binding within the nucleosome core. *Current opinion in structural biology*, **8**, 33-40.
8. Li, G. and Widom, J. (2004) Nucleosomes facilitate their own invasion. *Nature structural & molecular biology*, **11**, 763-769.
9. Olins, A.L. and Olins, D.E. (1974) Spheroid chromatin units (v bodies). *Science*, **183**, 330-332.
10. Simpson, R.T. (1978) Structure of the chromatosome, a chromatin particle containing 160 base pairs of DNA and all the histones. *Biochemistry*, **17**, 5524-5531.
11. Tremethick, D.J. (2007) Higher-order structures of chromatin: the elusive 30 nm fiber. *Cell*, **128**, 651-654.
12. Maeshima, K., Hihara, S. and Eltsov, M. (2010) Chromatin structure: does the 30-nm fibre exist in vivo? *Current opinion in cell biology*, **22**, 291-297.
13. Hardin, J., Bertoni, G.P. and L.J., K. (2012) *Becker's world of the cell* 8th ed. Benjamin Cummings.
14. Lanctot, C., Cheutin, T., Cremer, M., Cavalli, G. and Cremer, T. (2007) Dynamic genome architecture in the nuclear space: regulation of gene expression in three dimensions. *Nature reviews. Genetics*, **8**, 104-115.
15. Fillion, G.J., van Bommel, J.G., Braunschweig, U., Talhout, W., Kind, J., Ward, L.D., Brugman, W., de Castro, I.J., Kerkhoven, R.M., Bussemaker, H.J. *et al.* (2010) Systematic protein location mapping reveals five principal chromatin types in Drosophila cells. *Cell*, **143**, 212-224.
16. Kharchenko, P.V., Alekseyenko, A.A., Schwartz, Y.B., Minoda, A., Riddle, N.C., Ernst, J., Sabo, P.J., Larschan, E., Gorchakov, A.A., Gu, T. *et al.* (2011) Comprehensive analysis of the chromatin landscape in Drosophila melanogaster. *Nature*, **471**, 480-485.
17. Ernst, J. and Kellis, M. (2010) Discovery and characterization of chromatin states for systematic annotation of the human genome. *Nature biotechnology*, **28**, 817-825.
18. Chen, H., Monte, E., Parvatiyar, M.S., Rosa-Garrido, M., Franklin, S. and Vondriska, T.M. (2012) Structural considerations for chromatin state models with transcription as a functional readout. *FEBS letters*, **586**, 3548-3554.
19. Hansen, J.C., Lu, X., Ross, E.D. and Woody, R.W. (2006) Intrinsic protein disorder, amino acid composition, and histone terminal domains. *The Journal of biological chemistry*, **281**, 1853-1856.
20. Nowak, S.J. and Corces, V.G. (2000) Phosphorylation of histone H3 correlates with transcriptionally active loci. *Genes & development*, **14**, 3003-3013.
21. Hendzel, M.J., Wei, Y., Mancini, M.A., Van Hooser, A., Ranalli, T., Brinkley, B.R., Bazett-Jones, D.P. and Allis, C.D. (1997) Mitosis-specific phosphorylation of histone H3 initiates



- primarily within pericentromeric heterochromatin during G2 and spreads in an ordered fashion coincident with mitotic chromosome condensation. *Chromosoma*, **106**, 348-360.
22. Strahl, B.D. and Allis, C.D. (2000) The language of covalent histone modifications. *Nature*, **403**, 41-45.
  23. Ruthenburg, A.J., Li, H., Patel, D.J. and Allis, C.D. (2007) Multivalent engagement of chromatin modifications by linked binding modules. *Nature reviews. Molecular cell biology*, **8**, 983-994.
  24. Jenuwein, T. and Allis, C.D. (2001) Translating the histone code. *Science*, **293**, 1074-1080.
  25. Wang, X., Moore, S.C., Laszczak, M. and Ausio, J. (2000) Acetylation increases the alpha-helical content of the histone tails of the nucleosome. *The Journal of biological chemistry*, **275**, 35013-35020.
  26. Potoyan, D.A. and Papoian, G.A. (2012) Regulation of the H4 tail binding and folding landscapes via Lys-16 acetylation. *Proceedings of the National Academy of Sciences of the United States of America*, **109**, 17857-17862.
  27. Shogren-Knaak, M., Ishii, H., Sun, J.M., Pazin, M.J., Davie, J.R. and Peterson, C.L. (2006) Histone H4-K16 acetylation controls chromatin structure and protein interactions. *Science*, **311**, 844-847.
  28. Wilkins, B.J., Rall, N.A., Ostwal, Y., Kruitwagen, T., Hiragami-Hamada, K., Winkler, M., Barral, Y., Fischle, W. and Neumann, H. (2014) A cascade of histone modifications induces chromatin condensation in mitosis. *Science*, **343**, 77-80.
  29. Robert, F., Pokholok, D.K., Hannett, N.M., Rinaldi, N.J., Chandy, M., Rolfe, A., Workman, J.L., Gifford, D.K. and Young, R.A. (2004) Global position and recruitment of HATs and HDACs in the yeast genome. *Molecular cell*, **16**, 199-209.
  30. Hodawadekar, S.C. and Marmorstein, R. (2007) Chemistry of acetyl transfer by histone modifying enzymes: structure, mechanism and implications for effector design. *Oncogene*, **26**, 5528-5540.
  31. Brownell, J.E. and Allis, C.D. (1996) Special HATs for special occasions: linking histone acetylation to chromatin assembly and gene activation. *Current opinion in genetics & development*, **6**, 176-184.
  32. Arrowsmith, C.H., Bountra, C., Fish, P.V., Lee, K. and Schapira, M. (2012) Epigenetic protein families: a new frontier for drug discovery. *Nature reviews. Drug discovery*, **11**, 384-400.
  33. Smolle, M. and Workman, J.L. (2013) Transcription-associated histone modifications and cryptic transcription. *Biochimica et biophysica acta*, **1829**, 84-97.
  34. Gray, S.G. and Ekstrom, T.J. (2001) The human histone deacetylase family. *Experimental cell research*, **262**, 75-83.
  35. Allfrey, V.G. and Mirsky, A.E. (1964) Structural Modifications of Histones and their Possible Role in the Regulation of RNA Synthesis. *Science*, **144**, 559.
  36. Sobel, R.E., Cook, R.G., Perry, C.A., Annunziato, A.T. and Allis, C.D. (1995) Conservation of deposition-related acetylation sites in newly synthesized histones H3 and H4. *Proceedings of the National Academy of Sciences of the United States of America*, **92**, 1237-1241.
  37. Chen, C.C., Carson, J.J., Feser, J., Tamburini, B., Zabaronick, S., Linger, J. and Tyler, J.K. (2008) Acetylated lysine 56 on histone H3 drives chromatin assembly after repair and signals for the completion of repair. *Cell*, **134**, 231-243.
  38. McCool, K.W., Xu, X., Singer, D.B., Murdoch, F.E. and Fritsch, M.K. (2007) The role of histone acetylation in regulating early gene expression patterns during early embryonic stem cell differentiation. *The Journal of biological chemistry*, **282**, 6696-6706.
  39. Ikura, T., Ogryzko, V.V., Grigoriev, M., Groisman, R., Wang, J., Horikoshi, M., Scully, R., Qin, J. and Nakatani, Y. (2000) Involvement of the TIP60 histone acetylase complex in DNA repair and apoptosis. *Cell*, **102**, 463-473.
  40. Legube, G. and Trouche, D. (2003) Regulating histone acetyltransferases and deacetylases. *EMBO reports*, **4**, 944-947.
  41. Zeng, L. and Zhou, M.M. (2002) Bromodomain: an acetyl-lysine binding domain. *FEBS letters*, **513**, 124-128.
  42. Zeng, L., Zhang, Q., Li, S., Plotnikov, A.N., Walsh, M.J. and Zhou, M.M. (2010) Mechanism and regulation of acetylated histone binding by the tandem PHD finger of DPF3b. *Nature*, **466**, 258-262.

43. Owen, D.J., Ornaghi, P., Yang, J.C., Lowe, N., Evans, P.R., Ballario, P., Neuhaus, D., Filetici, P. and Travers, A.A. (2000) The structural basis for the recognition of acetylated histone H4 by the bromodomain of histone acetyltransferase *gcn5p*. *The EMBO journal*, **19**, 6141-6149.
44. Dreveny, I., Deeves, S.E., Fulton, J., Yue, B., Messmer, M., Bhattacharya, A., Collins, H.M. and Heery, D.M. (2013) The double PHD finger domain of MOZ/MYST3 induces alpha-helical structure of the histone H3 tail to facilitate acetylation and methylation sampling and modification. *Nucleic acids research*.
45. Lu, X., Simon, M.D., Chodaparambil, J.V., Hansen, J.C., Shokat, K.M. and Luger, K. (2008) The effect of H3K79 dimethylation and H4K20 trimethylation on nucleosome and chromatin structure. *Nature structural & molecular biology*, **15**, 1122-1124.
46. Frederiks, F., Tzouros, M., Oudgenoeg, G., van Welsem, T., Fornerod, M., Krijgsveld, J. and van Leeuwen, F. (2008) Nonprocessive methylation by Dot1 leads to functional redundancy of histone H3K79 methylation states. *Nature structural & molecular biology*, **15**, 550-557.
47. Rea, S., Eisenhaber, F., O'Carroll, D., Strahl, B.D., Sun, Z.W., Schmid, M., Opravil, S., Mechtler, K., Ponting, C.P., Allis, C.D. *et al.* (2000) Regulation of chromatin structure by site-specific histone H3 methyltransferases. *Nature*, **406**, 593-599.
48. Tschiersch, B., Hofmann, A., Krauss, V., Dorn, R., Korge, G. and Reuter, G. (1994) The protein encoded by the *Drosophila* position-effect variegation suppressor gene *Su(var)3-9* combines domains of antagonistic regulators of homeotic gene complexes. *The EMBO journal*, **13**, 3822-3831.
49. Jones, R.S. and Gelbart, W.M. (1993) The *Drosophila* Polycomb-group gene Enhancer of zeste contains a region with sequence similarity to trithorax. *Molecular and cellular biology*, **13**, 6357-6366.
50. Stassen, M.J., Bailey, D., Nelson, S., Chinwalla, V. and Harte, P.J. (1995) The *Drosophila* trithorax proteins contain a novel variant of the nuclear receptor type DNA binding domain and an ancient conserved motif found in other chromosomal proteins. *Mechanisms of development*, **52**, 209-223.
51. Dillon, S.C., Zhang, X., Trievel, R.C. and Cheng, X. (2005) The SET-domain protein superfamily: protein lysine methyltransferases. *Genome biology*, **6**, 227.
52. Karytinis, A., Forneris, F., Profumo, A., Ciossani, G., Battaglioli, E., Binda, C. and Mattevi, A. (2009) A novel mammalian flavin-dependent histone demethylase. *The Journal of biological chemistry*, **284**, 17775-17782.
53. Tsukada, Y., Fang, J., Erdjument-Bromage, H., Warren, M.E., Borchers, C.H., Tempst, P. and Zhang, Y. (2006) Histone demethylation by a family of JmjC domain-containing proteins. *Nature*, **439**, 811-816.
54. Nottke, A., Colaiacovo, M.P. and Shi, Y. (2009) Developmental roles of the histone lysine demethylases. *Development*, **136**, 879-889.
55. Kim, J., Daniel, J., Espejo, A., Lake, A., Krishna, M., Xia, L., Zhang, Y. and Bedford, M.T. (2006) Tudor, MBT and chromo domains gauge the degree of lysine methylation. *EMBO reports*, **7**, 397-403.
56. Yun, M., Wu, J., Workman, J.L. and Li, B. (2011) Readers of histone modifications. *Cell research*, **21**, 564-578.
57. Collins, R.E., Northrop, J.P., Horton, J.R., Lee, D.Y., Zhang, X., Stallcup, M.R. and Cheng, X. (2008) The ankyrin repeats of G9a and GLP histone methyltransferases are mono- and dimethyllysine binding modules. *Nature structural & molecular biology*, **15**, 245-250.
58. Jacobs, S.A. and Khorasanizadeh, S. (2002) Structure of HP1 chromodomain bound to a lysine 9-methylated histone H3 tail. *Science*, **295**, 2080-2083.
59. Al-Sady, B., Madhani, H.D. and Narlikar, G.J. (2013) Division of labor between the chromodomains of HP1 and Suv39 methylase enables coordination of heterochromatin spread. *Molecular cell*, **51**, 80-91.
60. Fischle, W., Wang, Y., Jacobs, S.A., Kim, Y., Allis, C.D. and Khorasanizadeh, S. (2003) Molecular basis for the discrimination of repressive methyl-lysine marks in histone H3 by Polycomb and HP1 chromodomains. *Genes & development*, **17**, 1870-1881.
61. Black, J.C., Van Rechem, C. and Whetstine, J.R. (2012) Histone lysine methylation dynamics: establishment, regulation, and biological impact. *Molecular cell*, **48**, 491-507.

62. Trojer, P. and Reinberg, D. (2007) Facultative heterochromatin: is there a distinctive molecular signature? *Molecular cell*, **28**, 1-13.
63. Santaguida, S. and Musacchio, A. (2009) The life and miracles of kinetochores. *The EMBO journal*, **28**, 2511-2531.
64. Regnier, V., Vagnarelli, P., Fukagawa, T., Zerjal, T., Burns, E., Trouche, D., Earnshaw, W. and Brown, W. (2005) CENP-A is required for accurate chromosome segregation and sustained kinetochore association of BubR1. *Molecular and cellular biology*, **25**, 3967-3981.
65. Allshire, R.C. and Karpen, G.H. (2008) Epigenetic regulation of centromeric chromatin: old dogs, new tricks? *Nature reviews. Genetics*, **9**, 923-937.
66. Sullivan, B.A. and Karpen, G.H. (2004) Centromeric chromatin exhibits a histone modification pattern that is distinct from both euchromatin and heterochromatin. *Nature structural & molecular biology*, **11**, 1076-1083.
67. Grewal, S.I. and Elgin, S.C. (2007) Transcription and RNA interference in the formation of heterochromatin. *Nature*, **447**, 399-406.
68. Schotta, G., Lachner, M., Sarma, K., Ebert, A., Sengupta, R., Reuter, G., Reinberg, D. and Jenuwein, T. (2004) A silencing pathway to induce H3-K9 and H4-K20 trimethylation at constitutive heterochromatin. *Genes & development*, **18**, 1251-1262.
69. Dambacher, S., Hahn, M. and Schotta, G. (2013) The compact view on heterochromatin. *Cell cycle*, **12**, 2925-2926.
70. Nagano, T., Mitchell, J.A., Sanz, L.A., Pauler, F.M., Ferguson-Smith, A.C., Feil, R. and Fraser, P. (2008) The Air noncoding RNA epigenetically silences transcription by targeting G9a to chromatin. *Science*, **322**, 1717-1720.
71. Bulut-Karslioglu, A., Perrera, V., Scaranaro, M., de la Rosa-Velazquez, I.A., van de Nobelen, S., Shukeir, N., Popow, J., Gerle, B., Opravil, S., Pagani, M. *et al.* (2012) A transcription factor-based mechanism for mouse heterochromatin formation. *Nature structural & molecular biology*, **19**, 1023-1030.
72. Loyola, A., Tagami, H., Bonaldi, T., Roche, D., Quivy, J.P., Imhof, A., Nakatani, Y., Dent, S.Y. and Almouzni, G. (2009) The HP1alpha-CAF1-SetDB1-containing complex provides H3K9me1 for Suv39-mediated K9me3 in pericentric heterochromatin. *EMBO reports*, **10**, 769-775.
73. Pinheiro, I., Margueron, R., Shukeir, N., Eisold, M., Fritzsche, C., Richter, F.M., Mittler, G., Genoud, C., Goyama, S., Kurokawa, M. *et al.* (2012) Prdm3 and Prdm16 are H3K9me1 methyltransferases required for mammalian heterochromatin integrity. *Cell*, **150**, 948-960.
74. Lachner, M., O'Carroll, D., Rea, S., Mechtler, K. and Jenuwein, T. (2001) Methylation of histone H3 lysine 9 creates a binding site for HP1 proteins. *Nature*, **410**, 116-120.
75. Richart, A.N., Brunner, C.I., Stott, K., Murzina, N.V. and Thomas, J.O. (2012) Characterization of chromoshadow domain-mediated binding of heterochromatin protein 1alpha (HP1alpha) to histone H3. *The Journal of biological chemistry*, **287**, 18730-18737.
76. Nielsen, A.L., Oulad-Abdelghani, M., Ortiz, J.A., Remboutsika, E., Chambon, P. and Losson, R. (2001) Heterochromatin formation in mammalian cells: interaction between histones and HP1 proteins. *Molecular cell*, **7**, 729-739.
77. Lehnertz, B., Ueda, Y., Derijck, A.A., Braunschweig, U., Perez-Burgos, L., Kubicek, S., Chen, T., Li, E., Jenuwein, T. and Peters, A.H. (2003) Suv39h-mediated histone H3 lysine 9 methylation directs DNA methylation to major satellite repeats at pericentric heterochromatin. *Current biology : CB*, **13**, 1192-1200.
78. Hahn, M., Dambacher, S., Dulev, S., Kuznetsova, A.Y., Eck, S., Worz, S., Sadic, D., Schulte, M., Mallm, J.P., Maiser, A. *et al.* (2013) Suv4-20h2 mediates chromatin compaction and is important for cohesin recruitment to heterochromatin. *Genes & development*, **27**, 859-872.
79. Clarke, A. and Orr-Weaver, T.L. (2006) Sister chromatid cohesion at the centromere: confrontation between kinases and phosphatases? *Developmental cell*, **10**, 544-547.
80. Ishiguro, K. and Watanabe, Y. (2007) Chromosome cohesion in mitosis and meiosis. *Journal of cell science*, **120**, 367-369.
81. Lo, W.S., Trievel, R.C., Rojas, J.R., Duggan, L., Hsu, J.Y., Allis, C.D., Marmorstein, R. and Berger, S.L. (2000) Phosphorylation of serine 10 in histone H3 is functionally linked in vitro and in vivo to Gcn5-mediated acetylation at lysine 14. *Molecular cell*, **5**, 917-926.

82. Zhong, S., Goto, H., Inagaki, M. and Dong, Z. (2003) Phosphorylation at serine 28 and acetylation at lysine 9 of histone H3 induced by trichostatin A. *Oncogene*, **22**, 5291-5297.
83. Lau, P.N. and Cheung, P. (2011) Histone code pathway involving H3 S28 phosphorylation and K27 acetylation activates transcription and antagonizes polycomb silencing. *Proceedings of the National Academy of Sciences of the United States of America*, **108**, 2801-2806.
84. Gehani, S.S., Agrawal-Singh, S., Dietrich, N., Christophersen, N.S., Helin, K. and Hansen, K. (2010) Polycomb group protein displacement and gene activation through MSK-dependent H3K27me3S28 phosphorylation. *Molecular cell*, **39**, 886-900.
85. Metzger, E., Yin, N., Wissmann, M., Kunowska, N., Fischer, K., Friedrichs, N., Patnaik, D., Higgins, J.M., Potier, N., Scheidtmann, K.H. *et al.* (2008) Phosphorylation of histone H3 at threonine 11 establishes a novel chromatin mark for transcriptional regulation. *Nature cell biology*, **10**, 53-60.
86. Metzger, E., Imhof, A., Patel, D., Kahl, P., Hoffmeyer, K., Friedrichs, N., Muller, J.M., Greschik, H., Kirfel, J., Ji, S. *et al.* (2010) Phosphorylation of histone H3T6 by PKCbeta(I) controls demethylation at histone H3K4. *Nature*, **464**, 792-796.
87. Johansen, K.M. and Johansen, J. (2006) Regulation of chromatin structure by histone H3S10 phosphorylation. *Chromosome research : an international journal on the molecular, supramolecular and evolutionary aspects of chromosome biology*, **14**, 393-404.
88. Kim, J.Y., Kim, K.B., Son, H.J., Chae, Y.C., Oh, S.T., Kim, D.W., Pak, J.H. and Seo, S.B. (2012) H3K27 methylation and H3S28 phosphorylation-dependent transcriptional regulation by INHAT subunit SET/TAF-Ibeta. *FEBS letters*, **586**, 3159-3165.
89. Wei, Y., Mizzen, C.A., Cook, R.G., Gorovsky, M.A. and Allis, C.D. (1998) Phosphorylation of histone H3 at serine 10 is correlated with chromosome condensation during mitosis and meiosis in Tetrahymena. *Proceedings of the National Academy of Sciences of the United States of America*, **95**, 7480-7484.
90. Fischle, W., Tseng, B.S., Dormann, H.L., Ueberheide, B.M., Garcia, B.A., Shabanowitz, J., Hunt, D.F., Funabiki, H. and Allis, C.D. (2005) Regulation of HP1-chromatin binding by histone H3 methylation and phosphorylation. *Nature*, **438**, 1116-1122.
91. Dai, J., Sultan, S., Taylor, S.S. and Higgins, J.M. (2005) The kinase haspin is required for mitotic histone H3 Thr 3 phosphorylation and normal metaphase chromosome alignment. *Genes & development*, **19**, 472-488.
92. Winter, S., Simboeck, E., Fischle, W., Zupkovitz, G., Dohnal, I., Mechtler, K., Ammerer, G. and Seiser, C. (2008) 14-3-3 proteins recognize a histone code at histone H3 and are required for transcriptional activation. *The EMBO journal*, **27**, 88-99.
93. Jeyaprakash, A.A., Basquin, C., Jayachandran, U. and Conti, E. (2011) Structural basis for the recognition of phosphorylated histone h3 by the survivin subunit of the chromosomal passenger complex. *Structure*, **19**, 1625-1634.
94. Hansen, J.C. (2002) Conformational dynamics of the chromatin fiber in solution: determinants, mechanisms, and functions. *Annual review of biophysics and biomolecular structure*, **31**, 361-392.
95. Freitas, M.A., Sklenar, A.R. and Parthun, M.R. (2004) Application of mass spectrometry to the identification and quantification of histone post-translational modifications. *Journal of cellular biochemistry*, **92**, 691-700.
96. North, J.A., Shimko, J.C., Javaid, S., Mooney, A.M., Shoffner, M.A., Rose, S.D., Bundschuh, R., Fishel, R., Ottesen, J.J. and Poirier, M.G. (2012) Regulation of the nucleosome unwrapping rate controls DNA accessibility. *Nucleic acids research*, **40**, 10215-10227.
97. Xu, F., Zhang, K. and Grunstein, M. (2005) Acetylation in histone H3 globular domain regulates gene expression in yeast. *Cell*, **121**, 375-385.
98. Li, Q., Zhou, H., Wurtele, H., Davies, B., Horazdovsky, B., Verreault, A. and Zhang, Z. (2008) Acetylation of histone H3 lysine 56 regulates replication-coupled nucleosome assembly. *Cell*, **134**, 244-255.
99. Xie, W., Song, C., Young, N.L., Sperling, A.S., Xu, F., Sridharan, R., Conway, A.E., Garcia, B.A., Plath, K., Clark, A.T. *et al.* (2009) Histone h3 lysine 56 acetylation is linked to the core transcriptional network in human embryonic stem cells. *Molecular cell*, **33**, 417-427.

100. Yu, Y., Song, C., Zhang, Q., DiMaggio, P.A., Garcia, B.A., York, A., Carey, M.F. and Grunstein, M. (2012) Histone H3 lysine 56 methylation regulates DNA replication through its interaction with PCNA. *Molecular cell*, **46**, 7-17.
101. Jack, A.P., Bussemer, S., Hahn, M., Punzeler, S., Snyder, M., Wells, M., Csankovszki, G., Solovei, I., Schotta, G. and Hake, S.B. (2013) H3K56me3 is a novel, conserved heterochromatic mark that largely but not completely overlaps with H3K9me3 in both regulation and localization. *PLoS one*, **8**, e51765.
102. Davey, C.A., Sargent, D.F., Luger, K., Maeder, A.W. and Richmond, T.J. (2002) Solvent mediated interactions in the structure of the nucleosome core particle at 1.9 Å resolution. *Journal of molecular biology*, **319**, 1097-1113.
103. Neumann, H., Hancock, S.M., Buning, R., Routh, A., Chapman, L., Somers, J., Owen-Hughes, T., van Noort, J., Rhodes, D. and Chin, J.W. (2009) A method for genetically installing site-specific acetylation in recombinant histones defines the effects of H3 K56 acetylation. *Molecular cell*, **36**, 153-163.
104. Watanabe, S., Resch, M., Lilyestrom, W., Clark, N., Hansen, J.C., Peterson, C. and Luger, K. (2010) Structural characterization of H3K56Q nucleosomes and nucleosomal arrays. *Biochimica et biophysica acta*, **1799**, 480-486.
105. Suto, R.K., Edayathumangalam, R.S., White, C.L., Melander, C., Gottesfeld, J.M., Dervan, P.B. and Luger, K. (2003) Crystal structures of nucleosome core particles in complex with minor groove DNA-binding ligands. *Journal of molecular biology*, **326**, 371-380.
106. Hall, M.A., Shundrovsky, A., Bai, L., Fulbright, R.M., Lis, J.T. and Wang, M.D. (2009) High-resolution dynamic mapping of histone-DNA interactions in a nucleosome. *Nature structural & molecular biology*, **16**, 124-129.
107. Shimko, J.C., North, J.A., Bruns, A.N., Poirier, M.G. and Ottesen, J.J. (2011) Preparation of fully synthetic histone H3 reveals that acetyl-lysine 56 facilitates protein binding within nucleosomes. *Journal of molecular biology*, **408**, 187-204.
108. Simon, M., North, J.A., Shimko, J.C., Forties, R.A., Ferdinand, M.B., Manohar, M., Zhang, M., Fishel, R., Ottesen, J.J. and Poirier, M.G. (2011) Histone fold modifications control nucleosome unwrapping and disassembly. *Proceedings of the National Academy of Sciences of the United States of America*, **108**, 12711-12716.
109. Bowman, A., Ward, R., El-Mkami, H., Owen-Hughes, T. and Norman, D.G. (2010) Probing the (H3-H4)<sub>2</sub> histone tetramer structure using pulsed EPR spectroscopy combined with site-directed spin labelling. *Nucleic acids research*, **38**, 695-707.
110. Schneider, J., Bajwa, P., Johnson, F.C., Bhaumik, S.R. and Shilatifard, A. (2006) Rtt109 is required for proper H3K56 acetylation: a chromatin mark associated with the elongating RNA polymerase II. *The Journal of biological chemistry*, **281**, 37270-37274.
111. Das, C., Lucia, M.S., Hansen, K.C. and Tyler, J.K. (2009) CBP/p300-mediated acetylation of histone H3 on lysine 56. *Nature*, **459**, 113-117.
112. Tjeertes, J.V., Miller, K.M. and Jackson, S.P. (2009) Screen for DNA-damage-responsive histone modifications identifies H3K9Ac and H3K56Ac in human cells. *The EMBO journal*, **28**, 1878-1889.
113. Zhang, L., Eugeni, E.E., Parthun, M.R. and Freitas, M.A. (2003) Identification of novel histone post-translational modifications by peptide mass fingerprinting. *Chromosoma*, **112**, 77-86.
114. Garcia, B.A., Hake, S.B., Diaz, R.L., Kauer, M., Morris, S.A., Recht, J., Shabanowitz, J., Mishra, N., Strahl, B.D., Allis, C.D. *et al.* (2007) Organismal differences in post-translational modifications in histones H3 and H4. *The Journal of biological chemistry*, **282**, 7641-7655.
115. Aslam, A. and Logie, C. (2010) Histone H3 serine 57 and lysine 56 interplay in transcription elongation and recovery from S-phase stress. *PLoS one*, **5**, e10851.
116. Fischle, W., Wang, Y. and Allis, C.D. (2003) Binary switches and modification cassettes in histone biology and beyond. *Nature*, **425**, 475-479.
117. Tropberger, P., Pott, S., Keller, C., Kamieniarsz-Gdula, K., Caron, M., Richter, F., Li, G., Mittler, G., Liu, E.T., Buhler, M. *et al.* (2013) Regulation of transcription through acetylation of H3K122 on the lateral surface of the histone octamer. *Cell*, **152**, 859-872.
118. Iwasaki, W., Tachiwana, H., Kawaguchi, K., Shibata, T., Kagawa, W. and Kurumizaka, H. (2011) Comprehensive structural analysis of mutant nucleosomes containing lysine to

- glutamine (KQ) substitutions in the H3 and H4 histone-fold domains. *Biochemistry*, **50**, 7822-7832.
119. Manohar, M., Mooney, A.M., North, J.A., Nakkula, R.J., Picking, J.W., Edon, A., Fishel, R., Poirier, M.G. and Ottesen, J.J. (2009) Acetylation of histone H3 at the nucleosome dyad alters DNA-histone binding. *The Journal of biological chemistry*, **284**, 23312-23321.
  120. Muthurajan, U.M., Park, Y.J., Edayathumangalam, R.S., Suto, R.K., Chakravarthy, S., Dyer, P.N. and Luger, K. (2003) Structure and dynamics of nucleosomal DNA. *Biopolymers*, **68**, 547-556.
  121. Flaus, A. and Owen-Hughes, T. (2003) Dynamic properties of nucleosomes during thermal and ATP-driven mobilization. *Molecular and cellular biology*, **23**, 7767-7779.
  122. Bohm, V., Hieb, A.R., Andrews, A.J., Gansen, A., Rocker, A., Toth, K., Luger, K. and Langowski, J. (2011) Nucleosome accessibility governed by the dimer/tetramer interface. *Nucleic acids research*, **39**, 3093-3102.
  123. Kruger, W., Peterson, C.L., Sil, A., Coburn, C., Arents, G., Moudrianakis, E.N. and Herskowitz, I. (1995) Amino acid substitutions in the structured domains of histones H3 and H4 partially relieve the requirement of the yeast SWI/SNF complex for transcription. *Genes & development*, **9**, 2770-2779.
  124. Kumar, A., Kashyap, M., Bhavesh, N.S., Yogavel, M. and Sharma, A. (2012) Structural delineation of histone post-translation modifications in histone-nucleosome assembly protein complex. *Journal of structural biology*, **180**, 1-9.
  125. Park, J.H., Cosgrove, M.S., Youngman, E., Wolberger, C. and Boeke, J.D. (2002) A core nucleosome surface crucial for transcriptional silencing. *Nature genetics*, **32**, 273-279.
  126. Thompson, J.S., Snow, M.L., Giles, S., McPherson, L.E. and Grunstein, M. (2003) Identification of a functional domain within the essential core of histone H3 that is required for telomeric and HM silencing in *Saccharomyces cerevisiae*. *Genetics*, **163**, 447-452.
  127. Lacoste, N., Utley, R.T., Hunter, J.M., Poirier, G.G. and Cote, J. (2002) Disruptor of telomeric silencing-1 is a chromatin-specific histone H3 methyltransferase. *The Journal of biological chemistry*, **277**, 30421-30424.
  128. van Leeuwen, F., Gafken, P.R. and Gottschling, D.E. (2002) Dot1p modulates silencing in yeast by methylation of the nucleosome core. *Cell*, **109**, 745-756.
  129. Singer, M.S., Kahana, A., Wolf, A.J., Meisinger, L.L., Peterson, S.E., Goggin, C., Mahowald, M. and Gottschling, D.E. (1998) Identification of high-copy disruptors of telomeric silencing in *Saccharomyces cerevisiae*. *Genetics*, **150**, 613-632.
  130. Janzen, C.J., Hake, S.B., Lowell, J.E. and Cross, G.A. (2006) Selective di- or trimethylation of histone H3 lysine 76 by two DOT1 homologs is important for cell cycle regulation in *Trypanosoma brucei*. *Molecular cell*, **23**, 497-507.
  131. Fingerman, I.M., Li, H.C. and Briggs, S.D. (2007) A charge-based interaction between histone H4 and Dot1 is required for H3K79 methylation and telomere silencing: identification of a new trans-histone pathway. *Genes & development*, **21**, 2018-2029.
  132. Altaf, M., Utley, R.T., Lacoste, N., Tan, S., Briggs, S.D. and Cote, J. (2007) Interplay of chromatin modifiers on a short basic patch of histone H4 tail defines the boundary of telomeric heterochromatin. *Molecular cell*, **28**, 1002-1014.
  133. Dover, J., Schneider, J., Tawiah-Boateng, M.A., Wood, A., Dean, K., Johnston, M. and Shilatifard, A. (2002) Methylation of histone H3 by COMPASS requires ubiquitination of histone H2B by Rad6. *The Journal of biological chemistry*, **277**, 28368-28371.
  134. Shilatifard, A. (2006) Chromatin modifications by methylation and ubiquitination: implications in the regulation of gene expression. *Annual review of biochemistry*, **75**, 243-269.
  135. Lee, J.S., Shukla, A., Schneider, J., Swanson, S.K., Washburn, M.P., Florens, L., Bhaumik, S.R. and Shilatifard, A. (2007) Histone crosstalk between H2B monoubiquitination and H3 methylation mediated by COMPASS. *Cell*, **131**, 1084-1096.
  136. McGinty, R.K., Kim, J., Chatterjee, C., Roeder, R.G. and Muir, T.W. (2008) Chemically ubiquitylated histone H2B stimulates hDot1L-mediated intranucleosomal methylation. *Nature*, **453**, 812-816.
  137. Nguyen, A.T. and Zhang, Y. (2011) The diverse functions of Dot1 and H3K79 methylation. *Genes & development*, **25**, 1345-1358.

138. Bheda, P., Swatkoski, S., Fiedler, K.L., Boeke, J.D., Cotter, R.J. and Wolberger, C. (2012) Biotinylation of lysine method identifies acetylated histone H3 lysine 79 in *Saccharomyces cerevisiae* as a substrate for Sir2. *Proceedings of the National Academy of Sciences of the United States of America*, **109**, E916-925.
139. Daujat, S., Weiss, T., Mohn, F., Lange, U.C., Ziegler-Birling, C., Zeissler, U., Lappe, M., Schubeler, D., Torres-Padilla, M.E. and Schneider, R. (2009) H3K64 trimethylation marks heterochromatin and is dynamically remodeled during developmental reprogramming. *Nature structural & molecular biology*, **16**, 777-781.
140. Di Cerbo, V., Mohn, F., Ryan, D.P., Montellier, E., Kacem, S., Tropberger, P., Kallis, E., Holzner, M., Hoerner, L., Feldmann, A. *et al.* (2014) Acetylation of histone H3 at lysine 64 regulates nucleosome dynamics and facilitates transcription. *eLife*, **3**, e01632.
141. Ku, M., Jaffe, J.D., Koche, R.P., Rheinbay, E., Endoh, M., Koseki, H., Carr, S.A. and Bernstein, B.E. (2012) H2A.Z landscapes and dual modifications in pluripotent and multipotent stem cells underlie complex genome regulatory functions. *Genome biology*, **13**, R85.
142. Pichler, G., Jack, A., Wolf, P. and Hake, S.B. (2012) Versatile toolbox for high throughput biochemical and functional studies with fluorescent fusion proteins. *PloS one*, **7**, e36967.
143. Talbert, P.B. and Henikoff, S. (2010) Histone variants--ancient wrap artists of the epigenome. *Nature reviews. Molecular cell biology*, **11**, 264-275.
144. Watanabe, S., Radman-Livaja, M., Rando, O.J. and Peterson, C.L. (2013) A histone acetylation switch regulates H2A.Z deposition by the SWR-C remodeling enzyme. *Science*, **340**, 195-199.
145. Chin, H.G., Pradhan, M., Esteve, P.O., Patnaik, D., Evans, T.C., Jr. and Pradhan, S. (2005) Sequence specificity and role of proximal amino acids of the histone H3 tail on catalysis of murine G9A lysine 9 histone H3 methyltransferase. *Biochemistry*, **44**, 12998-13006.
146. Rathert, P., Dhayalan, A., Murakami, M., Zhang, X., Tamas, R., Jurkowska, R., Komatsu, Y., Shinkai, Y., Cheng, X. and Jeltsch, A. (2008) Protein lysine methyltransferase G9a acts on non-histone targets. *Nature chemical biology*, **4**, 344-346.
147. Tachibana, M., Sugimoto, K., Fukushima, T. and Shinkai, Y. (2001) Set domain-containing protein, G9a, is a novel lysine-preferring mammalian histone methyltransferase with hyperactivity and specific selectivity to lysines 9 and 27 of histone H3. *The Journal of biological chemistry*, **276**, 25309-25317.
148. Trojer, P., Zhang, J., Yonezawa, M., Schmidt, A., Zheng, H., Jenuwein, T. and Reinberg, D. (2009) Dynamic Histone H1 Isoform 4 Methylation and Demethylation by Histone Lysine Methyltransferase G9a/KMT1C and the Jumonji Domain-containing JMJD2/KDM4 Proteins. *The Journal of biological chemistry*, **284**, 8395-8405.
149. Weiss, T., Hergeth, S., Zeissler, U., Izzo, A., Tropberger, P., Zee, B.M., Dunder, M., Garcia, B.A., Daujat, S. and Schneider, R. (2010) Histone H1 variant-specific lysine methylation by G9a/KMT1C and Glp1/KMT1D. *Epigenetics & chromatin*, **3**, 7.
150. Krishnan, S., Horowitz, S. and Trievel, R.C. (2011) Structure and function of histone H3 lysine 9 methyltransferases and demethylases. *Chembiochem : a European journal of chemical biology*, **12**, 254-263.
151. Wu, H., Min, J., Lunin, V.V., Antoshenko, T., Dombrowski, L., Zeng, H., Allali-Hassani, A., Campagna-Slater, V., Vedadi, M., Arrowsmith, C.H. *et al.* (2010) Structural biology of human H3K9 methyltransferases. *PloS one*, **5**, e8570.
152. Sanli, D., Keskin, O., Gursoy, A. and Erman, B. (2011) Structural cooperativity in histone H3 tail modifications. *Protein science : a publication of the Protein Society*, **20**, 1982-1990.
153. Peters, A.H., O'Carroll, D., Scherthan, H., Mechtler, K., Sauer, S., Schofer, C., Weipoltshammer, K., Pagani, M., Lachner, M., Kohlmaier, A. *et al.* (2001) Loss of the Suv39h histone methyltransferases impairs mammalian heterochromatin and genome stability. *Cell*, **107**, 323-337.
154. Wang, H., An, W., Cao, R., Xia, L., Erdjument-Bromage, H., Chatton, B., Tempst, P., Roeder, R.G. and Zhang, Y. (2003) mAM facilitates conversion by ESET of dimethyl to trimethyl lysine 9 of histone H3 to cause transcriptional repression. *Molecular cell*, **12**, 475-487.

155. Lange, U.C., Siebert, S., Wossidlo, M., Weiss, T., Ziegler-Birling, C., Walter, J., Torres-Padilla, M.E., Daujat, S. and Schneider, R. (2013) Dissecting the role of H3K64me3 in mouse pericentromeric heterochromatin. *Nature communications*, **4**, 2233.
156. Fritsch, L., Robin, P., Mathieu, J.R., Souidi, M., Hinaux, H., Rougeulle, C., Harel-Bellan, A., Ameyar-Zazoua, M. and Ait-Si-Ali, S. (2010) A subset of the histone H3 lysine 9 methyltransferases Suv39h1, G9a, GLP, and SETDB1 participate in a multimeric complex. *Molecular cell*, **37**, 46-56.
157. Tachibana, M., Sugimoto, K., Nozaki, M., Ueda, J., Ohta, T., Ohki, M., Fukuda, M., Takeda, N., Niida, H., Kato, H. *et al.* (2002) G9a histone methyltransferase plays a dominant role in euchromatic histone H3 lysine 9 methylation and is essential for early embryogenesis. *Genes & development*, **16**, 1779-1791.
158. Dong, K.B., Maksakova, I.A., Mohn, F., Leung, D., Appanah, R., Lee, S., Yang, H.W., Lam, L.L., Mager, D.L., Schubeler, D. *et al.* (2008) DNA methylation in ES cells requires the lysine methyltransferase G9a but not its catalytic activity. *The EMBO journal*, **27**, 2691-2701.
159. Kondo, Y., Shen, L., Ahmed, S., Boumber, Y., Sekido, Y., Haddad, B.R. and Issa, J.P. (2008) Downregulation of histone H3 lysine 9 methyltransferase G9a induces centrosome disruption and chromosome instability in cancer cells. *PLoS one*, **3**, e2037.
160. Krishnan, S. and Trievel, R.C. (2013) Structural and functional analysis of JMJD2D reveals molecular basis for site-specific demethylation among JMJD2 demethylases. *Structure*, **21**, 98-108.
161. Banerjee, T. and Chakravarti, D. (2011) A peek into the complex realm of histone phosphorylation. *Molecular and cellular biology*, **31**, 4858-4873.
162. Cowieson, N.P., Partridge, J.F., Allshire, R.C. and McLaughlin, P.J. (2000) Dimerisation of a chromo shadow domain and distinctions from the chromodomain as revealed by structural analysis. *Current biology : CB*, **10**, 517-525.
163. Vempati, R.K., Jayani, R.S., Notani, D., Sengupta, A., Galande, S. and Haldar, D. (2010) p300-mediated acetylation of histone H3 lysine 56 functions in DNA damage response in mammals. *The Journal of biological chemistry*, **285**, 28553-28564.
164. Probst, A.V., Dunleavy, E. and Almouzni, G. (2009) Epigenetic inheritance during the cell cycle. *Nature reviews. Molecular cell biology*, **10**, 192-206.
165. Zhang, Z., Shibahara, K. and Stillman, B. (2000) PCNA connects DNA replication to epigenetic inheritance in yeast. *Nature*, **408**, 221-225.
166. Henderson, D.S., Banga, S.S., Grigliatti, T.A. and Boyd, J.B. (1994) Mutagen sensitivity and suppression of position-effect variegation result from mutations in mus209, the Drosophila gene encoding PCNA. *The EMBO journal*, **13**, 1450-1459.
167. Moldovan, G.L., Pfander, B. and Jentsch, S. (2006) PCNA controls establishment of sister chromatid cohesion during S phase. *Molecular cell*, **23**, 723-732.
168. Bernard, P., Maure, J.F., Partridge, J.F., Genier, S., Javerzat, J.P. and Allshire, R.C. (2001) Requirement of heterochromatin for cohesion at centromeres. *Science*, **294**, 2539-2542.
169. Aagaard, L., Schmid, M., Warburton, P. and Jenuwein, T. (2000) Mitotic phosphorylation of SUV39H1, a novel component of active centromeres, coincides with transient accumulation at mammalian centromeres. *Journal of cell science*, **113 ( Pt 5)**, 817-829.
170. Lee, K.J., Lin, Y.F., Chou, H.Y., Yajima, H., Fattah, K.R., Lee, S.C. and Chen, B.P. (2011) Involvement of DNA-dependent protein kinase in normal cell cycle progression through mitosis. *The Journal of biological chemistry*, **286**, 12796-12802.
171. Smith, G.C. and Jackson, S.P. (1999) The DNA-dependent protein kinase. *Genes & development*, **13**, 916-934.
172. Tanaka, A., Tanizawa, H., Sriswasdi, S., Iwasaki, O., Chatterjee, A.G., Speicher, D.W., Levin, H.L., Noguchi, E. and Noma, K. (2012) Epigenetic regulation of condensin-mediated genome organization during the cell cycle and upon DNA damage through histone H3 lysine 56 acetylation. *Molecular cell*, **48**, 532-546.
173. Dubey, R.N., Nakwal, N., Bisht, K.K., Saini, A., Haldar, S. and Singh, J. (2009) Interaction of APC/C-E3 ligase with Swi6/HP1 and Clr4/Suv39 in heterochromatin assembly in fission yeast. *The Journal of biological chemistry*, **284**, 7165-7176.



174. Gunesdogan, U., Jackle, H. and Herzig, A. (2010) A genetic system to assess in vivo the functions of histones and histone modifications in higher eukaryotes. *EMBO reports*, **11**, 772-776.
175. Peters, A.H., Kubicek, S., Mechtler, K., O'Sullivan, R.J., Derijck, A.A., Perez-Burgos, L., Kohlmaier, A., Opravil, S., Tachibana, M., Shinkai, Y. *et al.* (2003) Partitioning and plasticity of repressive histone methylation states in mammalian chromatin. *Molecular cell*, **12**, 1577-1589.
176. O'Carroll, D., Scherthan, H., Peters, A.H., Opravil, S., Haynes, A.R., Laible, G., Rea, S., Schmid, M., Lebersorger, A., Jerratsch, M. *et al.* (2000) Isolation and characterization of Suv39h2, a second histone H3 methyltransferase gene that displays testis-specific expression. *Molecular and cellular biology*, **20**, 9423-9433.
177. Towbin, B.D., Gonzalez-Aguilera, C., Sack, R., Gaidatzis, D., Kalck, V., Meister, P., Askjaer, P. and Gasser, S.M. (2012) Step-wise methylation of histone H3K9 positions heterochromatin at the nuclear periphery. *Cell*, **150**, 934-947.
178. Kind, J. and van Steensel, B. (2010) Genome-nuclear lamina interactions and gene regulation. *Current opinion in cell biology*, **22**, 320-325.
179. Therizols, P., Fairhead, C., Cabal, G.G., Genovesio, A., Olivo-Marin, J.C., Dujon, B. and Fabre, E. (2006) Telomere tethering at the nuclear periphery is essential for efficient DNA double strand break repair in subtelomeric region. *The Journal of cell biology*, **172**, 189-199.
180. Hiraga, S., Botsios, S. and Donaldson, A.D. (2008) Histone H3 lysine 56 acetylation by Rtt109 is crucial for chromosome positioning. *The Journal of cell biology*, **183**, 641-651.
181. Pokholok, D.K., Harbison, C.T., Levine, S., Cole, M., Hannett, N.M., Lee, T.I., Bell, G.W., Walker, K., Rolfe, P.A., Herbolsheimer, E. *et al.* (2005) Genome-wide map of nucleosome acetylation and methylation in yeast. *Cell*, **122**, 517-527.
182. Li, B., Carey, M. and Workman, J.L. (2007) The role of chromatin during transcription. *Cell*, **128**, 707-719.
183. Luger, K. (2006) Dynamic nucleosomes. *Chromosome research : an international journal on the molecular, supramolecular and evolutionary aspects of chromosome biology*, **14**, 5-16.
184. Williams, S.K., Truong, D. and Tyler, J.K. (2008) Acetylation in the globular core of histone H3 on lysine-56 promotes chromatin disassembly during transcriptional activation. *Proceedings of the National Academy of Sciences of the United States of America*, **105**, 9000-9005.
185. Tan, Y., Xue, Y., Song, C. and Grunstein, M. (2013) Acetylated histone H3K56 interacts with Oct4 to promote mouse embryonic stem cell pluripotency. *Proceedings of the National Academy of Sciences of the United States of America*, **110**, 11493-11498.
186. Lo, K.A., Bauchmann, M.K., Baumann, A.P., Donahue, C.J., Thiede, M.A., Hayes, L.S., des Etages, S.A. and Fraenkel, E. (2011) Genome-wide profiling of H3K56 acetylation and transcription factor binding sites in human adipocytes. *PloS one*, **6**, e19778.
187. Heintzman, N.D., Hon, G.C., Hawkins, R.D., Kheradpour, P., Stark, A., Harp, L.F., Ye, Z., Lee, L.K., Stuart, R.K., Ching, C.W. *et al.* (2009) Histone modifications at human enhancers reflect global cell-type-specific gene expression. *Nature*, **459**, 108-112.
188. He, H.H., Meyer, C.A., Shin, H., Bailey, S.T., Wei, G., Wang, Q., Zhang, Y., Xu, K., Ni, M., Lupien, M. *et al.* (2010) Nucleosome dynamics define transcriptional enhancers. *Nature genetics*, **42**, 343-347.
189. Heintzman, N.D., Stuart, R.K., Hon, G., Fu, Y., Ching, C.W., Hawkins, R.D., Barrera, L.O., Van Calcar, S., Qu, C., Ching, K.A. *et al.* (2007) Distinct and predictive chromatin signatures of transcriptional promoters and enhancers in the human genome. *Nature genetics*, **39**, 311-318.
190. Creyghton, M.P., Cheng, A.W., Welstead, G.G., Kooistra, T., Carey, B.W., Steine, E.J., Hanna, J., Lodato, M.A., Frampton, G.M., Sharp, P.A. *et al.* (2010) Histone H3K27ac separates active from poised enhancers and predicts developmental state. *Proceedings of the National Academy of Sciences of the United States of America*, **107**, 21931-21936.
191. Chen, C.Y., Morris, Q. and Mitchell, J.A. (2012) Enhancer identification in mouse embryonic stem cells using integrative modeling of chromatin and genomic features. *BMC genomics*, **13**, 152.

192. Whyte, W.A., Orlando, D.A., Hnisz, D., Abraham, B.J., Lin, C.Y., Kagey, M.H., Rahl, P.B., Lee, T.I. and Young, R.A. (2013) Master transcription factors and mediator establish super-enhancers at key cell identity genes. *Cell*, **153**, 307-319.
193. Tolhuis, B., Palstra, R.J., Splinter, E., Grosveld, F. and de Laat, W. (2002) Looping and interaction between hypersensitive sites in the active beta-globin locus. *Molecular cell*, **10**, 1453-1465.
194. Schwabish, M.A. and Struhl, K. (2004) Evidence for eviction and rapid deposition of histones upon transcriptional elongation by RNA polymerase II. *Molecular and cellular biology*, **24**, 10111-10117.
195. Rufiange, A., Jacques, P.E., Bhat, W., Robert, F. and Nourani, A. (2007) Genome-wide replication-independent histone H3 exchange occurs predominantly at promoters and implicates H3 K56 acetylation and Asf1. *Molecular cell*, **27**, 393-405.
196. Sekinger, E.A. and Gross, D.S. (1999) SIR repression of a yeast heat shock gene: UAS and TATA footprints persist within heterochromatin. *The EMBO journal*, **18**, 7041-7055.
197. Sekinger, E.A. and Gross, D.S. (2001) Silenced chromatin is permissive to activator binding and PIC recruitment. *Cell*, **105**, 403-414.
198. Varv, S., Kristjuhan, K., Peil, K., Looke, M., Mahlakoiv, T., Paapsi, K. and Kristjuhan, A. (2010) Acetylation of H3 K56 is required for RNA polymerase II transcript elongation through heterochromatin in yeast. *Molecular and cellular biology*, **30**, 1467-1477.
199. Bitoun, E., Oliver, P.L. and Davies, K.E. (2007) The mixed-lineage leukemia fusion partner AF4 stimulates RNA polymerase II transcriptional elongation and mediates coordinated chromatin remodeling. *Human molecular genetics*, **16**, 92-106.
200. Mueller, D., Bach, C., Zeisig, D., Garcia-Cuellar, M.P., Monroe, S., Sreekumar, A., Zhou, R., Nesvizhskii, A., Chinnaiyan, A., Hess, J.L. *et al.* (2007) A role for the MLL fusion partner ENL in transcriptional elongation and chromatin modification. *Blood*, **110**, 4445-4454.
201. Wang, Z., Zang, C., Rosenfeld, J.A., Schones, D.E., Barski, A., Cuddapah, S., Cui, K., Roh, T.Y., Peng, W., Zhang, M.Q. *et al.* (2008) Combinatorial patterns of histone acetylations and methylations in the human genome. *Nature genetics*, **40**, 897-903.
202. Steger, D.J., Lefterova, M.I., Ying, L., Stonestrom, A.J., Schupp, M., Zhuo, D., Vakoc, A.L., Kim, J.E., Chen, J., Lazar, M.A. *et al.* (2008) DOT1L/KMT4 recruitment and H3K79 methylation are ubiquitously coupled with gene transcription in mammalian cells. *Molecular and cellular biology*, **28**, 2825-2839.
203. Kim, S.K., Jung, I., Lee, H., Kang, K., Kim, M., Jeong, K., Kwon, C.S., Han, Y.M., Kim, Y.S., Kim, D. *et al.* (2012) Human histone H3K79 methyltransferase DOT1L protein [corrected] binds actively transcribing RNA polymerase II to regulate gene expression. *The Journal of biological chemistry*, **287**, 39698-39709.
204. Stulemeijer, I.J., Pike, B.L., Faber, A.W., Verzijlbergen, K.F., van Welsem, T., Frederiks, F., Lenstra, T.L., Holstege, F.C., Gasser, S.M. and van Leeuwen, F. (2011) Dot1 binding induces chromatin rearrangements by histone methylation-dependent and -independent mechanisms. *Epigenetics & chromatin*, **4**, 2.
205. Ooga, M., Suzuki, M.G. and Aoki, F. (2013) Involvement of DOT1L in the remodeling of heterochromatin configuration during early preimplantation development in mice. *Biology of reproduction*, **89**, 145.
206. Schulze, J.M., Jackson, J., Nakanishi, S., Gardner, J.M., Hentrich, T., Haug, J., Johnston, M., Jaspersen, S.L., Kobor, M.S. and Shilatifard, A. (2009) Linking cell cycle to histone modifications: SBF and H2B monoubiquitination machinery and cell-cycle regulation of H3K79 dimethylation. *Molecular cell*, **35**, 626-641.
207. Cecere, G., Hoersch, S., Jensen, M.B., Dixit, S. and Grishok, A. (2013) The ZFP-1(AF10)/DOT-1 complex opposes H2B ubiquitination to reduce Pol II transcription. *Molecular cell*, **50**, 894-907.
208. Schulze, J.M., Hentrich, T., Nakanishi, S., Gupta, A., Emberly, E., Shilatifard, A. and Kobor, M.S. (2011) Splitting the task: Ubp8 and Ubp10 deubiquitinate different cellular pools of H2BK123. *Genes & development*, **25**, 2242-2247.
209. Feng, Q., Wang, H., Ng, H.H., Erdjument-Bromage, H., Tempst, P., Struhl, K. and Zhang, Y. (2002) Methylation of H3-lysine 79 is mediated by a new family of HMTases without a SET domain. *Current biology : CB*, **12**, 1052-1058.

210. Jones, B., Su, H., Bhat, A., Lei, H., Bajko, J., Hevi, S., Baltus, G.A., Kadam, S., Zhai, H., Valdez, R. *et al.* (2008) The histone H3K79 methyltransferase Dot1L is essential for mammalian development and heterochromatin structure. *PLoS genetics*, **4**, e1000190.
211. Harrison, P.M., Kumar, A., Lang, N., Snyder, M. and Gerstein, M. (2002) A question of size: the eukaryotic proteome and the problems in defining it. *Nucleic acids research*, **30**, 1083-1090.
212. Barski, A., Cuddapah, S., Cui, K., Roh, T.Y., Schones, D.E., Wang, Z., Wei, G., Chepelev, I. and Zhao, K. (2007) High-resolution profiling of histone methylations in the human genome. *Cell*, **129**, 823-837.
213. Zhang, W., Xia, X., Reisenauer, M.R., Hemenway, C.S. and Kone, B.C. (2006) Dot1a-AF9 complex mediates histone H3 Lys-79 hypermethylation and repression of ENaC $\alpha$  in an aldosterone-sensitive manner. *The Journal of biological chemistry*, **281**, 18059-18068.
214. Buttner, N., Johnsen, S.A., Kugler, S. and Vogel, T. (2010) Af9/Mllt3 interferes with Tbr1 expression through epigenetic modification of histone H3K79 during development of the cerebral cortex. *Proceedings of the National Academy of Sciences of the United States of America*, **107**, 7042-7047.
215. Schubeler, D., MacAlpine, D.M., Scalzo, D., Wirbelauer, C., Kooperberg, C., van Leeuwen, F., Gottschling, D.E., O'Neill, L.P., Turner, B.M., Delrow, J. *et al.* (2004) The histone modification pattern of active genes revealed through genome-wide chromatin analysis of a higher eukaryote. *Genes & development*, **18**, 1263-1271.
216. Vakoc, C.R., Sachdeva, M.M., Wang, H. and Blobel, G.A. (2006) Profile of histone lysine methylation across transcribed mammalian chromatin. *Molecular and cellular biology*, **26**, 9185-9195.
217. Shahbazian, M.D., Zhang, K. and Grunstein, M. (2005) Histone H2B ubiquitylation controls processive methylation but not monomethylation by Dot1 and Set1. *Molecular cell*, **19**, 271-277.
218. Liu, T., Rechtsteiner, A., Egelhofer, T.A., Vielle, A., Latorre, I., Cheung, M.S., Ercan, S., Ikegami, K., Jensen, M., Kolasinska-Zwierz, P. *et al.* (2011) Broad chromosomal domains of histone modification patterns in *C. elegans*. *Genome research*, **21**, 227-236.
219. Ho, L.L., Sinha, A., Verzi, M., Bernt, K.M., Armstrong, S.A. and Shivdasani, R.A. (2013) DOT1L-mediated H3K79 methylation in chromatin is dispensable for Wnt pathway-specific and other intestinal epithelial functions. *Molecular and cellular biology*, **33**, 1735-1745.
220. Bentley, D.L. and Groudine, M. (1986) A block to elongation is largely responsible for decreased transcription of c-myc in differentiated HL60 cells. *Nature*, **321**, 702-706.
221. Gilmour, D.S. and Lis, J.T. (1986) RNA polymerase II interacts with the promoter region of the noninduced hsp70 gene in *Drosophila melanogaster* cells. *Molecular and cellular biology*, **6**, 3984-3989.
222. Blackburn, E.H. (1991) Structure and function of telomeres. *Nature*, **350**, 569-573.
223. Westhorpe, F.G. and Straight, A.F. (2013) Functions of the centromere and kinetochore in chromosome segregation. *Current opinion in cell biology*, **25**, 334-340.
224. Grewal, S.I. and Jia, S. (2007) Heterochromatin revisited. *Nature reviews. Genetics*, **8**, 35-46.
225. Lee, J.Y. and Lee, T.H. (2012) Effects of DNA methylation on the structure of nucleosomes. *Journal of the American Chemical Society*, **134**, 173-175.
226. Henikoff, S. (1990) Position-effect variegation after 60 years. *Trends in genetics : TIG*, **6**, 422-426.
227. Ng, H.H., Feng, Q., Wang, H., Erdjument-Bromage, H., Tempst, P., Zhang, Y. and Struhl, K. (2002) Lysine methylation within the globular domain of histone H3 by Dot1 is important for telomeric silencing and Sir protein association. *Genes & development*, **16**, 1518-1527.
228. Rossmann, M.P., Luo, W., Tsaponina, O., Chabes, A. and Stillman, B. (2011) A common telomeric gene silencing assay is affected by nucleotide metabolism. *Molecular cell*, **42**, 127-136.
229. Takahashi, Y.H., Schulze, J.M., Jackson, J., Hentrich, T., Seidel, C., Jaspersen, S.L., Kobar, M.S. and Shilatifard, A. (2011) Dot1 and histone H3K79 methylation in natural telomeric and HM silencing. *Molecular cell*, **42**, 118-126.
230. van Welsem, T., Frederiks, F., Verzijlbergen, K.F., Faber, A.W., Nelson, Z.W., Egan, D.A., Gottschling, D.E. and van Leeuwen, F. (2008) Synthetic lethal screens identify gene silencing

- processes in yeast and implicate the acetylated amino terminus of Sir3 in recognition of the nucleosome core. *Molecular and cellular biology*, **28**, 3861-3872.
231. Moretti, P., Freeman, K., Coodly, L. and Shore, D. (1994) Evidence that a complex of SIR proteins interacts with the silencer and telomere-binding protein RAP1. *Genes & development*, **8**, 2257-2269.
232. Luo, K., Vega-Palas, M.A. and Grunstein, M. (2002) Rap1-Sir4 binding independent of other Sir, yKu, or histone interactions initiates the assembly of telomeric heterochromatin in yeast. *Genes & development*, **16**, 1528-1539.
233. Aparicio, O.M., Billington, B.L. and Gottschling, D.E. (1991) Modifiers of position effect are shared between telomeric and silent mating-type loci in *S. cerevisiae*. *Cell*, **66**, 1279-1287.
234. Ehrentraut, S., Hassler, M., Oppikofer, M., Kueng, S., Weber, J.M., Mueller, J.W., Gasser, S.M., Ladurner, A.G. and Ehrenhofer-Murray, A.E. (2011) Structural basis for the role of the Sir3 AAA+ domain in silencing: interaction with Sir4 and unmethylated histone H3K79. *Genes & development*, **25**, 1835-1846.
235. Armache, K.J., Garlick, J.D., Canzio, D., Narlikar, G.J. and Kingston, R.E. (2011) Structural basis of silencing: Sir3 BAH domain in complex with a nucleosome at 3.0 Å resolution. *Science*, **334**, 977-982.
236. Ng, H.H., Ciccone, D.N., Morshead, K.B., Oettinger, M.A. and Struhl, K. (2003) Lysine-79 of histone H3 is hypomethylated at silenced loci in yeast and mammalian cells: a potential mechanism for position-effect variegation. *Proceedings of the National Academy of Sciences of the United States of America*, **100**, 1820-1825.
237. Fu, H., Maunakea, A.K., Martin, M.M., Huang, L., Zhang, Y., Ryan, M., Kim, R., Lin, C.M., Zhao, K. and Aladjem, M.I. (2013) Methylation of histone H3 on lysine 79 associates with a group of replication origins and helps limit DNA replication once per cell cycle. *PLoS genetics*, **9**, e1003542.
238. Gassen, A., Brechtefeld, D., Schandry, N., Arteaga-Salas, J.M., Israel, L., Imhof, A. and Janzen, C.J. (2012) DOT1A-dependent H3K76 methylation is required for replication regulation in *Trypanosoma brucei*. *Nucleic acids research*, **40**, 10302-10311.
239. Callebaut, I., Courvalin, J.C. and Mornon, J.P. (1999) The BAH (bromo-adjacent homology) domain: a link between DNA methylation, replication and transcriptional regulation. *FEBS letters*, **446**, 189-193.
240. Cesare, A.J. and Reddel, R.R. (2010) Alternative lengthening of telomeres: models, mechanisms and implications. *Nature reviews. Genetics*, **11**, 319-330.
241. Hyland, E.M., Cosgrove, M.S., Molina, H., Wang, D., Pandey, A., Cottee, R.J. and Boeke, J.D. (2005) Insights into the role of histone H3 and histone H4 core modifiable residues in *Saccharomyces cerevisiae*. *Molecular and cellular biology*, **25**, 10060-10070.
242. Xu, F., Zhang, Q., Zhang, K., Xie, W. and Grunstein, M. (2007) Sir2 deacetylates histone H3 lysine 56 to regulate telomeric heterochromatin structure in yeast. *Molecular cell*, **27**, 890-900.
243. Oppikofer, M., Kueng, S., Martino, F., Soeroes, S., Hancock, S.M., Chin, J.W., Fischle, W. and Gasser, S.M. (2011) A dual role of H4K16 acetylation in the establishment of yeast silent chromatin. *The EMBO journal*, **30**, 2610-2621.
244. Celic, I., Masumoto, H., Griffith, W.P., Meluh, P., Cotter, R.J., Boeke, J.D. and Verreault, A. (2006) The sirtuins hst3 and Hst4p preserve genome integrity by controlling histone h3 lysine 56 deacetylation. *Current biology : CB*, **16**, 1280-1289.
245. Maas, N.L., Miller, K.M., DeFazio, L.G. and Toczyski, D.P. (2006) Cell cycle and checkpoint regulation of histone H3 K56 acetylation by Hst3 and Hst4. *Molecular cell*, **23**, 109-119.
246. Yang, B., Miller, A. and Kirchmaier, A.L. (2008) HST3/HST4-dependent deacetylation of lysine 56 of histone H3 in silent chromatin. *Molecular biology of the cell*, **19**, 4993-5005.
247. Aygun, O., Mehta, S. and Grewal, S.I. (2013) HDAC-mediated suppression of histone turnover promotes epigenetic stability of heterochromatin. *Nature structural & molecular biology*, **20**, 547-554.
248. Michishita, E., McCord, R.A., Berber, E., Kioi, M., Padilla-Nash, H., Damian, M., Cheung, P., Kusumoto, R., Kawahara, T.L., Barrett, J.C. *et al.* (2008) SIRT6 is a histone H3 lysine 9 deacetylase that modulates telomeric chromatin. *Nature*, **452**, 492-496.

249. Gil, R., Barth, S., Kanfi, Y. and Cohen, H.Y. (2013) SIRT6 exhibits nucleosome-dependent deacetylase activity. *Nucleic acids research*, **41**, 8537-8545.
250. Palacios, J.A., Herranz, D., De Bonis, M.L., Velasco, S., Serrano, M. and Blasco, M.A. (2010) SIRT1 contributes to telomere maintenance and augments global homologous recombination. *The Journal of cell biology*, **191**, 1299-1313.
251. de Boer, J., Walf-Vorderwulbecke, V. and Williams, O. (2013) In focus: MLL-rearranged leukemia. *Leukemia*, **27**, 1224-1228.
252. Milne, T.A., Briggs, S.D., Brock, H.W., Martin, M.E., Gibbs, D., Allis, C.D. and Hess, J.L. (2002) MLL targets SET domain methyltransferase activity to Hox gene promoters. *Molecular cell*, **10**, 1107-1117.
253. Bernt, K.M., Zhu, N., Sinha, A.U., Vempati, S., Faber, J., Krivtsov, A.V., Feng, Z., Punt, N., Daigle, A., Bullinger, L. *et al.* (2011) MLL-rearranged leukemia is dependent on aberrant H3K79 methylation by DOT1L. *Cancer cell*, **20**, 66-78.
254. Okada, Y., Feng, Q., Lin, Y., Jiang, Q., Li, Y., Coffield, V.M., Su, L., Xu, G. and Zhang, Y. (2005) hDOT1L links histone methylation to leukemogenesis. *Cell*, **121**, 167-178.
255. Daigle, S.R., Olhava, E.J., Therkelsen, C.A., Basavapathruni, A., Jin, L., Boriack-Sjodin, P.A., Allain, C.J., Klaus, C.R., Raimondi, A., Scott, M.P. *et al.* (2013) Potent inhibition of DOT1L as treatment of MLL-fusion leukemia. *Blood*, **122**, 1017-1025.
256. Tomlins, S.A., Rhodes, D.R., Perner, S., Dhanasekaran, S.M., Mehra, R., Sun, X.W., Varambally, S., Cao, X., Tchinda, J., Kuefer, R. *et al.* (2005) Recurrent fusion of TMPRSS2 and ETS transcription factor genes in prostate cancer. *Science*, **310**, 644-648.
257. Kumar-Sinha, C., Tomlins, S.A. and Chinnaiyan, A.M. (2008) Recurrent gene fusions in prostate cancer. *Nature reviews. Cancer*, **8**, 497-511.
258. Mani, R.S. and Chinnaiyan, A.M. (2010) Triggers for genomic rearrangements: insights into genomic, cellular and environmental influences. *Nature reviews. Genetics*, **11**, 819-829.
259. Lin, C., Yang, L., Tanasa, B., Hutt, K., Ju, B.G., Ohgi, K., Zhang, J., Rose, D.W., Fu, X.D., Glass, C.K. *et al.* (2009) Nuclear receptor-induced chromosomal proximity and DNA breaks underlie specific translocations in cancer. *Cell*, **139**, 1069-1083.
260. Wu, D., Zhang, C., Shen, Y., Nephew, K.P. and Wang, Q. (2011) Androgen receptor-driven chromatin looping in prostate cancer. *Trends in endocrinology and metabolism: TEM*, **22**, 474-480.
261. Eckner, R., Ludlow, J.W., Lill, N.L., Oldread, E., Arany, Z., Modjtahedi, N., DeCaprio, J.A., Livingston, D.M. and Morgan, J.A. (1996) Association of p300 and CBP with simian virus 40 large T antigen. *Molecular and cellular biology*, **16**, 3454-3464.
262. Avantaggiati, M.L., Carbone, M., Graessmann, A., Nakatani, Y., Howard, B. and Levine, A.S. (1996) The SV40 large T antigen and adenovirus E1a oncoproteins interact with distinct isoforms of the transcriptional co-activator, p300. *The EMBO journal*, **15**, 2236-2248.
263. Lill, N.L., Tevethia, M.J., Eckner, R., Livingston, D.M. and Modjtahedi, N. (1997) p300 family members associate with the carboxyl terminus of simian virus 40 large tumor antigen. *Journal of virology*, **71**, 129-137.
264. Saenz Robles, M.T., Shivalila, C., Wano, J., Sorrells, S., Roos, A. and Pipas, J.M. (2013) Two Independent Regions of Simian Virus 40 T Antigen Increase CBP/p300 Levels, Alter Patterns of Cellular Histone Acetylation, and Immortalize Primary Cells. *Journal of virology*, **87**, 13499-13509.
265. Ferrari, R., Pellegrini, M., Horwitz, G.A., Xie, W., Berk, A.J. and Kurdistani, S.K. (2008) Epigenetic reprogramming by adenovirus e1a. *Science*, **321**, 1086-1088.
266. Henikoff, S. and Shilatifard, A. (2011) Histone modification: cause or cog? *Trends in genetics : TIG*, **27**, 389-396.
267. Arnaudo, A.M. and Garcia, B.A. (2013) Proteomic characterization of novel histone post-translational modifications. *Epigenetics & chromatin*, **6**, 24.
268. Garcia-Gimenez, J.L., Olaso, G., Hake, S.B., Bonisch, C., Wiedemann, S.M., Markovic, J., Dasi, F., Gimeno, A., Perez-Quilis, C., Palacios, O. *et al.* (2013) Histone h3 glutathionylation in proliferating mammalian cells destabilizes nucleosomal structure. *Antioxidants & redox signaling*, **19**, 1305-1320.

**H3K56me3 is a novel, conserved heterochromatic mark that largely but not completely overlaps with H3K9me3 in both regulation and localization**

PloS One 8(2), (2013)

**Jack AP**, Bussemer S, Hahn M, Pünzeler S, Snyder M, Wells M,  
Csankovszki G, Solovei I, Schotta G, Hake SB.

# H3K56me3 Is a Novel, Conserved Heterochromatic Mark That Largely but Not Completely Overlaps with H3K9me3 in Both Regulation and Localization

Antonia P. M. Jack<sup>1</sup>, Silva Bussemer<sup>1</sup>, Matthias Hahn<sup>1</sup>, Sebastian Pünzeler<sup>1</sup>, Martha Snyder<sup>2</sup>, Michael Wells<sup>2</sup>, Gyorgyi Csankovszki<sup>2</sup>, Irina Solovei<sup>3</sup>, Gunnar Schotta<sup>1</sup>, Sandra B. Hake<sup>1\*</sup>

**1** Center for Integrated Protein Science Munich (CIPSM) at the Adolf-Butenandt-Institute, Department of Molecular Biology, Ludwig-Maximilians-University Munich, Munich, Germany, **2** Department of MCDB, University of Michigan, Ann Arbor, Michigan, United States of America, **3** LMU Biozentrum, Department of Biology II, Ludwig-Maximilians-University Munich, Planegg-Martinsried, Germany

## Abstract

Histone lysine (K) methylation has been shown to play a fundamental role in modulating chromatin architecture and regulation of gene expression. Here we report on the identification of histone H3K56, located at the pivotal, nucleosome DNA entry/exit point, as a novel methylation site that is evolutionary conserved. We identify trimethylation of H3K56 (H3K56me3) as a modification that is present during all cell cycle phases, with the exception of S-phase, where it is underrepresented on chromatin. H3K56me3 is a novel heterochromatin mark, since it is enriched at pericentromeres but not telomeres and is thereby similar, but not identical, to the localization of H3K9me3 and H4K20me3. Possibly due to H3 sequence similarities, Suv39h enzymes, responsible for trimethylation of H3K9, also affect methylation of H3K56. Similarly, we demonstrate that trimethylation of H3K56 is removed by members of the JMJD2 family of demethylases that also target H3K9me3. Furthermore, we identify and characterize mouse Mjmd2E and its human homolog hKDM4L as novel, functionally active enzymes that catalyze the removal of two methyl groups from trimethylated H3K9 and K56. H3K56me3 is also found in *C. elegans*, where it co-localizes with H3K9me3 in most, but not all, tissues. Taken together, our findings raise interesting questions regarding how methylation of H3K9 and H3K56 is regulated in different organisms and their functional roles in heterochromatin formation and/or maintenance.

**Citation:** Jack APM, Bussemer S, Hahn M, Pünzeler S, Snyder M, et al. (2013) H3K56me3 Is a Novel, Conserved Heterochromatic Mark That Largely but Not Completely Overlaps with H3K9me3 in Both Regulation and Localization. PLoS ONE 8(2): e51765. doi:10.1371/journal.pone.0051765

**Editor:** Janet F. Partridge, St Jude Children's Research Hospital, United States of America

**Received:** August 1, 2012; **Accepted:** November 7, 2012; **Published:** February 22, 2013

**Copyright:** © 2013 Jack et al. This is an open-access article distributed under the terms of the Creative Commons Attribution License, which permits unrestricted use, distribution, and reproduction in any medium, provided the original author and source are credited.

**Funding:** This study was supported by grants from the DFG (HA 5437/3-1 and SFB TR5), as well as CIPSM to S.B.H. and from the National Institutes of Health (NIH) R01 GM079533 to G.C. I.S. was supported by DFG (SO1054/1) and Biomedizinisches Netzwerk Munich and G.S. by SFB TR5, SPP1356 and BMBF (EpiSys). A.P.M.J. and S.P. are members of the IMPRS/LS program. The funders had no role in study design, data collection and analysis, decision to publish, or preparation of the manuscript.

**Competing Interests:** The authors have declared that no competing interests exist.

\* E-mail: sandra.hake@med.uni-muenchen.de

## Introduction

Histones, the building blocks of chromatin, are subject to several posttranslational modifications including methylation, acetylation and phosphorylation that carry important functional information [1]. Over the last decades, it has become increasingly obvious that such chemical histone tags contribute to the regulation of DNA-related processes in a highly selective and specialized manner [2]. These posttranslational histone modifications (PTMs) either change nucleosome structure directly by affecting histone-DNA contacts or indirectly by recruiting PTM-binding proteins that act on the underlying chromatin structure, as has been proposed in the “histone code” hypothesis [3]. Although most marks are found on the flexible histone tail regions, some modifications have also been identified on core residues. One such core PTM, histone H3 lysine 56 acetylation (H3K56ac) [4], occurs in the  $\alpha$ -N-helical region near the entry-exit sites of the DNA superhelix and is conserved from yeast to man [5]. It is most abundant during S phase [6,7] and has been shown to play a pivotal role in DNA damage response [6], chromatin integrity [8,9] and replication-coupled nucleosome assembly [10]. In a previous mass spectrometry-based study, we

were not only able to verify the existence of H3K56 acetylation in humans but were also able to identify low levels of mono- and trimethylation of lysine 56 on histone H3 (H3K56me1 and H3K56me3, respectively) [11]. Recently, it was demonstrated that monomethylation of H3K56 regulates DNA replication through interaction with the replication processivity factor PCNA and is catalyzed by the lysine methyltransferase (KMT) G9a (KMT1C) [12]. The involvement of H3K56me1 in such an important biological event led us to ask how trimethylation of this residue might be regulated and impact cellular processes. Despite the known *in vivo* existence of H3K56me3 [11], no further information concerning this novel histone H3 core modification has been established. We set out to learn more about its functional role by deciphering its chromatin localization and by identifying enzymes that set (“writer”) and erase (“eraser”) this mark.

## Materials and Methods

### Cell lines

Human HeLa Kyoto cells [13], and mouse C127 (ATCC CRL-1616) cell lines were grown in DMEM medium (PAA) supplemented

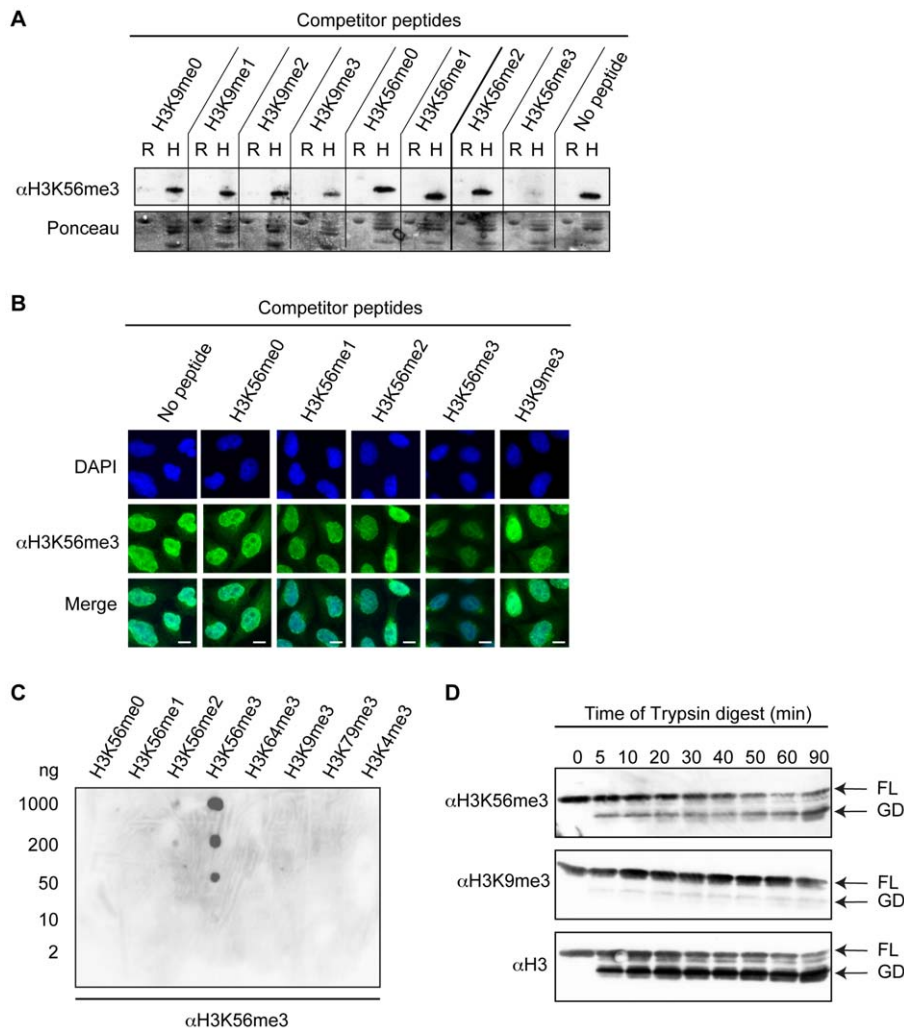


**Figure 1. Determination of  $\alpha$ H3K56me3 specificity and suitability in diverse applications.** (A) Immunoblot peptide competition experiment.  $\alpha$ H3K56me3 antibody was preincubated with competitor peptides before addition to immunoblots containing recombinant H3 protein (R) or acid extracted HeLa Kyoto histones (H) (top). Ponceau staining (bottom) serves as loading control. (B) IF microscopy peptide competition experiment.  $\alpha$ H3K56me3 antibody (green) was preincubated with competitor peptides before addition to fixed HeLa Kyoto cells. DAPI (blue) stains DNA. Scale bar = 5  $\mu$ m. (C) Spot-blot with different concentrations (5–1000 ng) of H3 peptides to determine  $\alpha$ H3K56me3-binding affinities. (D) Immunoblot of sequential tryptic digest of HeLa Kyoto-derived mononucleosomes using  $\alpha$ H3K56me3 (top),  $\alpha$ H3K9me3 (middle) and  $\alpha$ H3 (bottom). FL = full-length histone H3, GD = N-terminally deleted globular domain of histone H3. doi:10.1371/journal.pone.0051765.g001

with 10% FCS (Sigma) and 1% penicillin/streptomycin at 37°C and 5% CO<sub>2</sub>. Wild type, Suv39hDKO [14] and SUV4-20hDKO [15] mouse embryonic fibroblast (MEF) cell lines were grown in DMEM medium (PAA) supplemented with 18% FCS (Sigma), 1% penicillin/streptomycin, 1% non-essential amino acids (Invitrogen), 50 mM  $\beta$ -mercaptoethanol and 0.4% LIF at 37°C and 5% CO<sub>2</sub>. Cells were transfected using FuGene HD (Roche Applied Science) according to the manufacturer's instructions.

### Antibodies

Polyclonal rabbit antibody against H3K56me3 was developed by Pineda Antikörper-Service (Berlin, Germany) using a peptide with the following amino acid sequence for immunization and affinity purification: NH<sub>2</sub>-CRRYQ-K(me<sub>3</sub>)-STEL-CONH<sub>2</sub>. Commercially available antibodies used in this study include: Primary antibodies:  $\alpha$ H3 (C-terminus, Abcam),  $\alpha$ H4 (Antikörper-online),  $\alpha$ H3K4me2 (Abcam),  $\alpha$ H3K4me3 (Abcam),  $\alpha$ H3K9me1 (Millipore),  $\alpha$ H3K9me2 (Active Motif),  $\alpha$ H3K9me3 (Active Motif and

[16]; specificity tests are shown in Figure S1),  $\alpha$ H3K27me2 (Millipore),  $\alpha$ H3K27me3 (Millipore),  $\alpha$ H3K36me1 (Millipore),  $\alpha$ H3K36me2 (Active Motif),  $\alpha$ H3K36me3 (Abcam),  $\alpha$ H4K20me1 (Millipore),  $\alpha$ H4K20me2 (Millipore),  $\alpha$ H4K20me3 (Abcam),  $\alpha$ H3K56me1 (Millipore),  $\alpha$ H3K56me2 (Active Motif),  $\alpha$ H3K56ac (Active Motif). Secondary antibodies: for immunoblots (Amersham), for IF microscopy (Dianova).

### Peptide competition experiment

$\alpha$ H3K56me3 antibody in 1:1000 or 1:100 dilutions was preincubated with 2  $\mu$ g/ml of peptides (Table S1) before usage in either immunoblots or immunofluorescence (IF) microscopy, respectively. Peptides were N-terminally biotinylated and synthesized with higher than 80% purity by The Rockefeller University, GeneScript or the MPI for Biochemistry Munich. In case of immunoblots, acid extracted histones [17] and recombinant histone H3 [18] were used.



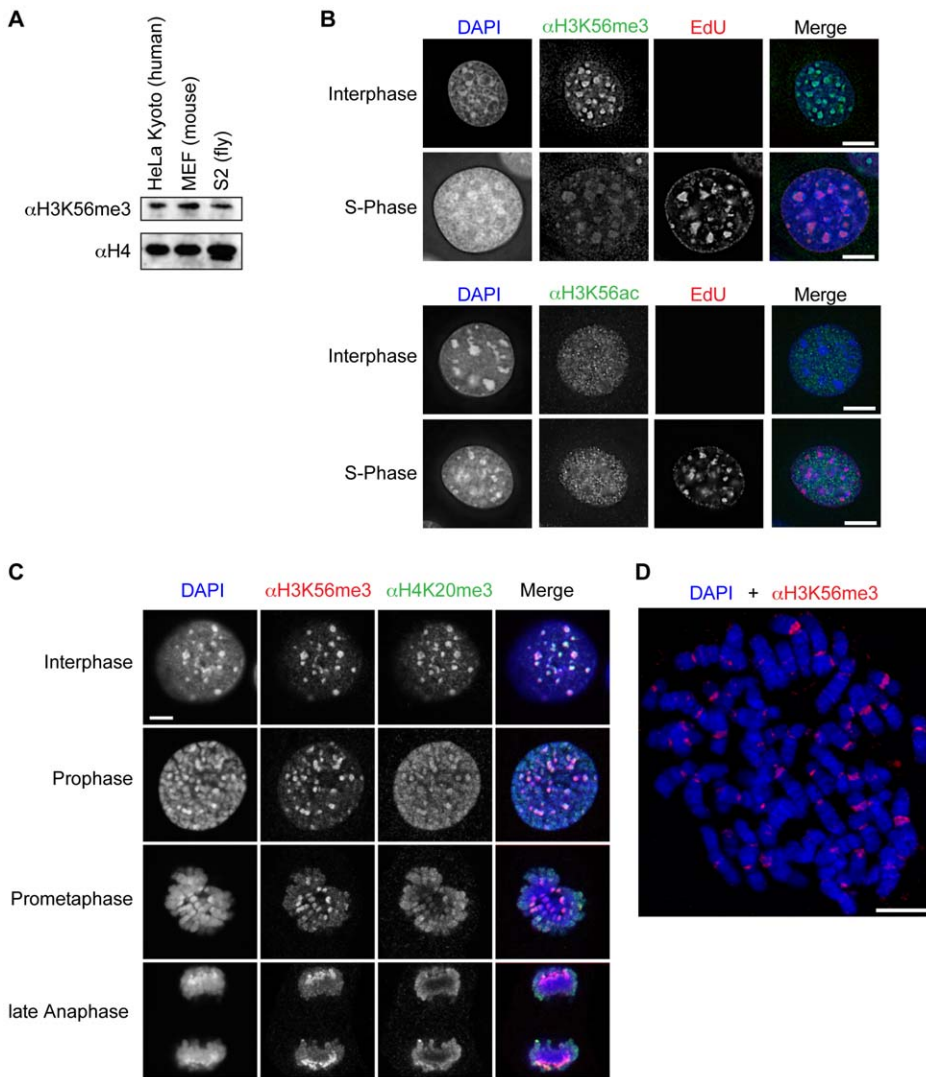


**Figure 2. H3K56me3 is evolutionary conserved, has a cell-cycle independent appearance and is part of pericentromeric heterochromatin.** (A) Immunoblot with acid extracted histones from human (HeLa Kyoto), mouse (MEF) and fly (S2) cell lines using  $\alpha$ H3K56me3 (top) and, as loading control,  $\alpha$ H4 (bottom) antibodies. (B) IF analysis of H3K56me3 (top) and H3K56ac (bottom) appearance in G1/G2 and S-phase cells. C127 cells were pulse-labeled with EdU (red) to visualize replication foci and to identify cells in S-phase. Cells were co-stained with  $\alpha$ H3K56me3 or  $\alpha$ H3K56ac (green) and DAPI (DNA, blue). Scale bar = 5  $\mu$ m. (C) IF microscopy of MEF cells in interphase and different stages of mitosis co-stained with  $\alpha$ H3K56me3 (red),  $\alpha$ H4K20me3 (red) and DAPI (DNA, blue). Scale bar = 5  $\mu$ m. (D) IF of chromosome spread from nocodazole-arrested HeLa cells with  $\alpha$ H3K56me3 (red) and DAPI (DNA, blue) staining. Scale bar = 5  $\mu$ m. doi:10.1371/journal.pone.0051765.g002

**Tryptic digest of mononucleosomes**

$6 \times 10^7$  HeLa Kyoto cells were incubated in PBS, 0.3% Triton X-100 and Protease Inhibitor Cocktail (Roche, Germany) for 10 min at 4°C. Nuclei were pelleted, washed once in PBS, resuspended in EX100 buffer (10 mM HEPES pH 7.6, 100 mM NaCl, 1.5 mM MgCl<sub>2</sub>, 0.5 mM EGTA, 10% (v/v) glycerol, 10 mM  $\beta$ -glycerol phosphate, 1 mM DTT, Protease Inhibitor Cocktail (Roche, Germany)) and CaCl<sub>2</sub> concentration adjusted to 2 mM. Resuspended nuclei were digested with 1.5 U MNase (Sigma) for 20 min at 26°C. The reaction was stopped by addition of EGTA to a final concentration of 10 mM followed by centrifugation for 10 min at 1000 rcf, 4°C. Mononucleosome containing supernatant was retained. NH<sub>4</sub>HCO<sub>3</sub> was added at a final concentration of 50 mM or until a pH of 7–8 was reached. 1.6  $\mu$ g Trypsin (Promega) was added and the reaction was incubated at 25°C. Samples were collected at different time

points and the reaction stopped by adding an equal volume of 1% trifluoroacetic acid. Fragments were size separated on a 15% SDS-PAGE probed with indicated antibodies.

**Spot-blot**

Peptide dilutions containing 2, 10, 50, 200 and 1000 ng in sterile water were spotted on nitrocellulose membrane and allowed to air-dry. The membrane was then blocked in PBS-Tween (0.1%) with milk powder (5%), followed by immunoblotting with  $\alpha$ H3K56me3.

**Immunofluorescence (IF) microscopy and cell cycle analysis**

**Mammalian cells.** Preparation of mammalian cells and chromosome spreads for IF microscopy was done as previously reported [19]. Staining of S-phase cells was performed as

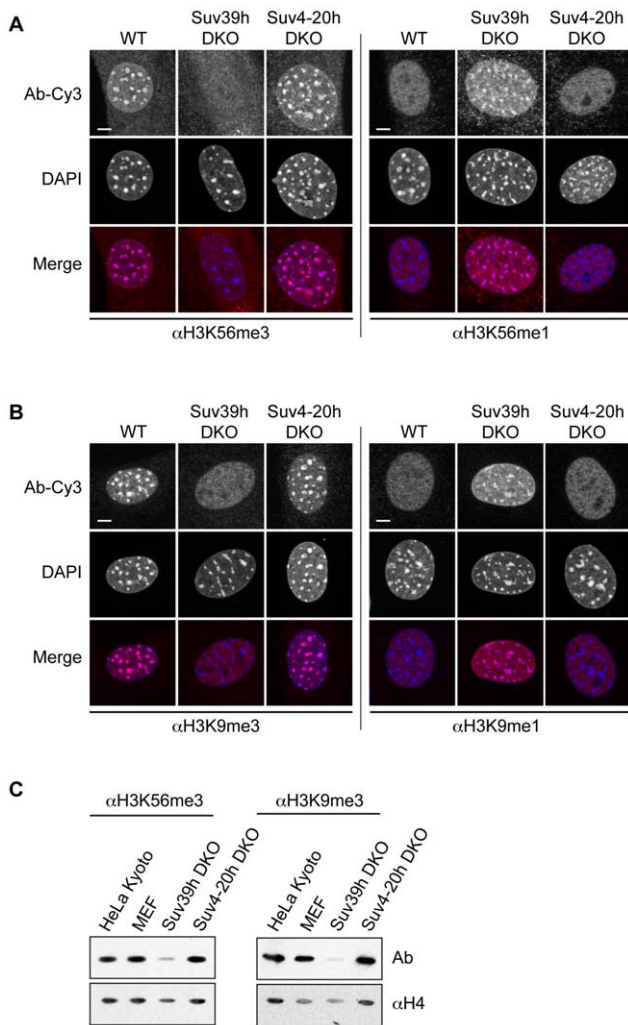


**Figure 3. Loss of Suv39h enzymes affect H3K56me3.** IF microscopy of wild type (WT), Suv39h double-null (Suv39h DKO) and Suv4-20h double-null (Suv4-20h DKO) MEF cells using various H3K56 (A) and H3K9 (B) methyl-specific antibodies (Ab-Cy3, red) and DAPI (DNA, blue). Scale bar = 5  $\mu$ m. (C) Immunoblots using acid extracted histones from HeLa Kyoto (positive control), wild type MEF, Suv39h DKO and Suv4-20h DKO cells. Blots were incubated with  $\alpha$ H3K56me3 (left, top) or  $\alpha$ H3K9me3 (right, top) antibodies, respectively. Blots shown at the bottom were incubated with  $\alpha$ H4 to ensure equal loading. doi:10.1371/journal.pone.0051765.g003

described in [18]. Wide-field IF imaging of EdU-stained C127 cells was performed on a PersonalDV microscope system (Applied Precision) equipped with a 60 $\times$ /1.42 PlanApo oil objective (Olympus), CoolSNAP ES2 interline CCD camera (Photometrics), Xenon illumination and appropriate filtersets. Iterative 3D deconvolution of image z-stacks was performed with the SoftWoRx 3.7 imaging software package (Applied Precision).

Confocal imaging of chromosome spreads was performed on a TCS SP5 II microscope system (Leica Microsystems, Wetzlar, Germany), equipped with a 63 $\times$ /1.3 HCX PL APO glycerol immersion objective. Z-stacks were recorded and subsequently deconvolved with Huygens Essential Software (SVI, Hilversum, The Netherlands).

Image stacks of immunostained MEF cells were collected using a Leica TCS SP5 confocal microscope with Plan Apo Lambda Blue 63 $\times$ /1.4 NA oil or 63 $\times$ /1.3 glycerol immersion objective.

**C. elegans.** Methanol/acetone fixation for immunostaining was performed as follows. Adult hermaphrodites were dissected in 1x sperm salts with and frozen on dry-ice for 20–30 minutes. The slides were fixed in methanol followed by acetone, 2 minutes each wash, at  $-20^{\circ}\text{C}$ . Slides were then washed once for ten minutes in PBST prior to incubation with primary antibody [1:200 or 1:100 (direct labeling)  $\alpha$ H3K56me3, 1:1000  $\alpha$ H3K9me3 (Abcam ab8898)]. Remainder of staining protocol was conducted as described previously [20]. Microscopy and imaging were conducted as described previously [21].

Images were capture with a Hamamatsu Orca-Erga close-coupled-device (CCD) camera mounted on an Olympus BX61 motorized Z-drive microscope using a 60X APO oil immersion objective. These images are projections of optical sections with a Z spacing of 0.2 micrometers. Scale bars were added using ImageJ (available at <http://rsb.info.nih.gov/ij>; developed by Wayne Rasband, National Institutes of Health, Bethesda, MD) and a template image created in Slidebook.

#### Quantitative PCR

qPCR was carried out as previously described [22] using Fast SYBR Green Master Mix (Applied Biosystems). Results were normalized to HPRT1 and GAPDH levels.

#### Cloning of GFP-jmjC constructs

pDONR entry clones of the JmjC subgroup [23] were recombined into the target vector pEGFP-N1-GW using LR clonase II enzyme mix (Invitrogen) according to the manufacturer's protocol.

#### C. elegans RNAi

RNA interference by feeding was performed with the Ahringer laboratory RNAi feeding library [24] in two generations as described previously [21].

## Results

### Development of a specific $\alpha$ H3K56me3 antibody

To gain insight into the biological function(s) of H3K56 trimethylation, we raised a polyclonal antibody against H3K56me3 ( $\alpha$ H3K56me3) and determined its specificity in various assays. Since H3K56me1 has previously been reported to be catalyzed by the H3K9me1-specific KMT G9a, maybe due to a conserved lysine-serine-threonine (K/S/T) motif at the site of both residues [12], we put special emphasis on testing a potential cross-reactivity of this antibody with H3K9me3. First, we performed peptide competition experiments using peptides spanning diverse regions of histone H3 with or without different methylation states. Specific antibody recognition of H3K56me3 in immunoblotting (Figure 1A) and immunofluorescence (IF) microscopy (Figure 1B) was efficiently competed out only with H3K56me3-containing peptides, but not with peptides containing other methylated or unmethylated histone regions. Next, we determined the relative binding affinity of  $\alpha$ H3K56me3 to its epitope by a peptide Spot-blot containing various concentrations of different histone peptides and observed that  $\alpha$ H3K56me3 detected as low as 50 ng of H3K56me3 peptides (Figure 1C). Notably,  $\alpha$ H3K56me3 does not recognize any other trimethylated peptides except H3K56me3. For further support of antibody specificity, we generated mononucleosomes from HeLa cells that were subsequently digested with different concentrations of Trypsin in order to generate histones lacking their flexible tail regions. In this way, we were able to determine if the antibody epitope resides in the H3 core region or N-terminal tail. In

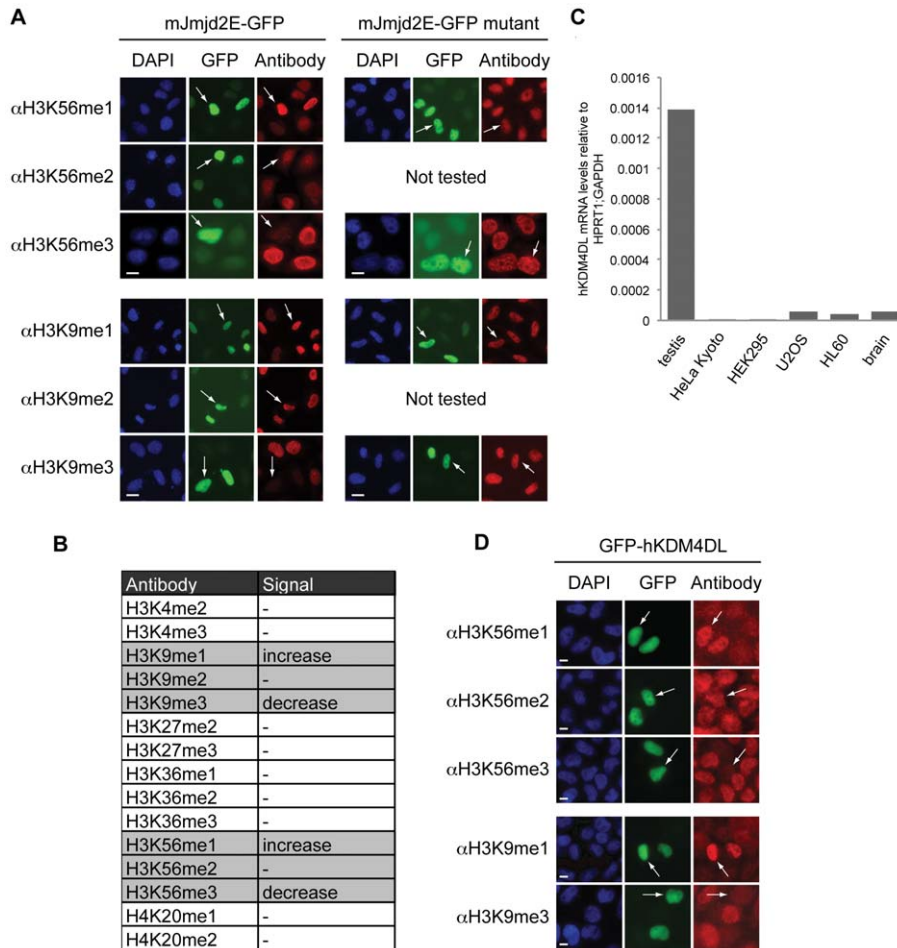


**Figure 4. Jmjd2E demethylase affects H3K56me3.** (A) IF microscopy of HeLa Kyoto cells transfected with mJmjd2E-GFP (green, left) or jmjcdomain mutated mJmjd2E-GFP (mutant, green, right) and stained with various H3K56 and H3K9 PTM-specific antibodies (red) and DAPI (DNA, blue). Arrows indicate transfected GFP-positive cells. Scale bar = 10  $\mu$ m. See also Figure S2A for IF results of cells transfected with other GFP-tagged mJMJD2 family members (mJmjd2a-d). (B) List of PTMs analyzed in IF after expression of mJmjd2E in HeLa Kyoto cells indicating changes in fluorescence intensities. See also Figure S2B for examples of IF results summarized in this table. (C) qPCR analysis with cDNAs from different human cell lines and tissues using primer pair specific for human Jmjd2E (hKDM4DL). Data were normalized to HPRT1 and GAPDH expression levels. (D) IF microscopy of HeLa Kyoto cells transfected with human GFP-hKDM4L (green) and stained with various H3K56 and H3K9 methyl-specific antibodies (red) and DAPI (DNA, blue). Arrows indicate transfected and GFP-positive cells. Scale bar = 10  $\mu$ m. doi:10.1371/journal.pone.0051765.g004

immunoblots,  $\alpha$ H3K56me3, but not the control  $\alpha$ H3K9me3 antibody, recognized both full-length (FL) and the N-terminus deleted globular domain (GD) of histone H3 (Figure 1D), demonstrating that  $\alpha$ H3K56me3 specifically binds to a modification in the core region of H3. In summary, these experiments provide compelling evidence that  $\alpha$ H3K56me3 is highly specific for this particular modification and can be applied in diverse biochemical assays.

### H3K56me3 is evolutionary conserved and localizes to pericentromeric heterochromatin outside of S-phase

Having demonstrated the high specificity of  $\alpha$ H3K56me3, we first examined the evolutionary occurrence of this novel mark by isolating histones from cell lines of diverse origins. Immunoblotting revealed that H3K56me3 was present in human, mouse and fly (Figure 2A), suggesting that this modification is conserved within, at least, metazoans.

Given that H3K56ac is highly conserved and that methylation and acetylation of the same residue are mutually exclusive we

wanted to investigate if there were correlations between the appearance of one mark and disappearance of the other. While in yeast H3K56ac has been shown to be cell cycle dependent, showing a significant increase during S-phase, [6,9,25], its cell cycle distribution in mammals remains controversial [26–28], with a high possibility of its occurrence in all cell cycle phases [29]. Therefore, we analyzed cell cycle appearance and nuclear localization of both acetylation and methylation of H3K56 in mammalian cells. To distinguish S-phase from interphase, mouse C127 cells were pulse-labeled with the thymidine analog EdU, which was chemically coupled to a fluorescent dye using a “click-chemistry” approach [30]. Co-staining of EdU-labeled cells with  $\alpha$ H3K56me3 revealed that, during interphase, H3K56me3 is found predominantly at DAPI-dense heterochromatic chromocenters and shows strongly diminished signal intensity in S-phase cells (Figure 2B top). Although, we observed a more or less equal appearance of H3K56ac signal in interphase and S-phase cells (Figure 2B, bottom), it is clearly distinct from the H3K56me3 signal. We also found H3K56me3 to be present throughout mitosis (Figure 2C), where it co-localizes with heterochromatin



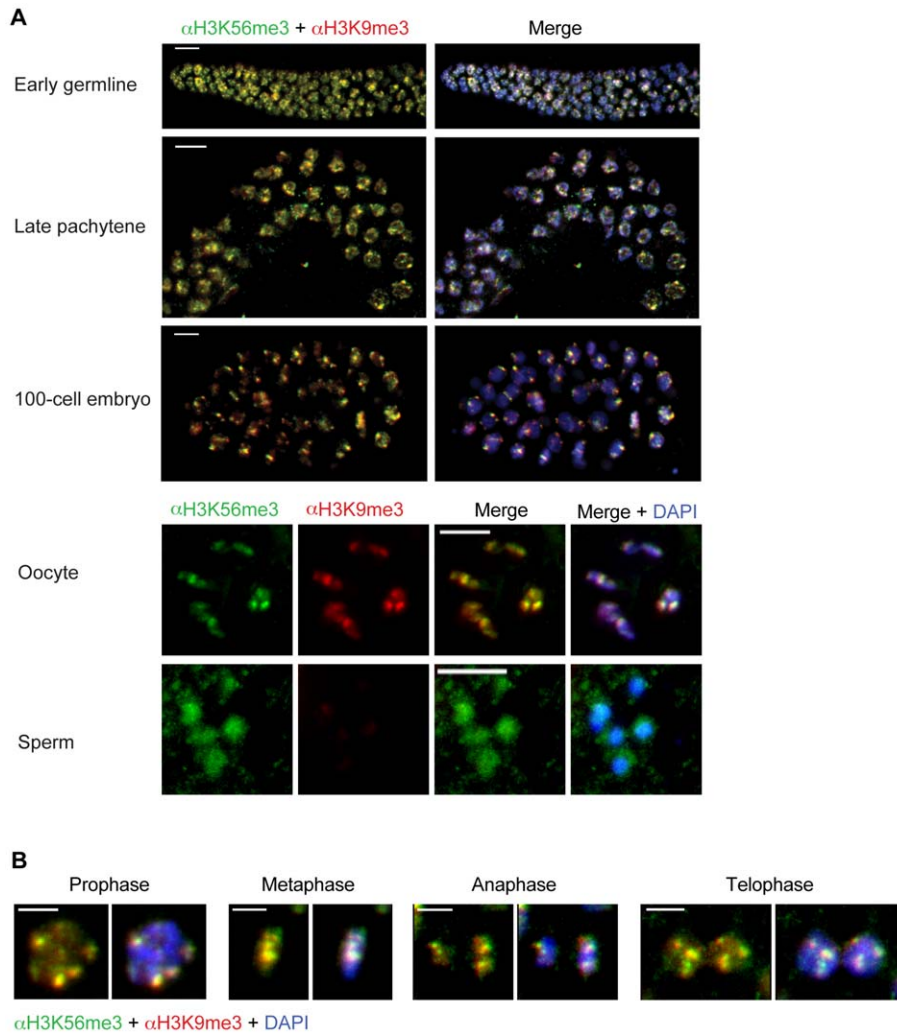


**Figure 5. H3K56me3 is conserved in *Caenorhabditis elegans*.** Shown are representative IF microscopy pictures from adult *C. elegans* hermaphrodite tissues. In all images H3K56me3 is shown in green, H3K9me3 in red, and DAPI (DNA) in blue. Scale bar = 5  $\mu$ m. A) H3K56me3 co-localizes with H3K9me3 in the early germline, late pachytene and in a 100-cell embryo (top picture). Interestingly, although H3K56me3 and H3K9me3 are both present in oocytes, only H3K56me3, but not H3K9me3, staining could be observed in sperm. (bottom, split channels) (B) H3K56me3 and H3K9me3 co-localize throughout all stages of mitosis. doi:10.1371/journal.pone.0051765.g005

foci, in an even more precise manner than the constitutive heterochromatin marker H4K20me3 [31]. To determine H3K56me3 localization in greater detail, human metaphase chromosomes were analyzed in IF microscopy. In accordance with H3K56me3 presence at chromocenters in interphase and heterochromatin foci in mitotic cells, this modification was present in a non-random manner and found predominantly at pericentromeric heterochromatin regions that include major satellite repeats (Figure 2D). Interestingly, H3K56me3 is, in contrast to H3K9me3, rarely found at telomeres [32], suggesting that the functional roles of these two modifications in heterochromatic regions might be different.

#### Mammalian methyltransferase Suv39h affects trimethylation of H3K56

To assess the functional relevance of posttranslational histone modifications, it is important to know their responsible enzymes. Several lysine methyltransferases (KMTs) that catalyze the methylation of histone lysine residues have been identified

previously [33,34]. Possibly due to the fact that both regions surrounding H3K56 and H3K9 contain a conserved K/S/T motif, monomethylation of H3K56 has been shown to be catalyzed by the H3K9me1-specific KMT G9a [12]. Additionally, both H3K9me3 and H3K56me3 localize to similar, albeit not identical, nuclear domains suggesting that H3K9 and H3K56 might share the same KMTs responsible for their trimethylation. Therefore, we first tested the H3K9me3-specific KMTs Suv39h1/2 (KMT1A and B) [35] for their ability to affect the methylation status of H3K56. Interestingly, we observed a complete loss of both H3K56me3 and H3K9me3 signals at chromocenters in Suv39h double-null MEF cells (Suv39h DKO, [14]). Accompanied with this loss of trimethyl signals, we observed an increase of the respective monomethyl marks at chromocenters (Figure 3A and B). This dramatic change in PTM localization upon the simultaneous lack of Suv39h1/2 suggests that these enzyme are involved in catalyzing trimethylation of both H3K9 and H3K56, the latter in either a direct or indirect manner. Since H3K56me3 showed a somewhat similar nuclear appearance as H4K20me3

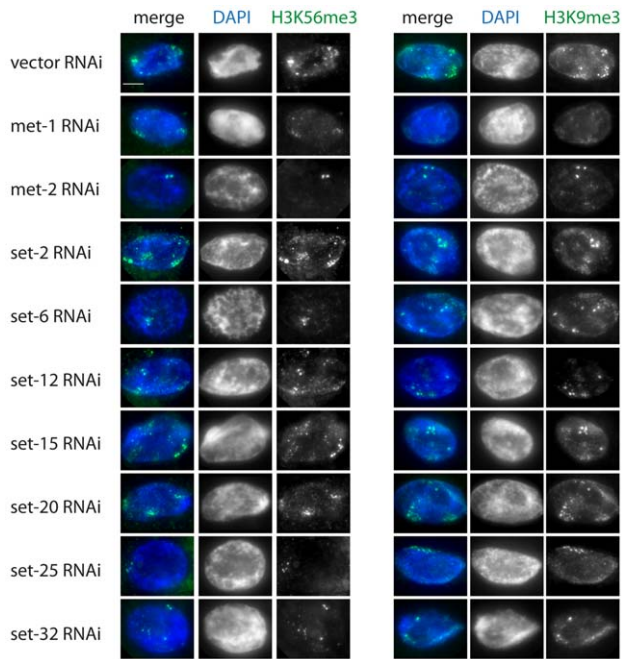


**Figure 6. *C. elegans* RNAi screen to identify H3K56me3-specific KMTs.** Shown are representative IF images from adult *C. elegans* hermaphrodite somatic intestinal nuclei following RNAi treatment. H3K56me3 (left) or H3K9me3 (right) staining is shown in green and DAPI (DNA) is shown in blue. CAPG-1 co-staining was used as a staining control (data not shown). Results show that *met-1* and *met-2* depletion severely affect both H3K56me3 and H3K9me3, while reduction of additional KMTs (*set-6*, *set-25* and *set-32*) has a stronger effect on H3K56me3 levels compared to H3K9me3. Scale bar = 5  $\mu$ m. doi:10.1371/journal.pone.0051765.g006

(Figure 2C), we wondered whether Suv4-20h1/h2 enzymes, responsible for methylating lysine 20 on histone H4 [15,31], might also target H3K56. Suv4-20h double null MEF cells (Suv4-20h DKO, [15]) showed no difference in abundance or localization of H3K56 methylation when compared to wild type cells (Figure 3A and B), demonstrating that these enzymes do not influence H3K56 methylation status. Similar results were also obtained with immunoblots, showing that the H3K56me3 signal is diminished in Suv39h DKO, but not Suv4-20 DKO acid extracted histones (Figure 3C).

#### Jmjd2E/KDM4DL is a novel lysine-demethylase specific for H3K9 and H3K56 trimethylation

Having shown that the same enzymes that methylate H3K9 also affect trimethylation of H3K56, we wondered whether the erasure of these modifications is catalyzed by identical lysine demethylases (KDMs) as well. Histone lysines are demethylated by two different classes of enzymes that are distinguished by their enzymatic active domains and methylation-state specificities [36]. We focused our attention on the Jumonji C-terminal domain (JmjC) family of KDMs, since they are able to remove all methyl-states, including trimethylation [37]. We therefore tested a panel of GFP-tagged members of the JMJD2 group-containing demethylases that are thought to partially work on H3K9me3 [23]. Over-expression of the respective mKDM in human cells was monitored by GFP signal in IF microscopy and effects on histone methylation were analyzed by co-staining with different histone PTM antibodies. This screen led to the identification of all members of the mJMJD2 family (mJmjd2A-E) able to affect H3K56me3 (Figure S2A and

Figure 4A). Since all members have previously been shown also to act on H3K9me3 [38], our results point once again towards a possible link between these two heterochromatic marks due, to a shared sequence motif (K/S/T). As one example, over-expression of mJmjd2D or mJmjd2E [39] strongly diminished H3K9me3, as well as H3K56me3 signals, in HeLa Kyoto cells (Figure 4A, left and Figure S2A). The loss of the respective trimethyl signal was accompanied with an increase in the monomethyl, but not dimethyl state, suggesting that these enzymes remove two methyl groups in total. Since over-expression of mJmjd2D-GFP caused severe cellular defects, its role on H3K56me3 was not further investigated and we focused subsequent analyses on mJmjd2E that acted solely on H3K9 and H3K56 trimethylation and not on other histone trimethylation marks (Figure 4B and Figure S2B). The observed changes in H3K9 and H3K56 methylation states upon mJmjd2E-GFP over-expression were dependent on the enzymatic active jmjC domain, since point mutations in that region completely abolished mJmjd2E's demethylase activity (Figure 4A, right). In the mouse, mJmjd2E is predicted to constitute a pseudogene and we therefore decided to analyze expression and function of the yet uncharacterized human homolog hKDM4DL. hKDM4DL mRNA is expressed predominantly in testis, with only residual levels present in U2OS (osteosarcoma) and HL60 (promyelocytic leukemia) cell lines and human brain tissue (Figure 4C). Over-expression of GFP-hKDM4DL in HeLa Kyoto cells showed identical results as seen for the mouse homolog, loss of H3K56 and H3K9 trimethylation with an accompanied gain of the respective monomethylation mark (Figure 4D). Taken together, we have identified the JMJD2 family to facilitate demethylation of H3K9 and H3K56 trimethyl states. Additionally, we showed that mJmjd2E, and its previously uncharacterized human homolog hKDM4DL, specifically remove two methyl groups from trimethylated H3K56 or H3K9 residues, depending on their catalytically active jmjC domain.

#### H3K56me3 is a novel chromatin mark in *C. elegans*

In order to learn more about H3K56me3 evolutionary conservation as a novel heterochromatic histone modification and its functions, we conducted IF microscopy analysis of wild type (WT) *C. elegans* hermaphrodite germlines and embryos (Figure 5A). H3K56me3 is present in both early germline and embryonic nuclei, as marked by DAPI morphology (Figure 5A, right). In almost all cells analyzed, we observed an H3K56me3 signal that strongly co-localized with H3K9me3 in most tissues (Figure 5A). Surprisingly, H3K56me3 staining was present in both types of germline cells, oocytes and sperm, whereas the H3K9me3 signal was restricted to oocytes only (Figure 5A, bottom). These data mirror previously obtained H3K9me3 results [40] and suggest that H3K56me3 might have an important H3K9me3-independent function in sperm development. Next, we wondered whether, similar to mammalian cells, H3K56 is trimethylated in cells during mitosis in *C. elegans*. Indeed, H3K56me3 is part of all mitotic stages and overlaps with H3K9me3 signals (Figure 5B), demonstrating the evolutionary high conservation of this novel mark.

Next, we sought to shed light on the enzymatic regulation of H3K56 trimethylation in *C. elegans* and performed an RNAi-based survey of known or predicted methyltransferases, including H3K9-specific enzymes [41]. The screen included RNAi targeting MET-2, a homolog of mammalian euchromatic H3K9 HMT SETDB1 [40–42], MET-1, a homolog of yeast Set2, an H3K36-specific methyltransferase, whose activity was reported to be required for normal levels of H3K9me3 [41], and SET-25, a distant homolog G9a, recently reported to deposit H3K9me3 in *C. elegans* embryos [42]. We also included RNAi against previously uncharacterized

SET domain containing proteins predicted to encode divergent H3K9-specific methyltransferases (*set-6*, *-12*, *-15*, *-20*, and *-32*). For control, we performed RNAi targeting an H3K4-specific methyltransferase SET-2, a homolog of SET1/MML. We conducted our screen in the intestine, where the large size of nuclei makes scoring easier. This screen identified several genes whose activity is required for normal levels of H3K56me3 and/or H3K9me3, some of which have been previously implicated in H3K9 methylation. H3K56me3 levels were severely reduced in *met-2* and *set-25* RNAi, consistent with the requirement for these genes for H3K9me3 levels in *C. elegans* embryos [42]. Interestingly, H3K9me3 levels were less affected in these conditions, indicating possible differences between the enzymes responsible for these marks and/or differences in antibody sensitivities. H3K56me3 levels were also reduced in *met-1* RNAi, and to a lesser extent in *set-6* and *set-32* RNAi. H3K9me3 levels were also reduced in *met-2* and *set-12* RNAi, possibly due to indirect effects (Figure 6). H3K9me3 levels were never reduced to background levels, perhaps due to partial redundancy between these enzymes. Knockdown of other known H3K9 methyltransferases or the H3K4 KMT *set-2* resulted in DAPI perturbations, but showed no effect on H3K56me3 staining (Figure 6).

In sum, H3K56me3, its relationship to H3K9me3, and its regulation by several H3K9 methyltransferases are conserved in *C. elegans*. However, some degree of divergence in the factors regulating H3K56me3 may have occurred in *C. elegans*.

## Discussion

Our study establishes the existence of a novel pericentric heterochromatin mark, H3K56me3, in several metazoan species. This novel modification is present in all cell cycle phases, with the exception of S-phase, where it is underrepresented. Enzymes targeting H3K9 also act on H3K56, as the KMTs Suv39h1/2 are important for trimethylation of both residues and KDM JMJD2 family members remove these modifications. Mouse Jmjd2E and its so far uncharacterized human homolog hKDM4DL are involved in the process of demethylating H3K56me3 to a monomethylated status. In *C. elegans*, H3K56me3 is a conserved feature of mitotic chromosomes that primarily co-localizes with H3K9me3 and is regulated by some but not all H3K9 methyltransferases.

Of particular interest is our observation in mammalian cells that H3K56me3 is found in chromocenters containing pericentric heterochromatin, but only outside of S-phase. During that particular cell cycle phase, H3K56me3-specific IF microscopy signals are strongly diminished. Such an effect can be caused either by a replication-specific removal of the trimethylation mark or by occlusion of the epitope through adjacent modifications, such as phosphorylation of H3S57, or association with a binding protein. As H3K56 is targeted by the lysine acetyltransferases CBP or GCN5 [26,43] prior to being deposited onto DNA during replication [7,44,45], it is highly likely that newly synthesized H3 histones with K56ac replace “old” H3K56me3-containing ones. Given that H3K56me3 has been recently shown to prevent binding of PCNA that specifically associates with the monomethylation state [12], it is plausible that H3K56me3 needs to be removed during replication to allow proper action of PCNA at the replication forks. With regard to adjacent modification sites, a serine and a threonine, potential phosphorylation sites, are located next to lysine 56. Although H3S57 phosphorylation was reported to exist in mammals *in vivo* [46], no data on its appearance during cell cycle, on responsible enzymes and its function in mammals are available due to the lack of a specific antibody. One study,

applying yeast mutants proposes a potential functional interplay between H3K56 and S57 in replicative stress recovery and transcriptional elongation [46]. However, because H3S57ph has thus far not been identified in yeast *in vivo*, it is not possible to relate such observations to the mammalian system. Concerning putative H3K56me3-specific binding partners, we applied peptide pull-down experiments followed by MS identification of precipitated proteins (data not shown). Although we repeated such experiment many times, we were not able to consistently pull-down any candidates when compared to unmodified control peptide pull-downs. It is likely that H3K56me3 is not directly recognized by any “reader” protein but, instead functions indirectly by preventing acetylation of H3K56 and its associated signaling pathways. Alternatively, since H3K56me3 is localized in the  $\alpha$ -N-helical region near the entry-exit sites of the DNA superhelix, it is possible that the correctly folded three-dimensional structure of this region (alone or in combination with DNA or other histones) is crucial for reader binding. Therefore, the use of peptides in such pull-down experiments will not suffice in reader binding. H3K56me3 histones or even nucleosomes containing this PTM will be needed for the identification of its potential reader(s) in the future.

Our finding that H3K56me3 constitutes another heterochromatin mark is in perfect agreement with previously published data, since H3K56 is monomethylated by G9A [12] that was initially described as a KMT responsible for H3K9me1 and H3K9me2 [47]. It is therefore plausible that H3K9me3-specific KMT(s) might also act on H3K56. We report here that the loss of Suv39h enzymes leads to diminished trimethylation of both H3K56 as well as H3K9. Based on our experimental set-up using Suv39h double-null cells, it is at the moment not possible to exclude that loss of H3K56me3 stems from an indirect effect. The chance of H3K9me3 influencing trimethylation of H3K56 by an, as yet, unknown mechanism, is conceivable albeit unlikely. Several observations argue for a direct enzymatic action of Suv39h on H3K56; the presence of a “K/S/T” motif in both regions and the fact that G9a, another H3K9-specific KMT is the responsible enzyme for H3K56me1 [12]. Therefore, we propose that Suv39h enzymes directly trimethylate H3K56 leading to a pericentric heterochromatin localization.

Although like both H3K9me3 and H4K20me3, H3K56me3 also constitutes a mark found in DAPI-dense regions, these modifications are not identical in their localization when looked at in greater detail. H3K9me3 stains telomeric repeats [32] and our results indicate that the majority of H3K56me3 does not. In contrast to H4K20me3, we found H3K56me3 in distinct chromatin foci during all mitotic phases, indicating that this novel mark is found in much more distinct heterochromatic loci. We plan to investigate this finding in future studies.

Besides our discovery of a novel histone modification site, our study raises one important question for many researchers dealing with PTMs and their biological functions. The finding that some enzymes might have several targets is supported by another recent study showing that pericentric localization of H3K64me3, another H3 core modification, also depends on Suv39h activity [48]. Therefore, the observed severe knock-down [14] and over-expression [49] phenotypes that were previously assigned to the sole loss or gain of H3K9me3, respectively, have to be reevaluated, since Suv39h enzymes affect not only H3K9, but also H3K64 as well as H3K56 trimethylation. It is possible that the assigned role of H3K9me3 in protecting genome stability and heterochromatic gene silencing [50] is in part shared by H3K56me3.

In agreement with the finding that H3K9-specific KMTs act on H3K56, we demonstrated a strong correlation between both

residues as to their KDM-specificity. Our study expands the list of known histone target residues of enzymes belonging to the JMJD2 family of demethylases since we could show that they act not only on H3K9me3 and, in some cases, H3K36me3 [38], but also on H3K56me3. Of particular interest is our characterization of mJmjd2E, a predicted pseudogene and its human homolog hKDM4DL, which codes for a, so far, uncharacterized protein. Because of hKDM4DL's strongest expression in human testis, it will be of great interest to determine if and why removal of the trimethylation of H3K9 and H3K56 is important in this special tissue. Perhaps it is crucial during the process of histone-protamine exchange and/or relaxation of pericentric heterochromatin in humans; a statement that will be difficult to address since the mouse enzyme is predicted to be a pseudogene and not expressed. hKDM4DL might, therefore, constitute a human or primate-specific protein. If so, then functional studies on hKDM4DL in testis will be hard, if not impossible to perform.

Our study clearly puts forward H3K56me3 as a novel modification, but we were unable to address its functional relevance. Usually, knock-down of the enzymes targeting the respective modification provide insights into its biological role; but since H3K9 and H3K56 methylations are affected by the same enzymatic machinery in mammals, we do not have any technical tool at hand to pinpoint, *in vivo*, one particular phenotype to H3K56me3. However, identification of genes that affect the two modifications slightly differently in the *C. elegans* intestine opens up the possibility of future functional studies, at least in this particular organism.

Interestingly, we identified MET-1, a H3K36 KMT homolog, as needed for wild type levels of both H3K9me3 and H3K56me3. It was previously suggested that H3K36 methylation might be a prerequisite for H3K9me3 in worms [41], and perhaps it is similarly required for H3K56me3 as well. Previous studies reported that H3K9me3 in the germline is independent of MET-2 [40], however H3K9me3 levels are significantly reduced in MET-2-depleted embryos [42]. These results indicate that different KMTs might be primarily used in different tissues. Consistent with this hypothesis, depletion of MET-2 and SET-25 significantly reduces H3K9me3 levels in embryos [42], and H3K56me3 levels in the intestine (this study), but their effect is less pronounced for H3K9me3 levels in the intestine. Future studies will be needed to reveal how the preference for different KMTs is regulated in different tissues.

We identified multiple KMTs required for normal levels of both H3K9me3 and H3K56me3. One possible explanation for the requirement of two or more methyltransferases is that one of these KMTs deposits mono- (and perhaps di-) methylation, while the second KMT deposits trimethylation, in a manner dependent on prior mono- or dimethylation. This model is similar to what was previously reported for MET-2 and SET-25 in embryos [42]. Alternative possibilities include indirect effects, perhaps involving non-histone targets for these proteins.

Early EM studies revealed that *C. elegans* embryos lack electron-dense material, classically associated with heterochromatin [51]. In addition, while in mammalian cells H3K9me3 co-localizes with DAPI-bright regions of pericentric heterochromatin, in *C. elegans*, H3K9me3 localizes to DAPI-faint regions [40], leading to the suggestion that *C. elegans* lacks heterochromatin or that heterochromatin is different in this species [40]. *C. elegans* chromosomes are holocentric, and in the absence of a localized centromere, the

phrase “pericentric “ does not apply. Instead, the brightest foci of H3K9me3 in *C. elegans* nuclei associate with the nuclear lamina [42]. H3K9me3 is coincident with H3K27me3 and nuclear lamina protein LEM-1, all of which are enriched along chromosome arms [42,52]. Therefore, these regions most likely are similar to mammalian heterochromatin near the nuclear periphery, or lamin associated domains, LADs [53]. Our results show that H3K56me3 colocalizes with H3K9me3 in worms, suggesting that H3K56me3 likely marks these lamin associated domains.

In agreement with a specialized role of H3K56me3 in testis is the finding that sperm cells in *C. elegans* contain solely trimethylation of H3K56 but not of H3K9. It will be of interest to see if H3K56me3 has an evolutionary conserved role in germline development, although its functional implication might be different in different metazoans.

## Supporting Information

**Figure S1 Immunoblot peptide competition experiments to determine specificity of  $\alpha$ H3K9me3 antibodies used in this study.**  $\alpha$ H3K9me3 antibodies from (A) Active Motif or (B) the Jenuwein laboratory [16] were pre-incubated with 2  $\mu$ g/ml competitor peptides before addition to immunoblots containing recombinant H3 protein (R) or acid extracted HeLa Kyoto histones (H) (top). Ponceau staining (bottom) serves as loading control. (TIF)

**Figure S2 Members of the JMJD2 family of demethylases affect H3K56me3.** (A) IF microscopy of HeLa Kyoto cells that were transfected with GFP-tagged mJmjd2a-d and human Jmjd2d homolog hKDM4 (green) and co-stained with  $\alpha$ H3K56me3 antibody (red) and DAPI (DNA, blue). Arrows indicate transfected and GFP-positive cells. Scale bar = 10  $\mu$ m. See also Figure 4A for detailed PTM analysis of HeLa cells transfected with mJmjd2E-GFP. (B) IF microscopy of HeLa Kyoto cells that were transfected with mJmjd2E-GFP (green) and co-stained with various histone PTM-specific antibodies (red) and DAPI (DNA, blue). Arrows indicate transfected and GFP-positive cells. Scale bar = 10  $\mu$ m. See also Figure 4B that contains a listing of the results depicted here. (TIF)

**Table S1 List of peptides used in peptide competition experiments.** (DOCX)

## Acknowledgments

We thank Christian Feller for providing histones from S2 cells. We are grateful to all members of the Hake laboratory, especially Raphael Kunisch, and we thank Lothar Schermelleh, Heinrich Leonhardt, and Boris Joffe for discussions and help.

## Author Contributions

Conceived and designed the experiments: APMJ MW GC IS GS SBH. Performed the experiments: APMJ SB MH SP MW IS MS. Analyzed the data: APMJ SB MH SP MW GC IS GS SBH. Contributed reagents/materials/analysis tools: APMJ SB MH SP MW GC IS GS SBH. Wrote the paper: SBH.

## References

1. Kouzarides T (2007) Chromatin modifications and their function. *Cell* 128: 693–705.
2. Campos EI, Reinberg D (2009) Histones: annotating chromatin. *Annu Rev Genet* 43: 559–599.

3. Strahl BD, Allis CD (2000) The language of covalent histone modifications. *Nature* 403: 41–45.
4. Xu F, Zhang K, Grunstein M (2005) Acetylation in histone H3 globular domain regulates gene expression in yeast. *Cell* 121: 375–385.
5. Xie W, Song C, Young NL, Sperling AS, Xu F, et al. (2009) Histone h3 lysine 56 acetylation is linked to the core transcriptional network in human embryonic stem cells. *Mol Cell* 33: 417–427.
6. Masumoto H, Hawke D, Kobayashi R, Verreault A (2005) A role for cell-cycle-regulated histone H3 lysine 56 acetylation in the DNA damage response. *Nature* 436: 294–298.
7. Recht J, Tsubota T, Tanny JC, Diaz RL, Berger JM, et al. (2006) Histone chaperone Asf1 is required for histone H3 lysine 56 acetylation, a modification associated with S phase in mitosis and meiosis. *Proc Natl Acad Sci U S A* 103: 6988–6993.
8. Celic I, Masumoto H, Griffith WP, Meluh P, Cotter RJ, et al. (2006) The sirtuins hst3 and Hst4p preserve genome integrity by controlling histone h3 lysine 56 deacetylation. *Curr Biol* 16: 1280–1289.
9. Driscoll R, Hudson A, Jackson SP (2007) Yeast Rtt109 promotes genome stability by acetylating histone H3 on lysine 56. *Science* 315: 649–652.
10. Li Q, Zhou H, Wurtele H, Davies B, Horadzovsky B, et al. (2008) Acetylation of histone H3 lysine 56 regulates replication-coupled nucleosome assembly. *Cell* 134: 244–255.
11. Garcia BA, Hake SB, Diaz RL, Kauer M, Morris SA, et al. (2007) Organismal differences in post-translational modifications in histones H3 and H4. *J Biol Chem* 282: 7641–7655.
12. Yu Y, Song C, Zhang Q, Dimaggio PA, Garcia BA, et al. (2012) Histone H3 Lysine 56 Methylation Regulates DNA Replication through Its Interaction with PCNA. *Mol Cell*.
13. Neumann B, Held M, Liebel U, Erfle H, Rogers P, et al. (2006) High-throughput RNAi screening by time-lapse imaging of live human cells. *Nat Methods* 3: 385–390.
14. Peters AH, O'Carroll D, Scherthan H, Mechtler K, Sauer S, et al. (2001) Loss of the Suv39h histone methyltransferases impairs mammalian heterochromatin and genome stability. *Cell* 107: 323–337.
15. Schotta G, Sengupta R, Kubicek S, Malin S, Kauer M, et al. (2008) A chromatin-wide transition to H4K20 monomethylation impairs genome integrity and programmed DNA rearrangements in the mouse. *Genes Dev* 22: 2048–2061.
16. Peters AH, Kubicek S, Mechtler K, O'Sullivan RJ, Derijck AA, et al. (2003) Partitioning and plasticity of repressive histone methylation states in mammalian chromatin. *Mol Cell* 12: 1577–1589.
17. Shechter D, Dormann HL, Allis CD, Hake SB (2007) Extraction, purification and analysis of histones. *Nat Protoc* 2: 1445–1457.
18. Bonisch C, Schneider K, Punzeler S, Wiedemann SM, Bielmeier C, et al. (2012) H2A.Z.2.2 is an alternatively spliced histone H2A.Z variant that causes severe nucleosome destabilization. *Nucleic Acids Res*.
19. Hake SB, Garcia BA, Kauer M, Baker SP, Shabanowitz J, et al. (2005) Serine 31 phosphorylation of histone variant H3.3 is specific to regions bordering centromeres in metaphase chromosomes. *Proc Natl Acad Sci U S A* 102: 6344–6349.
20. Csankovszki G, McDonel P, Meyer BJ (2004) Recruitment and spreading of the *C. elegans* dosage compensation complex along X chromosomes. *Science* 303: 1182–1185.
21. Wells MB, Snyder MJ, Custer LM, Csankovszki G (2012) *Caenorhabditis elegans* dosage compensation regulates histone H4 chromatin state on X chromosomes. *Mol Cell Biol* 32: 1710–1719.
22. Wiedemann SM, Mildner SN, Bonisch C, Israel L, Maiser A, et al. (2010) Identification and characterization of two novel primate-specific histone H3 variants, H3.X and H3.Y. *J Cell Biol* 190: 777–791.
23. Fodor BD, Kubicek S, Yonezawa M, O'Sullivan RJ, Sengupta R, et al. (2006) Jmjd2b antagonizes H3K9 trimethylation at pericentric heterochromatin in mammalian cells. *Genes Dev* 20: 1557–1562.
24. Kamath RS, Ahringer J (2003) Genome-wide RNAi screening in *Caenorhabditis elegans*. *Methods* 30: 313–321.
25. Ozdemir A, Masumoto H, Fitzjohn P, Verreault A, Logie C (2006) Histone H3 lysine 56 acetylation: a new twist in the chromosome cycle. *Cell Cycle* 5: 2602–2608.
26. Das C, Lucia MS, Hansen KC, Tyler JK (2009) CBP/p300-mediated acetylation of histone H3 on lysine 56. *Nature* 459: 113–117.
27. Vempati RK, Jayani RS, Notani D, Sengupta A, Galande S, et al. (2010) p300-mediated acetylation of histone H3 lysine 56 functions in DNA damage response in mammals. *J Biol Chem* 285: 28553–28564.
28. Yuan J, Pu M, Zhang Z, Lou Z (2009) Histone H3-K56 acetylation is important for genomic stability in mammals. *Cell Cycle* 8: 1747–1753.
29. Gu B, Watanabe K, Dai X (2012) Pygo2 regulates histone gene expression and H3 K56 acetylation in human mammary epithelial cells. *Cell Cycle* 11: 79–87.
30. Salic A, Mitchison TJ (2008) A chemical method for fast and sensitive detection of DNA synthesis in vivo. *Proc Natl Acad Sci U S A* 105: 2415–2420.
31. Schotta G, Lachner M, Sarma K, Ebert A, Sengupta R, et al. (2004) A silencing pathway to induce H3-K9 and H4-K20 trimethylation at constitutive heterochromatin. *Genes Dev* 18: 1251–1262.
32. Chadwick BP (2007) Variation in Xi chromatin organization and correlation of the H3K27me3 chromatin territories to transcribed sequences by microarray analysis. *Chromosoma* 116: 147–157.
33. Trievel RC (2004) Structure and function of histone methyltransferases. *Crit Rev Eukaryot Gene Expr* 14: 147–169.
34. Dambacher S, Hahn M, Schotta G (2010) Epigenetic regulation of development by histone lysine methylation. *Heredity (Edinb)* 105: 24–37.
35. Rea S, Eisenhaber F, O'Carroll D, Strahl BD, Sun ZW, et al. (2000) Regulation of chromatin structure by site-specific histone H3 methyltransferases. *Nature* 406: 593–599.
36. Tian X, Fang J (2007) Current perspectives on histone demethylases. *Acta Biochim Biophys Sin (Shanghai)* 39: 81–88.
37. Hou H, Yu H (2010) Structural insights into histone lysine demethylation. *Curr Opin Struct Biol* 20: 739–748.
38. Shin S, Janknecht R (2007) Diversity within the JMJD2 histone demethylase family. *Biochem Biophys Res Commun* 353: 973–977.
39. Whetstine JR, Nottke A, Lan F, Huarte M, Smolikov S, et al. (2006) Reversal of histone lysine trimethylation by the JMJD2 family of histone demethylases. *Cell* 125: 467–481.
40. Bessler JB, Andersen EC, Villeneuve AM (2010) Differential localization and independent acquisition of the H3K9me2 and H3K9me3 chromatin modifications in the *Caenorhabditis elegans* adult germ line. *PLoS Genet* 6: e1000830.
41. Andersen EC, Horvitz HR (2007) Two *C. elegans* histone methyltransferases repress lin-3 EGF transcription to inhibit vulval development. *Development* 134: 2991–2999.
42. Towbin BD, Gonzalez-Aguilera C, Sack R, Gaidatzis D, Kalck V, et al. (2012) Step-Wise Methylation of Histone H3K9 Positions Heterochromatin at the Nuclear Periphery. *Cell* 150: 934–947.
43. Tjeertes JV, Miller KM, Jackson SP (2009) Screen for DNA-damage-responsive histone modifications identifies H3K9Ac and H3K56Ac in human cells. *EMBO J* 28: 1878–1889.
44. Rufiange A, Jacques PE, Bhat W, Robert F, Nourani A (2007) Genome-wide replication-independent histone H3 exchange occurs predominantly at promoters and implicates H3 K56 acetylation and Asf1. *Mol Cell* 27: 393–405.
45. Williams SK, Truong D, Tyler JK (2008) Acetylation in the globular core of histone H3 on lysine-56 promotes chromatin disassembly during transcriptional activation. *Proc Natl Acad Sci U S A* 105: 9000–9005.
46. Aslam A, Logie C (2010) Histone H3 serine 57 and lysine 56 interplay in transcription elongation and recovery from S-phase stress. *PLoS One* 5: e10851.
47. Tachibana M, Sugimoto K, Nozaki M, Ueda J, Ohta T, et al. (2002) G9a histone methyltransferase plays a dominant role in euchromatic histone H3 lysine 9 methylation and is essential for early embryogenesis. *Genes Dev* 16: 1779–1791.
48. Daujat S, Weiss T, Mohn F, Lange UC, Ziegler-Birling C, et al. (2009) H3K64 trimethylation marks heterochromatin and is dynamically remodeled during developmental reprogramming. *Nat Struct Mol Biol* 16: 777–781.
49. Czvitkovich S, Sauer S, Peters AH, Deiner E, Wolf A, et al. (2001) Overexpression of the SUV39H1 histone methyltransferase induces altered proliferation and differentiation in transgenic mice. *Mech Dev* 107: 141–153.
50. Schotta G, Ebert A, Reuter G (2003) SU(VAR)3-9 is a conserved key function in heterochromatic gene silencing. *Genetica* 117: 149–158.
51. Leung B, Hermann GJ, Priess JR (1999) Organogenesis of the *Caenorhabditis elegans* intestine. *Dev Biol* 216: 114–134.
52. Gu SG, Fire A (2010) Partitioning the *C. elegans* genome by nucleosome modification, occupancy, and positioning. *Chromosoma* 119: 73–87.
53. Guelen L, Pagie L, Brasset E, Meuleman W, Faza MB, et al. (2008) Domain organization of human chromosomes revealed by mapping of nuclear lamina interactions. *Nature* 453: 948–951.



Supplementary Figure S1 (Jack et al.)

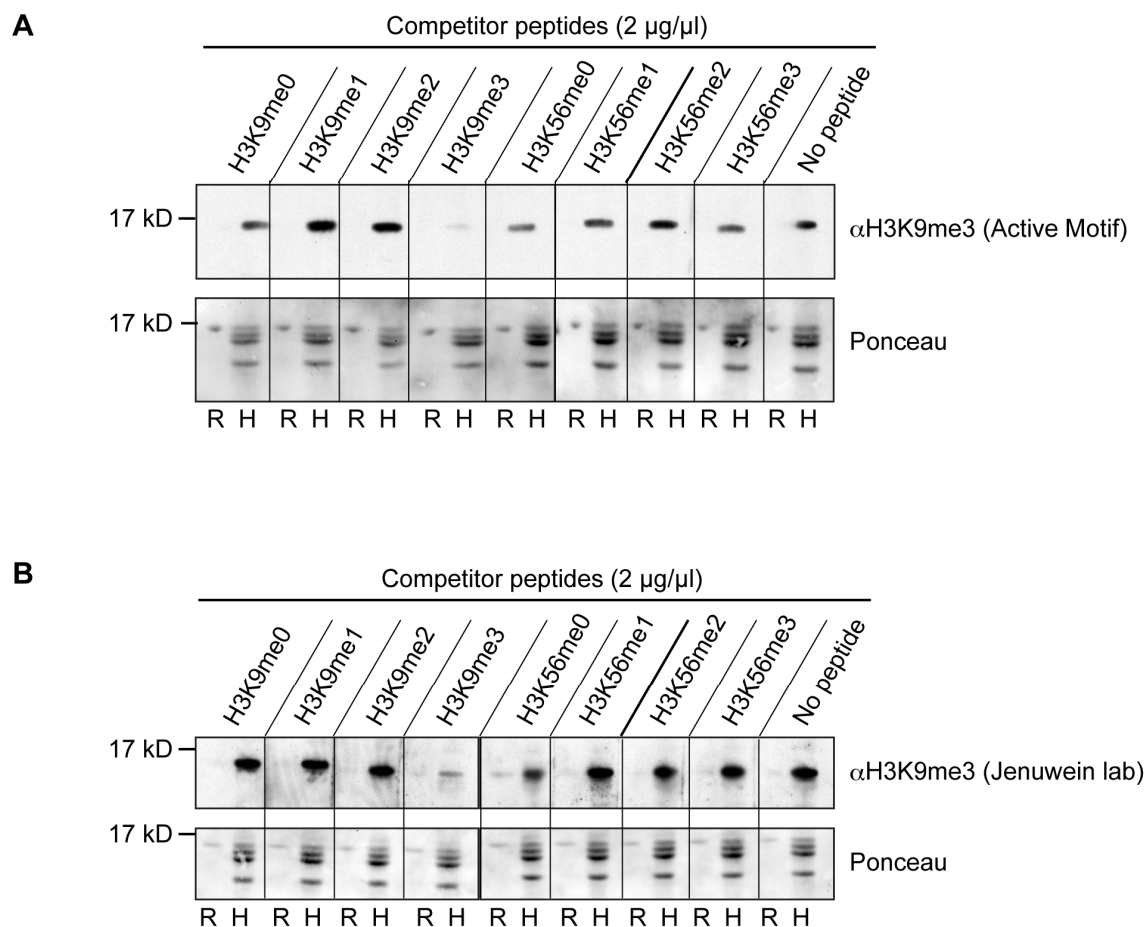


**Figure S1.**

**Immunoblot peptide competition experiments to determine specificity of  $\alpha$ H3K9me3 antibodies used in this study.**  $\alpha$ H3K9me3 antibodies from (A) Active Motif or (B) the Jenuwein laboratory [16] were pre-incubated with 2 µg/ml competitor peptides before addition to immunoblots containing recombinant H3 protein (R) or acid extracted HeLa Kyoto histones (H) (top). Ponceau staining (bottom) serves as loading control.

**Supplementary Table 1 (Jack et al.)**

Peptide	Sequence
H3K56me0	VALREIRRYQKSTELLIRKL
H3K56me1	VALREIRRYQK(me1)STELLIRKL
H3K56me2	VALREIRRYQK(me2)STELLIRKL
H3K56me3	VALREIRRYQK(me3)STELLIRKL
H3K9me0	ARTKQTARKSTGGKAPRKQL
H3K9me1	ARTKQTARK(me1)STGGKAPRKQL
H3K9me2	ARTKQTARK(me2)STGGKAPRKQL
H3K9me3	ARTKQTARK(me3)STGGKAPRKQL
H3K4me3	ARTK(me3)QTARKSTGGKAPRKQL
H3K64me3	YQKSTELLIRK(me3)LPFQRLVRE
H3K79me3	LVREIAQDFK(me3)TDLRFQS

**Table S1.**

List of peptides used in peptide competition experiments.

Supplementary Figure S2 (Jack et al.)

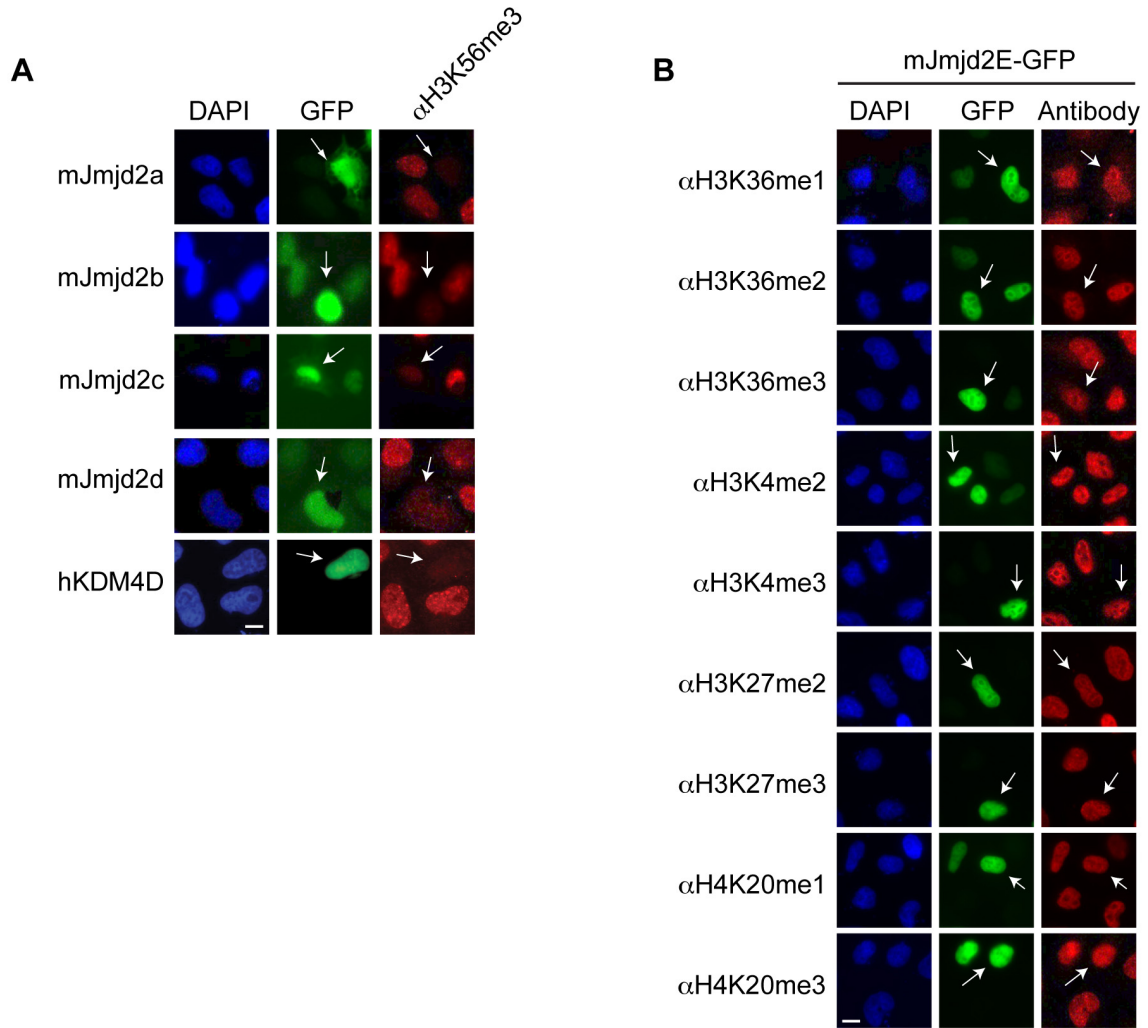


**Figure S2.**

**Members of the JMJD2 family of demethylases affect H3K56me3.** (A) IF microscopy of HeLa Kyoto cells that were transfected with GFP-tagged mJmjd2a-d and human Jmjd2d homolog hKDM4 (green) and co-stained with  $\alpha$ H3K56me3 antibody (red) and DAPI (DNA, blue). Arrows indicate transfected and GFP-positive cells. Scale bar = 10  $\mu$ m. See also [Figure 4A](#) for detailed PTM analysis of HeLa cells transfected with mJmjd2E-GFP. (B) IF microscopy of HeLa Kyoto cells that were transfected with mJmjd2E-GFP (green) and co-stained with various histone PTM-specific antibodies (red) and DAPI (DNA, blue). Arrows indicate transfected and GFP-positive cells. Scale bar = 10  $\mu$ m. See also [Figure 4B](#) that contains a listing of the results depicted here.

# **Versatile toolbox for high throughput biochemical and functional studies with fluorescent fusion proteins**

PloS One 7(5), (2012)

Pichler G, **Jack A**, Wolf P, Hake SB.

# Versatile Toolbox for High Throughput Biochemical and Functional Studies with Fluorescent Fusion Proteins

Garwin Pichler<sup>1\*</sup>, Antonia Jack<sup>2</sup>, Patricia Wolf<sup>1</sup>, Sandra B. Hake<sup>2</sup>

**1** Department of Biology II and Center for Integrated Protein Science Munich (CIPSM), Ludwig Maximilians University Munich, Planegg-Martinsried, Munich, Germany, **2** Center for Integrated Protein Science Munich at the Adolf-Butenandt Institute, Department of Molecular Biology, Ludwig Maximilians University of Munich, Munich, Germany

## Abstract

Fluorescent fusion proteins are widely used to study protein localization and interaction dynamics in living cells. However, to fully characterize proteins and to understand their function it is crucial to determine biochemical characteristics such as enzymatic activity and binding specificity. Here we demonstrate an easy, reliable and versatile medium/high-throughput method to study biochemical and functional characteristics of fluorescent fusion proteins. Using a new system based on 96-well micro plates comprising an immobilized GFP-binding protein (GFP-multitrap), we performed fast and efficient one-step purification of different GFP- and YFP-fusion proteins from crude cell lysate. After immobilization we determined highly reproducible binding ratios of cellular expressed GFP-fusion proteins to histone-tail peptides, DNA or selected RFP-fusion proteins. In particular, we found Cbx1 preferentially binding to di- and trimethylated H3K9 that is abolished by phosphorylation of the adjacent serine. DNA binding assays showed, that the MBD domain of MeCP2 discriminates between fully methylated over unmethylated DNA and protein-protein interactions studies demonstrate, that the PBD domain of Dnmt1 is essential for binding to PCNA. Moreover, using an ELISA-based approach, we detected endogenous PCNA and histone H3 bound at GFP-fusions. In addition, we quantified the level of H3K4me2 on nucleosomes containing different histone variants. In summary, we present an innovative medium/high-throughput approach to analyse binding specificities of fluorescently labeled fusion proteins and to detect endogenous interacting factors in a fast and reliable manner *in vitro*.

**Citation:** Pichler G, Jack A, Wolf P, Hake SB (2012) Versatile Toolbox for High Throughput Biochemical and Functional Studies with Fluorescent Fusion Proteins. PLoS ONE 7(5): e36967. doi:10.1371/journal.pone.0036967

**Editor:** Pierre-Antoine Defosse, Université Paris-Diderot, France

**Received:** January 12, 2012; **Accepted:** April 10, 2012; **Published:** May 11, 2012

**Copyright:** © 2012 Pichler et al. This is an open-access article distributed under the terms of the Creative Commons Attribution License, which permits unrestricted use, distribution, and reproduction in any medium, provided the original author and source are credited.

**Funding:** GP was supported by the International Doctorate Program NanoBioTechnology (IDK-NBT, <http://www.cens.de/doctorate-program/>) and GP and AJ by the International Max Planck Research School for Molecular and Cellular Life Sciences (IMPRS-LS, <https://www.imprs-ls.de/>). PW is a fellow of the Graduate School Life Science Munich (LSM, <http://www.lsm.bio.lmu.de/>). SBH was supported by CIPSM (<http://www.cipsm.de/en/index.html>) and the DFG (<http://www.dfg.de/index.jsp>). The funders had no role in study design, data collection and analysis, decision to publish, or preparation of the manuscript.

**Competing Interests:** The authors have declared that no competing interests exist.

\* E-mail: [pichler@bio.lmu.de](mailto:pichler@bio.lmu.de)

## Introduction

Over the past decade a variety of proteomic approaches have been used to identify cellular components in order to understand the mechanism and inner workings of cells [1]. For example, mass spectrometry-based proteomics uncovered the proteome of many different organisms as well as cell-type specific differences in protein expression. However, to understand and characterize the function of single proteins, as well as the interplay between different factors, it is essential to gain further insights into their abundance, localization, dynamic interactions and substrate specificities.

Fluorescent proteins like the green fluorescent proteins (GFP) [2] and spectral variants have become popular tools to study the localization and dynamic interactions of proteins *in vivo*. Despite, the availability of a variety of commercial mono- and polyclonal antibodies against GFP and other fluorescent proteins [3,4] (e.g. Abcam, UK; Sigma, USA; Roche, Germany, ChromoTek, Germany), proteins are mostly fused to a small epitope tag such as FLAG or c-Myc to analyze biochemical characteristics like enzymatic activities and/or binding specificities. Thus, integration of such *in vitro* data with *in vivo* data obtained with fluorescently labeled proteins has, in part, been impeded by the simple fact that

different protein tags are used for different applications. The gold standard to examine binding affinities is surface plasmon resonance (SPR) [5]. One drawback of this method is the need of large amount of proteins. Such proteins have to be expressed and purified from bacterial systems (e.g. *E. coli*) or lower eukaryotes such as yeast (e.g. *S. cerevisiae*). Thus, the recombinant proteins lack essential post-translational modifications or are not folded properly possibly leading to different binding properties and inaccurate results. In addition with SPR measurements one can only determine the binding affinity to one substrate. This does not reflect the *in vivo* situation where most proteins have the choice between many different binding substrates in parallel.

Protein microarrays are an alternative to study protein-protein interactions in high-throughput manner [6]. Once more the drawback of this *in vitro* method is the laborative and time-consuming preparation of recombinant proteins or protein domains. Therefore protein microarrays are limited to domains that can be produced as soluble, well-folded proteins [6].

Recently, specific GFP binding proteins based on single domain antibodies derived from Lama alpaca have been described [7] (GFP-Trap ChromoTek, Germany). The GFP-Trap exclusively binds to wtGFP, eGFP and GFP<sup>S65T</sup> as well as to YFP and eYFP. Coupling to matrices including agarose beads or magnetic

particles the GFP-Trap allows for one-step purification of GFP-fusion proteins. Previous studies made use of the GFP-Trap to perform a broad range of different methods including mass spectrometry analysis [8], DNA binding, DNA methyltransferase activity assays [9], as-well-as histone-tail peptide binding assays [10]. One mayor disadvantage of the GFP-Trap is, that batch purification of GFP-fusions is very laborious and time-consuming and one cannot test different GFP-fusion and/or assay conditions in parallel. Here, we present an innovative and versatile high-throughput method to quantitatively measure binding specificities and to detect endogenous interacting factors in a fast and reliable manner *in vitro*: 96-well micro plates coated with immobilized GFP-Trap (GFP-multiTrap). To demonstrate the general suitability of our assays, we choose already known binding partners and compared our results with previous publications. Using this method, we could confirm that Cbx1 preferentially binds to di- and trimethylated histone H3 lysine 9 and that this binding is abolished by phosphorylation of the adjacent serine 10 [11–13]. In addition, we determined a 4-fold preference of the MBD domain of MeCP2 for fully over unmethylated DNA in accordance to [14–16]. Furthermore, we performed protein-protein interaction assays and found that the Dnmt1 binds to PCNA in a PBD domain-dependent manner consistent to [17,18]. In contrast, LigaseIII binds Xrcc1 but does not interact with PCNA [19,20]. Using an ELISA-based assay, we were able to detect endogenous PCNA bound to immunoprecipitated Dnmt1, Fen1 and PCNA itself. In accordance with our protein-protein interaction data, Dnmt1 lacking the PBD domain (Dnmt1 $\Delta$ PBD) could not co-immunoprecipitate with PCNA. Consistent with our histone-tail peptide binding data, we could detect endogenous histone H3 bound to Cbx1. Finally, we quantified specific histone modifications on nucleosomes comprising different histone variants. All of these data clearly demonstrate the versatility and easy handling of this high-throughput approach and its immense benefit to many researchers.

## Results

### One-step Purification of GFP-fusion Proteins

In a first step, we tested the efficiency of the GFP-multiTrap to purify GFP-fusion proteins from cellular extracts. First, we examined the pull-down efficiency of a GFP-tagged protein and chose GFP-Cbx1 as a model protein. Cbx1 is a chromodomain-containing protein related to the *Drosophila* HP1 $\beta$ , a well-studied heterochromatin-associated protein [11]. We used cell extracts from HEK293T cells transiently expressing GFP-Cbx1 or GFP, purified the GFP-fusions using the GFP-multiTrap, eluted the bound fractions, separated them by SDS-PAGE and visualized the bound proteins by coomassie staining. The bound fractions displayed mainly GFP as well as GFP-Cbx1 with only minor impurities (Figure 1A), providing therefore a reliable tool for downstream biochemical analyses. Notably, the washing conditions can be varied according to the downstream applications. In addition to these qualitative results, we performed experiments to quantify the pull-down efficiency. For this purpose we quantified the amount of bound GFP with varying concentrations of input GFP from cellular extracts. After binding, the single wells were subjected to several washing steps and bound GFP was analyzed by fluorescent read-out using a micro plate reader. Notably, the input amount of protein/substrate was measured in solution, whereas the bound fraction represents one value on the 96-well surface. We measured the fluorescence intensities of bound GFP and plotted the amount of bound GFP as a function of total GFP (Figure 1B). The amount of bound GFP increased linearly from 10

to 130 nM of total input and saturated between 130 and 400 nM. Next, we quantified the amount of bound GFP by immunoblotting. Therefore, we eluted the bound GFP fractions, separated them by SDS-PAGE, visualized the bound proteins by immunoblot analysis (Figure 1C) and quantified the GFP signal by measuring the mean intensity via Image J (Figure 1D). Similar to the quantification by fluorescent read out using a micro plate reader, the amount of bound GFP increases linearly from 10 to 130 nM of total input and saturates between 130 and 400 nM.

In summary, we demonstrated that the GFP-multiTrap allows for fast and efficient one-step purification of GFP-fusion proteins directly from crude cell lysates in a high-throughput manner. The method works well for both qualitative and quantitative measurements and the immunoprecipitated GFP-fusions can then be further tested in biochemical assays.

### In vitro Histone-tail Peptide and DNA Binding Assay

In the next assay we determined whether this approach is also feasible to quantify binding affinities between GFP-proteins and peptides or DNA. First, we analyzed histone-tail peptide binding specificities of the chromobox homolog 1, Cbx1, fused with a N-terminal GFP-tag using the GFP-multiTrap. GFP-Cbx1 was purified from mammalian cell lysate, as described above, and the bound protein was incubated with TAMRA-labeled histone-tail peptides. A set of 20 different histone-tail peptides (Table 1) was used in technical triplicates in parallel and GFP served as negative control (GFP data is not shown). After removal of unbound substrate the amounts of protein and histone-tail peptide were determined by fluorescence intensity measurements using a micro plate reader. Binding ratios were calculated by dividing the concentration of bound histone-tail peptide by the concentration of GFP fusion (Figure 2A). GFP-Cbx1 preferentially binds H3K9me3 and H3K9me2 histone-tail peptides consistent with previous studies [11,12]. As expected, the phosphorylation of serine 10 (S10p) next to the trimethylated lysine 9 leads prevents binding of Cbx1, which is in accordance with previous reports [13]. In addition to fluorescent quantification via a micro plate reader, we scanned the TAMRA signals using a Typhoon scanner (Figure 2B). Here, we detected TAMRA signals in the wells corresponding to di- and trimethylated H3K9. Notably, we did not detect differences in binding towards di- and trimethylated H3K9 using a micro plate reader. However, we could detect a preference for tri- over dimethylated H3K9 using a fluorescence scanner. These differences could result from different sensitivities of both methods. Furthermore, we performed a competition assay to demonstrate the specificity of the histone-tail peptide-binding assay. We incubated GFP-Cbx1 with TAMRA-labeled H3K9me3 in parallel with either biotinylated H3K9me3 or H3K9ac histone-tail peptides. As expected, the addition of biotinylated H3K9me3 histone-tail peptide significantly decreased the binding of Cbx1 to TAMRA-labeled H3K9me3, whereas the addition of biotinylated H3K9ac did not alter the binding ratios (Figure 2C). In previous studies [11,12], the binding affinities of the HP1 $\beta$  chromo domain, the *Drosophila* homolog of mammalian Cbx1, for both di- and trimethylated H3K9 peptides have been found to be 7 and 2.5  $\mu$ M, respectively. In contrast, we could not detect a significant difference in binding ratios between di- and trimethylated H3K9 histone tail peptides using a micro plate reader (Figure 2A). One explanation could be the use of different expression systems. While the binding ratios for the HP1 $\beta$  chromo domain were determined using bacterially expressed protein we used a fluorescent fusion protein derived from mammalian cells. In this context a recent study revealed that recombinant HP1 $\alpha$  prepared from mammalian cultured cells exhibited a stronger binding affinity for K9-



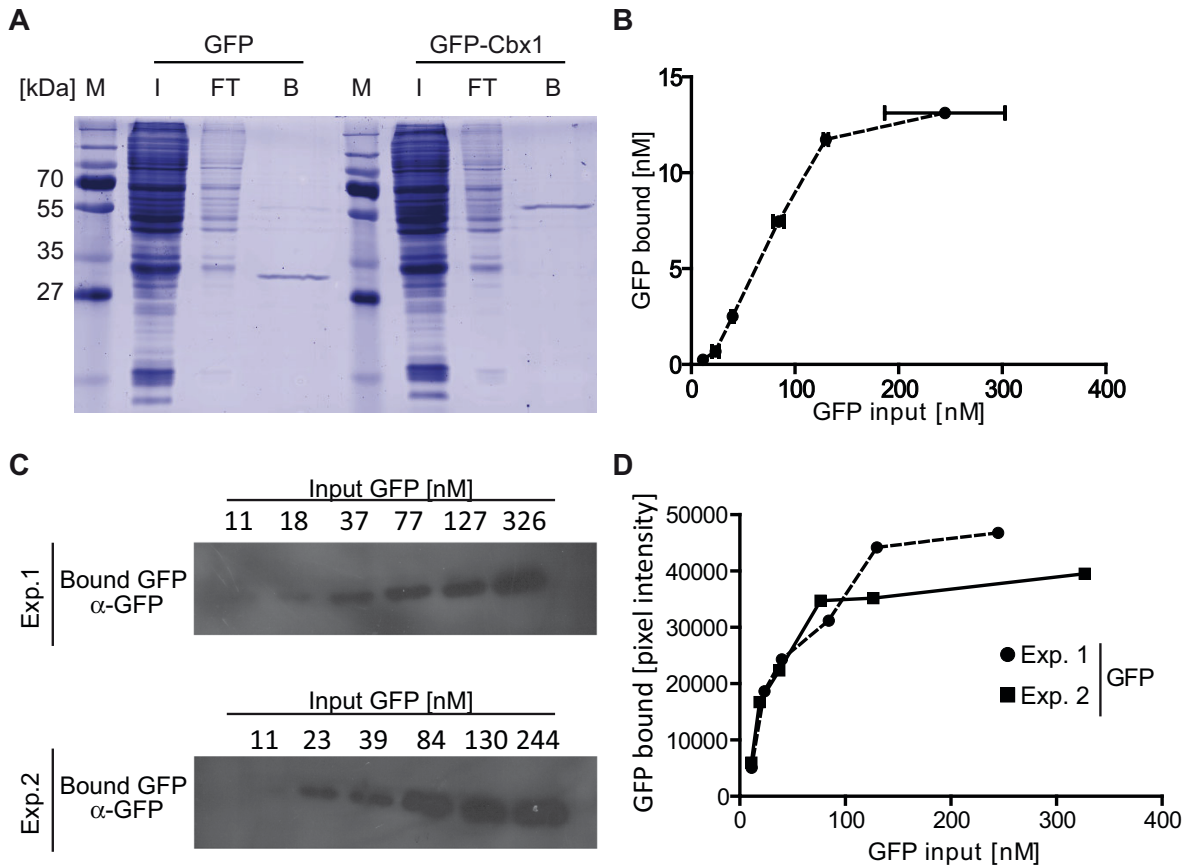


**Figure 1. One-step purification of GFP and GFP-fusion proteins.** Purification of GFP and GFP-Cbx1 expressed in HEK293T cells. All GFP concentrations were quantified via plate reader. **(A)** Purification of GFP and GFP-Cbx1 from HEK293T cell extracts, transiently transfected with the GFP-fusions. Input (I), flow-through (FT) and bound (B) fractions were separated by SDS-PAGE and visualized by coomassie staining. **(B)** Different amounts of GFP cell lysate were added into wells of a 96-well plate immobilized with the GFP-Trap (GFP-multiTrap). Shown are means  $\pm$  SD from two independent experiments. **(C)** Bound GFP fractions from both independent experiments (B) were eluted, separated by SDS-PAGE and visualized by immunoblot analysis using an anti-GFP mouse antibody (Roche, Germany). **(D)** Quantification of bound GFP fractions by immunoblotting. The mean intensities of the GFP signals were measured using Image J. doi:10.1371/journal.pone.0036967.g001

methylated histone H3 (H3K9me) in comparison to protein produced in *Escherichia coli* [21]. Biochemical analyses revealed that HP1 $\alpha$  was multiply phosphorylated at N-terminal serine residues (S11–14) in human and mouse cells and that this phosphorylation enhanced the affinity of HP1 $\alpha$  for H3K9me, displaying the importance of post-translational modifications for binding affinities [21]. To determine the binding affinity of GFP-Cbx1 to H3K9me3, we varied the input amount of histone-tail peptide. We plotted the amount of bound histone-tail peptide as a function of total peptide and fitted the values using GraphPad Prism and nonlinear regression (Figure 2D). The amount of bound H3K9me3 histone-tail peptide increases linearly and saturates at approximately 500 nM of input peptide. In contrast to H3K9me3, we could not detect any binding of Cbx1 to H3 histone-tail peptides. Notably, the exact determination of binding affinities was not possible due to differences in the technical measurement of input versus bound fractions. Here, the input amount of protein/substrate was measured in solution, whereas the bound fraction represents one value on the 96-well surface.

In addition to histone-tail peptide binding assays, we performed DNA-binding assays. We purified the methyl-binding domain (MBD) of MeCP2, fused with a C-terminal YFP tag, from cell extracts as described and performed competition binding analysis by incubating immobilized MBD-YFP with fluorescently labeled

un- and fully methylated DNA (Table 1). As a result we observed a five-fold preference of MBD for fully methylated DNA over unmethylated DNA (Figure 2E). In addition, we measured the amount of bound DNA to MBD-YFP by varying the input amount of DNA. We plotted the amount of total un- and fully methylated DNA as a function of total un- and fully methylated DNA and fitted the values using GraphPad Prism and nonlinear regression (Figure 2F). Similar to the relative binding ratios, MBD binds preferentially to fully methylated DNA. These results are in accordance with previous studies describing that MeCP2 interacts specifically with methylated DNA mediated by the MBD domain. In these studies, electrophoretic mobility shift assays (EMSA) using the isolated MBD domain expressed in *E. coli* were performed and dissociation constants of 14.7 and 1000 nM were calculated for symmetrically methylated and unmethylated DNA, respectively [14–16].

To assess the suitability of the *in vitro* histone-tail peptide and DNA binding assay for high-throughput applications, the Z-factor was calculated. For histone-tail peptide binding assays, we calculated the Z-factor using the relative binding ratios of H3K9me3 to GFP-Cbx1 as positive state and of H3K9me0 to GFP-Cbx1 as negative state. For the DNA binding assay, we calculated the Z-factor using the relative binding ratios of fully methylated DNA to MBD-YFP as positive state and of

**Table 1.** Sequences of DNA oligonucleotides and histone-tail peptides.

DNA oligos				
DNA substrate	DNA sequence			DNA labeling
CG-up	5'- CTAACAACAACTACCATCCGGACCAGAAGAGTCATCATGG -3'			No
MG-up	5'- CTAACAACAACTACCATCMGGACCAGAAGAGTCATCATGG -3'			No
um550	5'- CCATGATGACTCTTCTGGTCCGGATGGTAGTTAGTTGTTGAG -3'			ATTO550 at 5'end
um700	5'- CCATGATGACTCTTCTGGTCCGGATGGTAGTTAGTTGTTGAG -3'			ATTO700 at 5'end
mC700	5'- CCATGATGACTCTTCTGGTCMGGATGGTAGTTAGTTGTTGAG -3'			ATTO700 at 5'end
DNA substrates				
DNA substrate	CpG site	Label	Oligo I	Oligo II
UMB-550	unmethylated	550	CG-up	um550
UMB-700	unmethylated	700	CG-up	um700
FMB-700	Fully methylated	700	MG-up	mC700
DNA sets				
Binding set			Control set	
UMB-550			UMB-550	
FMB-700			UMB-700	
Histone-tail peptides				
H3 (1–20)	ART K QTARKSTGGKAPRKQLK			TAMRA at C-terminus
H3K4me1	ART X1 QTARKSTGGKAPRKQLK			
H3K4me2	ART X2 QTARKSTGGKAPRKQLK			
H3K4me3	ART X3 QTARKSTGGKAPRKQLK			
H3K4ac	ART Z QTARKSTGGKAPRKQLK			
H3K9me1	ARTKQATAR X1 S TGGKAPRKQLK			
H3K9me2	ARTKQATAR X2 S TGGKAPRKQLK			
H3K9me3	ARTKQATAR X3 S TGGKAPRKQLK			
H3K9me3S10p	ARTKQATAR X3 Z2 TGGKAPRKQLK			
H3K9ac	ARTKQATAR Z S TGGKAPRKQLK			
H3 (17–36)	RKQLATKAAR K SAPATGGVK			TAMRA at N-terminus
H3K27me1	RKQLATKAAR X1 SAPATGGVK			
H3K27me2	RKQLATKAAR X2 SAPATGGVK			
H3K27me3	RKQLATKAAR X3 SAPATGGVK			
H3K27ac	RKQLATKAAR Z SAPATGGVK			
H4 (10–29)	LGKGGAKRHR K VLRDNIQGI			
H4K20me1	LGKGGAKRHR X1 VLRDNIQGI			
H4K20me2	LGKGGAKRHR X2 VLRDNIQGI			
H4K20me3	LGKGGAKRHR X3 VLRDNIQGI			
H4K20ac	LGKGGAKRHR Z VLRDNIQGI			

X1: monomethylated Lysine; X2: dimethylated Lysine; X3: trimethylated Lysine; Z: acetylated Lysine; Z2: phosphorylated Serine.  
doi:10.1371/journal.pone.0036967.t001

unmethylated DNA to MBD-YFP as negative state (Table 2). The Z-factors of 0.766 for the histone-tail peptide binding assay and 0.756 for the DNA binding assay strongly indicate that both assays are robust, reproducible and suitable for high-throughput applications.

### In vitro Protein-protein Binding Assay

In addition to the detection of substrate specificity (e.g. histone-tail peptide) and DNA binding, analysis of the interaction with other cellular components and factors is essential to understand the function of proteins.

The use of fluorescence intensity read-out systems for the quantification of protein-protein interactions *in vitro* provides a new

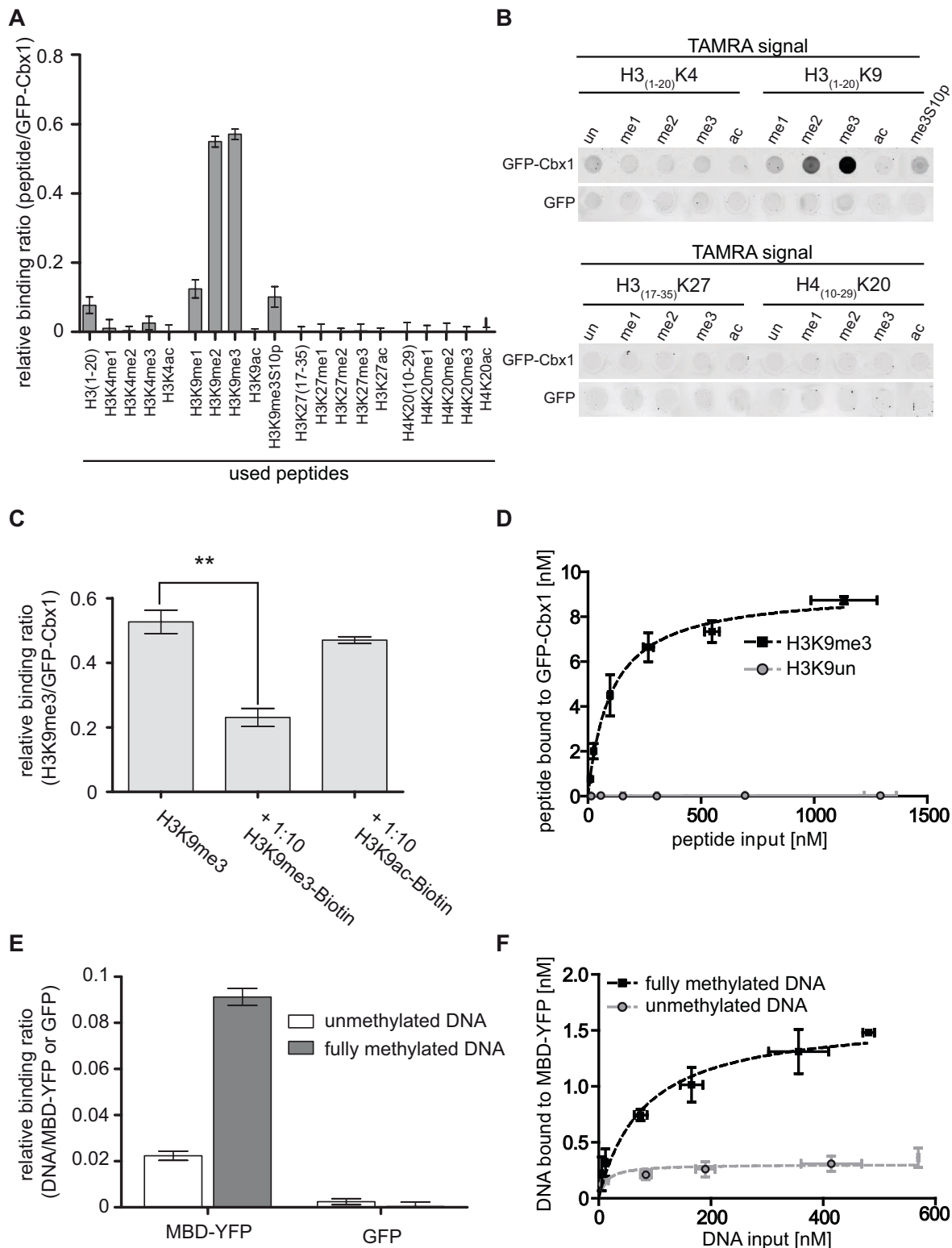


**Figure 2. In vitro histone-tail peptide and DNA binding assay.** *In vitro* binding ratios of fluorescently labeled substrates over bound GFP fusion proteins were determined. (A)–(D) *In vitro* histone-tail peptide binding assay with GFP-Cbx1. (A) Histone H3- and H4-tail binding specificities of Cbx1. A final concentration of 0.15  $\mu$ M TAMRA-labeled histone-tail peptide was added per well. Fluorescent signals of bound TAMRA-labeled histone-tail peptides and GFP-fusion protein were quantified via plate reader. Shown are means  $\pm$  SD from three independent experiments (B) Fluorescent signals of bound TAMRA-labeled histone-tail peptides visualized by fluorescent scanner. (C) Competition assay between TAMRA-labeled H3K9me3 and biotinylated histone-tail peptides with GFP-Cbx1. Shown are means  $\pm$  SD from three independent experiments. Statistical significance between the binding ratios is indicated; \*\* $P < 0.003$ . (D) Different amounts of TAMRA-labeled H3K9me3 and H3 histone-tail peptides were added to GFP-Cbx1. Three or two independent experiments for H3K9me3 or H3 histone-tail peptides were performed, respectively. Shown are means  $\pm$  SD and the amount of bound histone-tail peptide was plotted as a function of total histone-tail peptide. The curve was fitted using GraphPad Prism and



nonlinear regression. All input and bound fractions were quantified via a plate reader. **(E)** DNA binding specificities of the MBD domain of MeCP2 to un- and fully methylated DNA in direct competition. Shown are means  $\pm$  SD from three independent experiments. **(F)** Different amounts of Atto550-labeled unmethylated and Atto700-labeled fully methylated DNA in direct competition were added to purified MBD-YFP. Shown are means  $\pm$  SD from three independent experiments. The amount of bound DNA peptide was plotted as a function of total DNA. The curve was fitted using GraphPad Prism and nonlinear regression. All input and bound fractions were quantified via a plate reader. doi:10.1371/journal.pone.0036967.g002

and simple method avoiding laborious and inaccurate protein detection using conventional immunoblotting systems.

To address the question if such interaction analysis can be performed in a multi-well format we analyzed the interaction of single GFP-fusions with RFP-fusion proteins expressed in mammalian cells. More precisely, we determined quantitative binding ratios between nuclear located proteins involved in DNA-replication (PCNA) [17,18], DNA-methylation (Dnmt1) [22] as well as in DNA-repair (Xrcc1) [23]. As described, we immobilized GFP-fusions on the GFP-multiTrap and incubated them with cell lysate containing RFP-fusion proteins. After binding, we removed unbound material, measured the concentrations of RFP and GFP and calculated the molar binding ratios. Firstly, we determined the binding ratios of the green fluorescent PCNA-binding domain of Dnmt1 (GFP-PBD) to RFP-PCNA and used Dnmt1 $\Delta$ PBD as a negative control. By measuring the fluorescent signal intensities we detected that RFP-PCNA binds to GFP-PBD in a molar ratio of  $1.42 \pm 0.31$  but not to Dnmt1 $\Delta$ PBD (Figure 3A).

For a direct comparison we eluted the bound fractions, separated them by SDS-PAGE and visualized the proteins by immunoblotting (Figure 3B). Both, GFP-PBD and RFP-PCNA are detected in the input and bound fractions whereas RFP is not visible in the bound fraction of GFP-PBD (Figure 3B).

In addition, we measured the amount of bound RFP-fusion to GFP-PBD with varying the input amount of RFP-fusion. We plotted the amount of bound RFP-fusion as a function of total RFP-fusion and fitted the values using GraphPad Prism and nonlinear regression (Figure 3C). Similar to the relative binding ratios, GFP-PBD binds to RFP-PCNA but not to RFP.

These results are in accordance with previous findings that Dnmt1 associates with the replication machinery by directly binding to PCNA, a homotrimeric ring which serves as loading platform for replication factors, and that this binding depends on the PCNA-binding domain in the very N-terminus of Dnmt1 [17,18]. In addition by determining the quantitative binding ratio between both partner proteins our approach provides a more detailed insight in the binding events occurring at the central loading platform of the DNA replication.

Secondly, we determined the molar binding ratio of GFP-Ligase III to RFP-Xrcc1. Xrcc1 binds in a molar ratio of  $0.61 \pm 0.14$  to Ligase III but did not bind to other proteins such as GFP-PBD,

GFP-Dnmt1 $\Delta$ PBD or GFP. Previous studies demonstrated that DNA Ligase III was recruited to DNA repair sites via its BRCT domain mediated interaction with Xrcc1 [19,20].

For the protein-protein binding assays, we calculated the Z-factor using the protein binding ratios of RFP-PCNA to GFP-PBD as positive state and RFP to GFP-PBD as negative state (Table 2). The Z-factor of 0.56 indicated that the protein-protein binding assay is robust and reproducible.

In summary, we demonstrate a new quantitative and reliable high-throughput method to analyze protein-protein interactions using GFP- and RFP-fusion proteins.

### Enzyme-linked Immunosorbent Assay (ELISA)

Next we examined endogenous protein-protein interactions using an ELISA assay. For this purpose, we precipitated GFP-fusion proteins in the 96 well format on the GFP-multiTrap and cross-linked bound fractions with formaldehyde (CH<sub>2</sub>O) and/or treated the bound fractions with methanol (MeOH). Using specific antibodies against PCNA, we determined the binding of endogenous PCNA to GFP fusions of Dnmt1, Dnmt1 $\Delta$ PBD, PCNA, Fen1, which is a flap endonuclease and an essential DNA replication protein [24]. We could detect endogenous PCNA binding to Dnmt1 but not to Dnmt1 $\Delta$ PBD similar to the results obtained with the protein-protein interaction assay using RFP-PCNA (Figure 4A). In addition, we detected binding of endogenous PCNA to Fen1 but also to PCNA itself. These results fit well to former studies showing that Fen1 or maturation factor 1 associates with PCNA in a stoichiometric complex of three Fen1 molecules per PCNA trimer [25,26]. In addition to 100 described interacting partners, it is known that PCNA also interacts with itself and forms a trimeric ring, which is confirmed by our ELISA assay by giving a signal for endogenous PCNA binding to GFP-PCNA (Figure 4A).

Next, we determined the binding of Cbx1 to endogenous histone H3. Similar to PCNA, we precipitated GFP-Cbx1 and GFP and detected endogenous H3 via an H3-antibody coupled to HRP. In accordance with the experiments using TAMRA labeled histone 3 peptides, we observed an H3 ELISA signal for binding to Cbx1 but not to GFP. Using an H3K9me3-specific antibody, we could not detect an ELISA signal (data not shown), due to the fact that the tight binding of Cbx1 (Figure 2) to H3K9me3 most likely

**Table 2.** Overview of relative binding ratios and Z-factor values.

Relative binding ratios of Substrate/GFP- or YFP-fusion						
Fusion protein	Histone-tail peptide binding		DNA binding		Protein-protein binding	
	GFP-Cbx1		MBD-YFP		GFP-PBD	
Substrate	H3K9me3	H3K9un	Fully methylated DNA	Unmethylated DNA	RFP-PCNA	RFP
<b>Average ratio</b>	0,5715	0,0772	0,0912	0,0223	1,487	0,005
<b>Standard deviation</b>	0,0150	0,0236	0,0037	0,0019	0,2111	0,006
<b>Z-factor</b>	0,766		0,756		0,560	

Based on the average relative binding ratios and the standard deviations we calculated the Z-factor.

doi:10.1371/journal.pone.0036967.t002

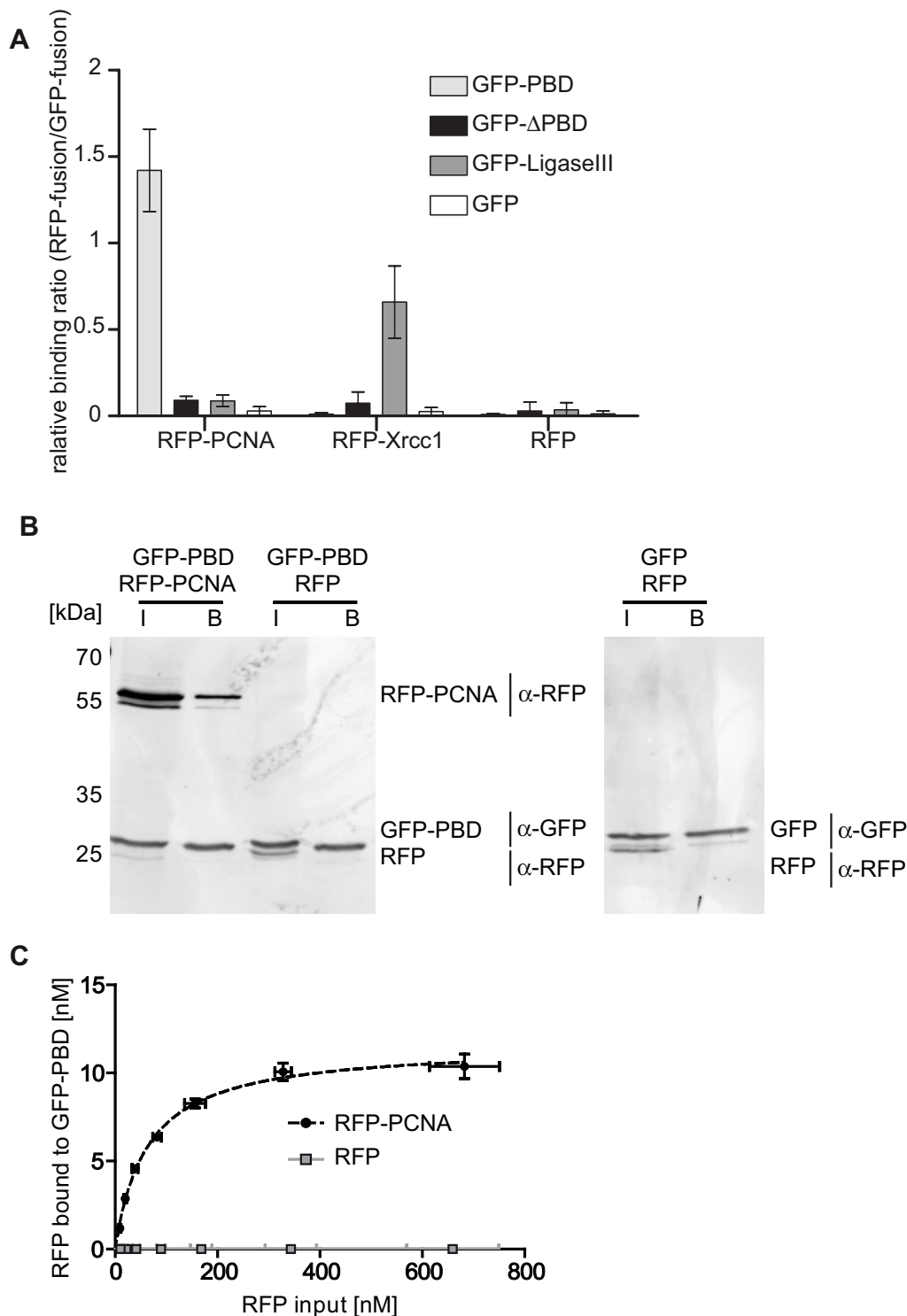


**Figure 3. In vitro Protein-Protein binding assay.** (A) *In vitro* binding ratios of RFP-fusion proteins over GFP-fusion proteins. Shown are means  $\pm$  SD from six independent experiments. (B) After immunoprecipitation input (I) and bound (B) fractions were separated by SDS-PAGE and visualized by immunoblot analysis using the anti-GFP rat monoclonal antibody, 3H9, and the anti-RFP rat monoclonal antibody, 5F8 (both ChromoTek, Germany). GFP-PBD: 30 kDa; RFP-PCNA: 56 kDa; GFP: 28 kDa, RFP: 26 kDa. (C) Different amounts of RFP-fusion protein were added to purified GFP-PBD. Shown are means  $\pm$  SD from two independent experiments. The amount of bound RFP was plotted as a function of total RFP. The curve was fitted using GraphPad Prism and nonlinear regression. All input and bound fractions were quantified via a plate reader. doi:10.1371/journal.pone.0036967.g003

occludes the antibody epitope, as has been proposed for HP1 binding to H3K9me3. In this study, the histone H3 trimethyl-lysine epitope is embedded in an aromatic cage blocking thereby

most likely the binding of any antibodies [27]. To further analyze the bound fractions, we eluted GFP-Cbx1 and GFP, separated them on an SDS-PAGE gel and visualized GFP and H3 by

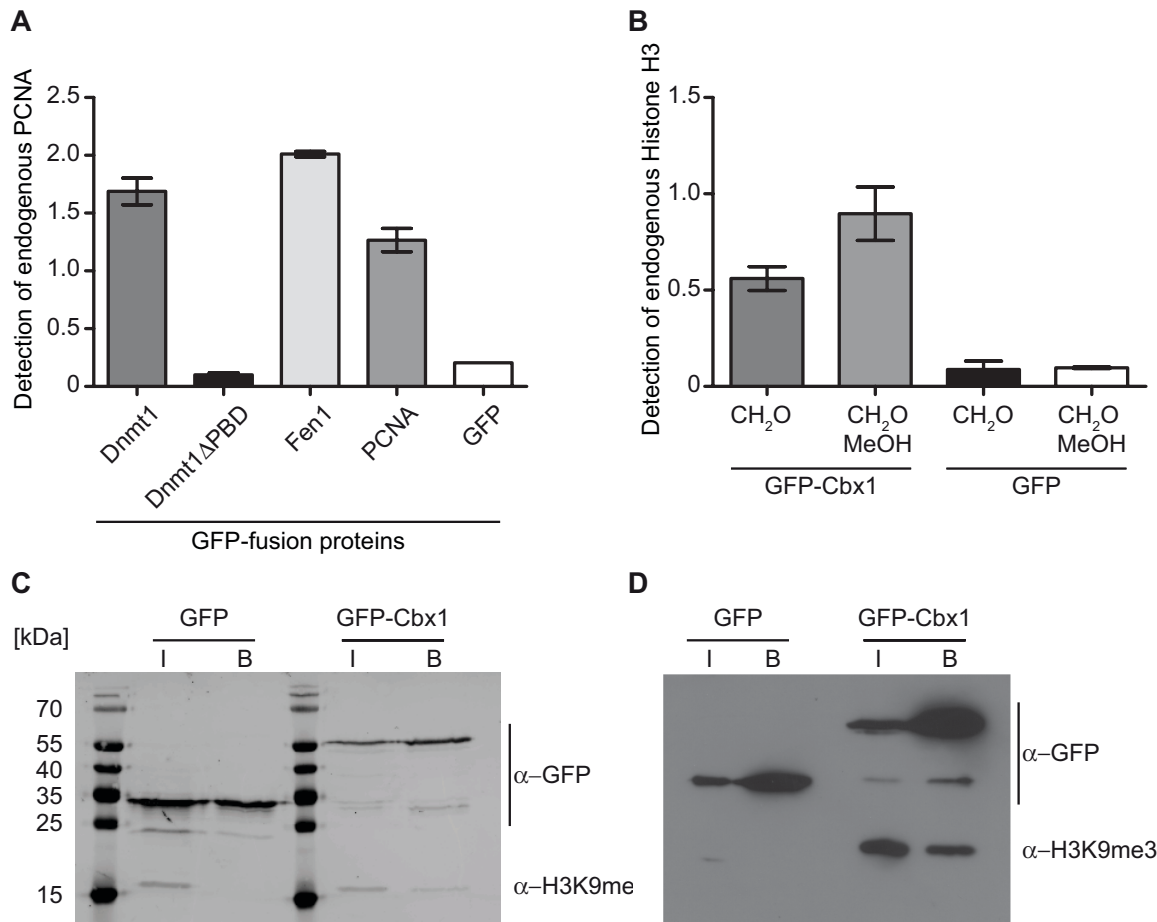


**Figure 4. Pulldown of endogenous interaction partners.** GFP-fusions were immunoprecipitated and endogenous interacting proteins were detected either by ELISA or immunoblot analysis. **(A)** ELISA signal (Absorbance at 450 nm) of bound endogenous PCNA detected by a PCNA antibody to purified GFP-fusion proteins. Shown are means  $\pm$  SD from three independent experiments. **(B)** ELISA signal (Absorbance at 450 nm) of bound endogenous Histone H3 detected by an H3 antibody to purified GFP-fusion proteins. Bound fractions were either cross-linked with 2% formaldehyde (CH<sub>2</sub>O) and/or additionally permeabilized with MeOH. Shown are means  $\pm$  SD from two independent experiments. **(C)** and **(D)** After immunoprecipitation input (I) and bound (B) fractions were separated by SDS-PAGE and visualized by immunoblot analysis. **(C)** The total protein concentration of the input fractions were adjusted. **(D)** The GFP concentrations of the input fractions were adjusted. doi:10.1371/journal.pone.0036967.g004

immunoblotting. Histone H3 was detectable in the input fractions of both GFP and GFP-Cbx1 but as expected, only in the bound fraction of GFP-Cbx1.

### Comparative Analysis of Posttranslational Histone Modifications

Histone posttranslational modifications play an important role in the structural organization of chromatin and often correlate to transcriptional activation or repression depending on their type and location. Recently, it has been shown that nucleosomal incorporation of histone variants can lead to alterations in modification patterning and that such changes may complement the properties brought by the variant itself [28].

In order to investigate the suitability of the GFP-multiTrap in comparing such histone posttranslational modifications, we isolated nucleosomes from HeLa cells expressing either GFP-H2A or GFP-H2A.Z and precipitated them with the 96 well micro plate. GFP levels were then recorded (data not shown) to ensure equal loading of substrate per well. In addition, as a negative control, the cytoplasmic supernatant fraction was also incubated with the GFP-multiTrap. An ELISA approach was then used to

quantify differences in histone H3K4me2 levels between the two different nucleosome compositions. Following cross-linking and permeabilization, bound nucleosomes were incubated with either anti-H3, directly conjugated to HRP or anti-H3K4me2 (both antibodies Abcam, UK). Histone H3K4me2 levels were then normalized to the histone H3 signal. In accordance with published data, H2A containing nucleosomes were depleted in H3K4me2 whereas those containing H2A.Z showed a large enrichment for this modification (Figure 5) [28].

### Discussion

One challenge of the proteomic era is the effective integration of proteomic, cell biological and biochemical data. Ideally, proteomic data on tissue and cell cycle-specific expression of specific proteins should be combined with subcellular localization and binding dynamics of fluorescent proteins. Additionally, it is crucial to determine cell biological and biochemical characteristics such as interacting factors, enzymatic activity and substrate binding specificities. The integration of all these different data has, in part, been impeded by the simple fact that different protein tags

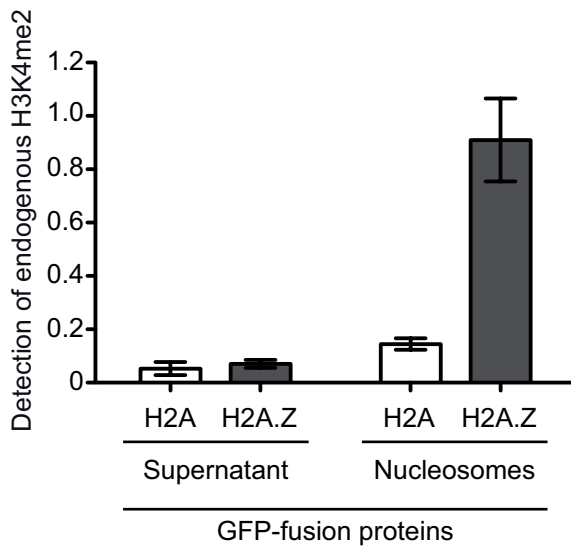


**Figure 5. Comparative analysis of posttranslational histone modifications.** Cytoplasmic supernatant (SN) or mononucleosome (MN) fractions prepared from HeLa cells expressing GFP-H2A or GFP-H2A.Z were precipitated and the levels of H3 and H3K4me2 were detected by ELISA (Absorbance at 450 nm). Shown are the H3K4me2 levels normalized to H3 and means  $\pm$  SD from two independent experiments.

doi:10.1371/journal.pone.0036967.g005

are used for different applications. Here, we present a new versatile, high-throughput method to determine *in vitro* binding specificities and to detect endogenous interacting factors of GFP-fusion proteins. We use 96-well micro plates with immobilized GFP-Trap (GFP-multiTrap) for fast and efficient purification of GFP-fusion proteins. We demonstrate the efficiency and purity of the GFP immunoprecipitation (Figure 1), a prerequisite to obtain reliable biochemical data on e.g. binding specificities. Moreover, we measured histone-tail binding, DNA and protein-protein binding ratios underlying the versatility of our approach (Figure 2 and 3 and Table 2). The suitability of the demonstrated assays for high-throughput biochemical and functional studies was assessed by calculating the Z-factors (Table 2). Therefore, our assay is suitable to examine an initial high-throughput screening for potential binding partners. Moreover, the assay can be used for compound screening. Additionally, our method allows for detection of endogenous interaction factors based on an ELISA assay (Figure 4 and 5).

In contrast to other high-throughput techniques like conventional microarrays, it does not require time-consuming recombinant protein expression and purification but allows for the direct biochemical analyses of GFP-fusion proteins expressed in mammalian cells. The versatile GFP-multiTrap combined with the widespread use of fluorescent fusion proteins now enables a fast and direct quantitative correlation of microscopic data concerning the subcellular localization and mobility of fluorescent fusion proteins with their enzymatic activity, interacting factors, and DNA binding properties combining cell biology and biochemistry with mutual benefits.

## Materials and Methods

### Expression Constructs, Cell Culture and Transfection

Mammalian expression constructs encoding GFP-Dnmt1, GFP-Dnmt1 $\Delta$ PBD, GFP-PBD, GFP-PCNA, RFP-PCNA, GFP-Ligase

III, mRFP, GFP, MBD-YFP, GFP-Fen1 and RFP-Xrcc1 were described previously [7,20,29–37]. Note that all constructs encode fusion proteins of GFP, RFP or yellow fluorescent protein (YFP). The Cbx1 expression construct was derived by PCR from mouse cDNA, cloned into pEGFP-C1 (Clontech, USA) and verified by DNA sequencing. Throughout this study enhanced GFP (eGFP) constructs were used and for simplicity referred to as GFP-fusions. HEK293T cells [30] and HeLa Kyoto [29] were cultured in DMEM supplemented with either 50  $\mu$ g/ml gentamicin (HEK293T) or 1% penicillin/streptomycin (HeLa Kyoto) and 10% fetal calf serum. For expression of GFP/RFP/YFP fusion proteins, HEK293T cells were transfected with the corresponding expression constructs using polyethylenimine (Sigma, USA). 2. HeLa Kyoto cells were transfected using FuGene HD (Roche, Germany) according to the manufacturer's instructions. The plasmid coding for GFP-H2A (H2A type 1, NP\_003501.1) was kindly provided by Emily Bernstein (Mount Sinai Hospital) and the plasmid coding for GFP-Z-1 was a gift from Sachihito Matsunaga (University of Tokyo). Stable cell lines were selected with 600  $\mu$ g/ml G418 (PAA, Austria) and individual cell clones sorted by using a FACSAria machine (Becton Dickinson, Germany).

### Histone-tail Peptides and DNA Substrate Preparation

Fluorescently labeled DNA substrates were prepared by mixing two HPLC-purified DNA oligonucleotides (IBA GmbH, Germany Table 1) in equimolar amounts, denaturation for 30 sec at 92°C and slow cool-down to 25°C allowing hybridization. Histone-tail peptides were purchased as TAMRA conjugates and/or biotinylated (PSL, Germany) and are listed in Table 1.

### Preparation of Protein Extracts

HEK293T cells were cultured and transfected as described [38]. For extract preparation 1 mg/ml DNaseI, 1 mM PMSF and Protease Inhibitor cocktail (Roche, Germany) were included in the lysis buffer (20 mM Tris-HCl pH 7.5, 150 mM NaCl, 2 mM MgCl<sub>2</sub>, 0.5% NP40) or nuclear extract buffer (10 mM HEPES pH 7.9, 10 mM KCl, 1.5 mM MgCl<sub>2</sub>, 0.34 M Sucrose, 10% Glycerol, 1 mM  $\beta$ -mercapto-ethanol). Cells were lysed for 30 minutes on ice followed by a centrifugation step (15/12000 rpm/4°C). Extracts from transfected 10 cm plates were diluted to 500  $\mu$ L with immunoprecipitation buffer (IP buffer; 20 mM Tris-HCl pH 7.5, 150 mM NaCl, 0.5 mM EDTA) or dilution buffer (20 mM HEPES pH 7.9, 150 mM KCl). An aliquot of 10  $\mu$ L (2%) were added to SDS-containing sample buffer (referred to as Input (I)).

### Purification and Elution of GFP/YFP/RFP- Fusions

For purification, 100  $\mu$ L or 50  $\mu$ L precleared cellular lysate for full-area plates or half-area plates, respectively, was added per well and incubated for 2 hours at 4°C on a GFP-multiTrap plate by continuous shaking. After removing the supernatant, wells were washed twice with 100  $\mu$ L of washing buffer (WB; 20 mM Tris-HCl pH 7.5, 100–300 mM NaCl, 0.5 mM EDTA) and 100  $\mu$ L of IP or dilution buffer was added for measurement. The amounts of bound protein were determined by fluorescence intensity measurements with a Tecan Infinite M1000 plate reader (Tecan, Austria). Wavelengths for excitation and emission of GFP are 490 $\pm$ 10 nm and 511 $\pm$ 10 nm, for RFP are 586 $\pm$ 5 nm and 608 $\pm$ 10 nm and for YFP 525 $\pm$ 5 nm and 538 $\pm$ 5 nm, respectively. The concentration of proteins was calculated using calibration curves that were determined by measuring the fluorescence signal of known concentrations of purified GFP, RFP and YFP. Notably, factors interfering with



fluorescence intensity measurements such as absorption of excitation light by cell lysates, auto fluorescence of the samples and/or scattering of the excitation/emission light by cell debris are negligible (Figure S1). Bound proteins were eluted with 300 mM Glycine pH 2.5 and subsequently buffered with 1 M Tris pH 7.5. Elution fractions were added to SDS-containing sample buffer (referred to as Bound (B)). Bound proteins were visualized by immunoblotting using the anti-GFP mouse monoclonal antibody (Roche, Germany).

### In vitro Histone-tail Peptide Binding Assay

The *in vitro* histone-tail binding assay was performed as described previously [10]. After one-step purification of GFP fusion proteins the wells were blocked with 100  $\mu$ L 3% milk solved in TBS-T (0.075% Tween) for 30 minutes at 4°C on a plate vortex, shaking gently. After blocking, the wells were equilibrated in 50  $\mu$ L IP buffer supplemented with 0.05% Tween. TAMRA-labeled histone-tail peptides were added either to a final concentration of 0.15  $\mu$ M or of the indicated concentrations and the binding reaction was performed at RT for 20 min on a plate vortex, shaking gently. After removal of unbound substrate the amounts of protein and histone-tail peptide were determined by fluorescence intensity measurements. The concentrations of bound TAMRA-labeled histone-tail peptides were calculated using calibration curves that were determined by measuring a serial dilution of TAMRA-labeled peptides with known concentrations.

Binding ratios were calculated dividing the concentration of bound histone-tail peptide by the concentration of GFP fusion. Wavelengths for excitation and emission of TAMRA were 560  $\pm$  5 nm and 586  $\pm$  5 nm, respectively.

### In vitro DNA Binding Assay

*In vitro* DNA binding assay was performed as described previously [9,10] with the following modifications. GFP/YFP fusions were purified from HEK293T extracts using the 96-well GFP-binder plates and incubated with two differentially labeled DNA substrates at a final concentration of either 100 nM or of the indicated concentration for 60 min at RT in IP buffer supplemented with 2 mM DTT and 100 ng/ $\mu$ L BSA. After removal of unbound substrate the amounts of protein and DNA were determined by fluorescence intensity measurements. The concentration of bound ATTO-labeled DNA substrates was calculated using calibration curves that were determined by measuring a serial dilution of DNA-coupled fluorophores with known concentrations. Binding ratios were calculated dividing the concentration of bound DNA substrate by the concentration of GFP/YFP fusion, corrected by values from a control experiment using DNA substrates of the same sequence but with different fluorescent label, and normalized by the total amount of bound DNA. Wavelengths for excitation and emission of ATTO550 were 545  $\pm$  5 nm and 575  $\pm$  5 nm and for ATTO700 700  $\pm$  10 nm and 720  $\pm$  10, respectively.

### Protein-Protein Interaction

GFP fusions were purified from HEK293T extracts using the 96-well GFP multiTrap plates, blocked with 3% milk and incubated with cellular extracts comprising the RFP fusions with the indicated concentrations for 30 min at RT. After removal of unbound RFP fusion (washing buffer) the amounts of proteins were determined by fluorescence intensity measurements. Binding ratios were calculated dividing the concentration of bound RFP fusion by the concentration of GFP fusion. Wavelengths for excitation and emission of RFP were 586  $\pm$  5 nm and 608  $\pm$  10 nm,

respectively. Bound proteins were eluted and separated by SDS-PAGE and visualized by immunoblotting using the anti-GFP rat monoclonal antibody; 3H9, and the anti-red rat monoclonal antibody, 5F8 (both ChromoTek, Germany).

### Enzyme-linked Immunosorbent Assay (ELISA)

GFP fusions were purified (from HEK293T extracts) using the 96-well GFP-multiTrap plates and were washed twice with dilution buffer (for nucleosome experiments salt concentration was adjusted to 300 mM). After washing bound fractions were either cross-linked with 2% formaldehyde and/or additionally permeabilized with 100% MeOH. After blocking with 3% milk solved in TBS-T (0.075% Tween) the wells were incubated with primary antibody (monoclonal rat anti-H3-HRP (Abcam, UK), polyclonal rabbit anti-H3K4me2 (Abcam, UK) or monoclonal rat anti-PCNA, 16D10 (ChromoTek, Germany) overnight at 4°C on a plate vortex, shaking gently. The wells were washed three times with 200  $\mu$ L TBS-T and horseradish peroxidase-conjugated secondary antibody (Sigma, USA) was incubated for 1 h at RT for the detection of PCNA or H3K4me2. The wells were washed again as described above. For PCNA experiments detection was carried out by incubating each well with 100  $\mu$ L TMB (3,3',5,5'-tetramethylbenzidine) for 10 minutes at RT. The reactions were stopped with the addition of 100  $\mu$ L 1 M H<sub>2</sub>SO<sub>4</sub>. For nucleosome experiments, detection was carried out using OPD (Sigma, USA) according to the manufacturers instructions. Bound histone H3, PCNA or H3K4me2 levels were quantified by determination of the absorbance at 450 nm using a Tecan Infinite M1000 plate reader (Tecan, Austria).

### Preparation of Mononucleosomes

$2 \times 10^7 - 10 \times 10^7$  HeLa cells, expressing either GFP-H2A or GFP-H2A.Z, were incubated in PBS, 0.3% Triton X-100 and Protease Inhibitor Cocktail (Roche, Germany) for 10 min at 4°C. Nuclei were pelleted and supernatant (SN) transferred and retained. The pellet was washed once in PBS, resuspended in EX100 buffer (10 mM Hepes pH 7.6, 100 mM NaCl, 1.5 mM MgCl<sub>2</sub>, 0.5 mM EGTA, 10% (v/v) glycerol, 10 mM  $\beta$ -glycerol phosphate 1 mM DTT, Protease Inhibitor Cocktail (Roche, Germany)) and CaCl<sub>2</sub> concentration adjusted to 2 mM. Resuspended nuclei were digested with 1.5 U MNase (Sigma, USA) for 20 min at 26°C. The reaction was stopped by addition of EGTA to a final concentration of 10 mM followed by centrifugation for 10 min at 1000 rcf, 4°C. Mononucleosome containing supernatant (MN) was retained.

### Calculation of the Z-factors

To assess the suitability of the assay for high-throughput biochemical and functional studies, the Z-factor was calculated using the equation  $Z = 1 - \frac{3 \times (\sigma_p + \sigma_n)}{|\mu_p - \mu_n|}$  [39]. In this equation,  $\sigma$  is the standard deviation of the positive (p) and the negative (n) control;  $\mu$  is the mean value for the molar binding ratio (for positive ( $\mu_p$ ) and negative ( $\mu_n$ ) controls). The values of three independent experiments were used to calculate the Z-factor and all values are listed in Table 2.

### Supporting Information

**Figure S1 Factors interfering the measured fluorescence intensities.** (A) The concentrations of GFP and RFP expressed in HEK293T cells were measured in serial dilutions of crude cell extracts. Shown are means  $\pm$  SD from two independent experiments. Fluorescence intensities were measured via a plate reader and the GFP and RFP concentrations were determined as described in the Material and Methods part. (B) Background GFP

and RFP signals in cell lysates of untransfected HEK293T cells. The fluorescence intensities (FI) were measured via a plate reader and the concentrations were determined as described in the Material and Methods part. (DOC)

## Acknowledgments

We thank Heinrich Leonhardt and Ulrich Rothbauer for comments on the manuscripts and discussion. We also thank ChromoTek for the supply of GFP-multiTrap.

## References

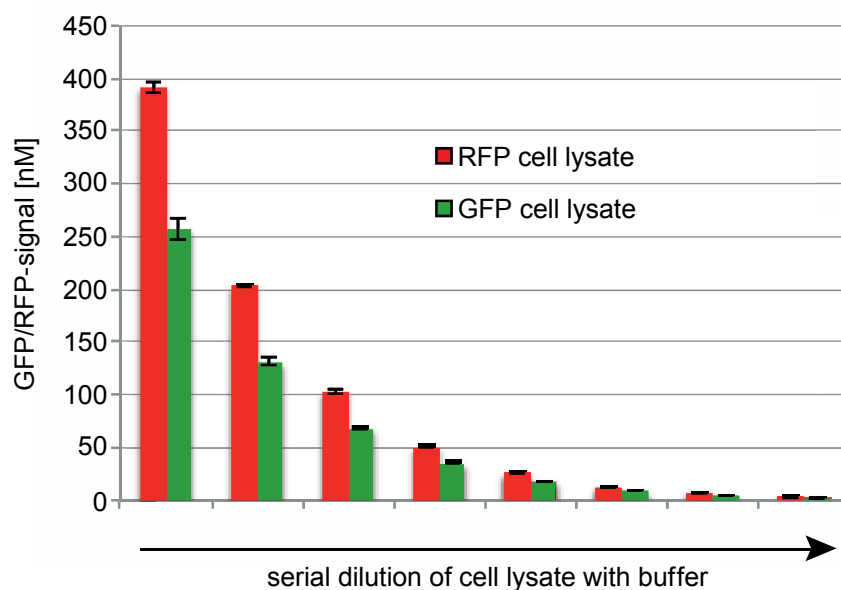
- Walther TC, Mann M (2010) Mass spectrometry-based proteomics in cell biology. *J Cell Biol* 190: 491–500. doi:10.1083/jcb.201004052.
- Chalfie M, Tu Y, Euskirchen G, Ward WW, Prasher DC (1994) Green fluorescent protein as a marker for gene expression. *Science* 263: 802–805.
- Cristea IM, Williams R, Chait BT, Rout MP (2005) Fluorescent proteins as proteomic probes. *Mol Cell Proteomics* 4: 1933–1941. doi:10.1074/mcp.M500227-MCP200.
- Rottach A, Kremmer E, Nowak D, Leonhardt H, Cardoso MC (2008) Generation and characterization of a rat monoclonal antibody specific for multiple red fluorescent proteins. *Hybridoma* 27: 337–343. doi:10.1089/hyb.2008.0031.
- Aslan K, Lakowicz JR, Geddes CD (2005) Plasmon light scattering in biology and medicine: new sensing approaches, visions and perspectives. *Curr Opin Chem Biol* 9: 538–544. doi:10.1016/j.cbpa.2005.08.021.
- Kaushansky A, Allen JE, Gordus A, Stiffler MA, Karp ES, et al. (2010) Quantifying protein-protein interactions in high throughput using protein domain microarrays. *Nat Protoc* 5: 773–790. doi:10.1038/nprot.2010.36.
- Rothbauer U, Zolghadr K, Muyldermans S, Schepers A, Cardoso MC, et al. (2008) A versatile nanotrapp for biochemical and functional studies with fluorescent fusion proteins. *Mol Cell Proteomics* 7: 282–289. doi:10.1074/mcp.M700342-MCP200.
- Trinkle-Mulcahy L, Boulton S, Lam YW, Urcia R, Boisvert FM, et al. (2008) Identifying specific protein interaction partners using quantitative mass spectrometry and bead proteomes. *J Cell Biol* 183: 223–239. doi:10.1083/jcb.200805092.
- Frauer C, Leonhardt H (2009) A versatile non-radioactive assay for DNA methyltransferase activity and DNA binding. *Nucleic Acids Research* 37: e22–e22. doi:10.1093/nar/gkn1029.
- Pichler G, Wolf P, Schmidt CS, Meilinger D, Schneider K, et al. (2011) Cooperative DNA and histone binding by Uhrf2 links the two major repressive epigenetic pathways. *J Cell Biochem* doi:10.1002/jcb.23185.
- Kaustov L, Quyang H, Amaya M, Lemak A, Nady N, et al. (2010) Recognition and specificity determinants of the human Cbx chromodomains. *J Biol Chem* doi:10.1074/jbc.M110.191411.
- Jacobs SA, Taverna SD, Zhang Y, Briggs SD, Li J, et al. (2001) Specificity of the HPI1 chromo domain for the methylated N-terminus of histone H3. *EMBO J* 20: 5232–5241. doi:10.1093/emboj/20.18.5232.
- Fischle W, Tseng BS, Dormann HL, Ueberheide BM, Garcia BA, et al. (2005) Regulation of HPI1-chromatin binding by histone H3 methylation and phosphorylation. *Nature* 438: 1116–1122. doi:10.1038/nature04219.
- Valinluck V, Tsai H-H, Rogstad DK, Burdzy A, Bird A, et al. (2004) Oxidative damage to methyl-CpG sequences inhibits the binding of the methyl-CpG binding domain (MBD) of methyl-CpG binding protein 2 (MeCP2). *Nucleic Acids Research* 32: 4100–4108. doi:10.1093/nar/gkh739.
- Nan X, Mehan RR, Bird A (1993) Dissection of the methyl-CpG binding domain from the chromosomal protein MeCP2. *Nucleic Acids Research* 21: 4886–4892.
- Free A, Wakefield RI, Smith BO, Dryden DT, Barlow PN, et al. (2001) DNA recognition by the methyl-CpG binding domain of MeCP2. *J Biol Chem* 276: 3353–3360. doi:10.1074/jbc.M007224200.
- Leonhardt H, Page AW, Weier HU, Bestor TH (1992) A targeting sequence directs DNA methyltransferase to sites of DNA replication in mammalian nuclei. *Cell* 71: 865–873.
- Chuang LS, Ian HI, Koh TW, Ng HH, Xu G, et al. (1997) Human DNA-(cytosine-5) methyltransferase-PCNA complex as a target for p21WAF1. *Science* 277: 1996–2000.
- Mortusewicz O, Leonhardt H (2007) XRCC1 and PCNA are loading platforms with distinct kinetic properties and different capacities to respond to multiple DNA lesions. *BMC Mol Biol* 8: 81. doi:10.1186/1471-2199-8-81.
- Mortusewicz O, Rothbauer U, Cardoso MC, Leonhardt H (2006) Differential recruitment of DNA Ligase I and III to DNA repair sites. *Nucleic Acids Research* 34: 3523–3532. doi:10.1093/nar/gkl492.
- Hiragami-Hamada K, Shimmyozu K, Hamada D, Tatsu Y, Uegaki K, et al. (2011) N-terminal phosphorylation of HPI1 promotes its chromatin binding. *Mol Cell Biol* 31: 1186–1200. doi:10.1128/MCB.01012–10.
- Bestor TH (2000) The DNA methyltransferases of mammals. *Human Molecular Genetics* 9: 2395–2402. doi:10.1093/hmg/9.16.2395.
- Caldecott KW (2003) XRCC1 and DNA strand break repair. *DNA repair* 2: 955–969.
- Tom S, Henriksen LA, Bambara RA (2000) Mechanism whereby proliferating cell nuclear antigen stimulates flap endonuclease 1. *J Biol Chem* 275: 10498–10505.
- Chen U, Chen S, Saha P, Dutta A (1996) p21Cip1/Waf1 disrupts the recruitment of human Fen1 by proliferating-cell nuclear antigen into the DNA replication complex. *Proc Natl Acad Sci USA* 93: 11597–11602.
- Jónsson ZO, Hindsger R, Hübscher U (1998) Regulation of DNA replication and repair proteins through interaction with the front side of proliferating cell nuclear antigen. *EMBO J* 17: 2412–2425. doi:10.1093/emboj/17.8.2412.
- Jacobs SA, Khorasanizadeh S (2002) Structure of HPI1 chromodomain bound to a lysine 9-methylated histone H3 tail. *Science* 295: 2080–2083. doi:10.1126/science.1069473.
- Viens A, Mechold U, Brouillard F, Gilbert C, Leclerc P, et al. (2006) Analysis of human histone H2AZ deposition in vivo argues against its direct role in epigenetic templating mechanisms. *Molecular and Cellular Biology* 26: 5325–5335. doi:10.1128/MCB.00584–06.
- Neumann B, Held M, Liebel U, Erfle H, Rogers P, et al. (2006) High-throughput RNAi screening by time-lapse imaging of live human cells. *Nat Methods* 3: 385–390. doi:10.1038/nmeth876.
- DuBridge RB, Tang P, Hsia HC, Leong PM, Miller JH, et al. (1987) Analysis of mutation in human cells by using an Epstein-Barr virus shuttle system. *Molecular and Cellular Biology* 7: 379–387.
- Brero A (2005) Methyl CpG-binding proteins induce large-scale chromatin reorganization during terminal differentiation. *J Cell Biol* 169: 733–743. doi:10.1083/jcb.200502062.
- Sporbert A, Domaing P, Leonhardt H, Cardoso MC (2005) PCNA acts as a stationary loading platform for transiently interacting Okazaki fragment maturation proteins. *Nucleic Acids Research* 33: 3521–3528. doi:10.1093/nar/gki665.
- Leonhardt H, Rahn HP, Weinzierl P, Sporbert A, Cremer T, et al. (2000) Dynamics of DNA replication factories in living cells. *J Cell Biol* 149: 271–280.
- Schermelleh L, Spada F, Easwaran HP, Zolghadr K, Margot JB, et al. (2005) Trapped in action: direct visualization of DNA methyltransferase activity in living cells. *Nat Methods* 2: 751–756. doi:10.1038/nmeth794.
- Easwaran HP, Schermelleh L, Leonhardt H, Cardoso MC (2004) Replication-independent chromatin loading of Dnmt1 during G2 and M phases. *EMBO Rep* 5: 1181–1186. doi:10.1038/sj.embor.7400295.
- Mortusewicz O, Schermelleh L, Walter J, Cardoso MC, Leonhardt H (2005) Recruitment of DNA methyltransferase I to DNA repair sites. *Proc Natl Acad Sci USA* 102: 8905–8909. doi:10.1073/pnas.0501034102.
- Campbell RE, Tour O, Palmer AE, Steinbach PA, Baird GS, et al. (2002) A monomeric red fluorescent protein. *Proc Natl Acad Sci USA* 99: 7877–7882. doi:10.1073/pnas.082243699.
- Schermelleh L, Haemmer A, Spada F, Rosing N, Meilinger D, et al. (2007) Dynamics of Dnmt1 interaction with the replication machinery and its role in postreplicative maintenance of DNA methylation. *Nucleic Acids Research* 35: 4301–4312. doi:10.1093/nar/gkm432.
- Zhang J, Chung T, Oldenburg K (1999) A Simple Statistical Parameter for Use in Evaluation and Validation of High Throughput Screening Assays. *J Biomol Screen* 4: 67–73.

## Author Contributions

Conceived and designed the experiments: GP SBH. Performed the experiments: GP AJ PW. Analyzed the data: GP AJ PW. Contributed reagents/materials/analysis tools: SBH. Wrote the paper: GP SBH.

## Supporting material

A



B

	GFP channel		RFP channel	
	cell lysate untransfected	blank	cell lysate untransfected	blank
FI	<b>33</b>	<b>14.5</b>	<b>206</b>	<b>228</b>
FI - blank	<b>18.5</b>	<b>0</b>	<b>0</b>	<b>0</b>
[nM]	<b>0.78</b>	<b>0</b>	<b>0</b>	<b>0</b>

### Figure S1: Factors interfering the measured fluorescence intensities. (A)

The concentrations of GFP and RFP expressed in HEK293T cells were measured in serial dilutions of crude cell extracts. Shown are means  $\pm$  SD from two independent experiments. Fluorescence intensities were measured via a plate reader and the GFP and RFP concentrations were determined as described in the Material and Methods part. (B) Background GFP and RFP signals in cell lysates of untransfected HEK293T cells. The fluorescence intensities (FI) were measured via a plate reader and the concentrations were determined as described in the Material and Methods part.

## APPENDIX

### Contributions

Declaration of contributions to **“H3K56me3 is a novel, conserved heterochromatic mark that largely but not completely overlaps with H3K9me3 in both regulation and localization”**

This project was conceived by Sandra B. Hake. I performed all antibody specificity tests for  $\alpha$ H3K56me1 (which was the original focus of the project), tests for  $\alpha$ H3K56me3 (Figure 1a, 1d) and tests for two  $\alpha$ H3K9me3 antibodies (Figure S1). In addition, I performed the screen of known histone demethylases (provided by Gunnar Schotta), initially analyzing H3K56me1 and H3K56me2. From this screen we established JMJD2D and JMJD2E as potential candidates for H3K56me regulation (parts of Figure 4a and Figure S2). Finally, I analyzed H3K56me3 conservation (Figure 2a) and also extracted histones and performed WBs for Figure C. I supervised Silva Bussemer, who carried out her Master’s work in our lab, and am therefore indirectly involved in the generation of the figures she produced for the manuscript Figure 1b, 1c: Silva Bussemer. Figure 2b: Sebastian Pünzeler; 2c: Irina Solovei 2d: Silva Bussemer. Figure 3a,3b: Matthias Hahn. Figure 4: Silva Bussemer. Figure 5 and 6: Martha Snyder and Michael Wells. I made all the figures. Sandra B. Hake wrote the manuscript.

Declaration of contributions to **“Versatile toolbox for high throughput biochemical and functional studies with fluorescent fusion proteins.”**

This manuscript was a collaboration with Dr. Garwin Pichler, from the lab of Heinrich Leonhardt, who conceived the idea and contributed Figures 1-4. I used an ELISA-based approach to test the utility of a new tool “GFP-multiTRAP” for analyzing PTMs on GFP-tagged histone variants (Figure 5).

Declaration of contributions to **“Getting down to the CORE of HISTONE MODIFICATIONS”**. Section 1.4 “Modification of histone H3 core residues and their implications on nucleosome structure” in my thesis introduction and section 2.2 “Genome-wide localization of H3 core modifications and their functional implications” in my discussion. These parts were taken from the review and slightly modified. I conceived the structure of the review and wrote it.



## Curriculum Vitae

### Personal Information

Name Antonia Prema Margaret Jack

Date of birth 16<sup>th</sup> November 1983

Place of birth Glasgow (Scotland)

Nationality British

### Higher Education

05/09-current **Graduate student**

International Max Planck Research School for Life Sciences / Ludwig-Maximilians-Universität, Munich, Germany

Priv.-Doz. Dr. Sandra B. Hake (Adolf-Butenandt-Institute, chair Prof. Dr. Peter B. Becker)

Project: Characterization of H3K56me, a novel, core histone modification (published)

10/03-07/07 **Undergraduate + Master Molecular and Cellular Biology**

University of Bath, Bath, England

Dr. Vasanta Subramanian

Project: Development of a system to make neuromuscular junctions *in vitro* through the co-culture of cell lines.

University of Utah, Utah, USA (one year scholarship)

Prof. Alejandro Sánchez-Alvarado

Project: Characterization of spliced-leader trans-splicing in Planarians (published)

09/00-06/02 **A-Levels**

Pate's Grammar School, Cheltenham, England

**Publications**

**Jack, A.P.**, Hake, S.B. (2014) Getting down to the CORE of HISTONE MODIFICATIONS. *Chromosoma*. Accepted.

**Jack, A.P.**, Bussemer, S., Hahn, M., Punzeler, S., Snyder, M., Wells, M., Csankovszki, G., Solovei, I., Schotta, G. and Hake, S.B. (2013) H3K56me3 is a novel, conserved heterochromatic mark that largely but not completely overlaps with H3K9me3 in both regulation and localization. *PloS one*, **8**, e51765.

Pichler, G., **Jack, A.**, Wolf, P. and Hake, S.B. (2012) Versatile toolbox for high throughput biochemical and functional studies with fluorescent fusion proteins. *PloS one*, **7**, e36967.

Rossi, A., Ross, E.J., **Jack, A.** and Sanchez Alvarado, A. (2014) Molecular cloning and characterization of SL3: a stem cell-specific SL RNA from the planarian *Schmidtea mediterranea*. *Gene*, **533**, 156-167.

## **Acknowledgements**

I would like to give tremendous thanks to Priv.-Doz. Dr. Sandra Hake for giving me the opportunity to work in her lab- I couldn't have asked for a better boss! Her enthusiasm and constant encouragement provided the foundation for a great working atmosphere. In this regard, I would also like to thank my colleagues, both past and present, for being ever humourful and turning bad days into good ones. Moreover, many have become good friends and I am looking forward to seeing where we all end up.

As chair of the Adolf-Butenandt-Institute and member of my thesis advisory committee, Prof. Peter Becker was a great role model and I appreciate his honest comments and passion for science. Likewise, I am thankful to the other members of my thesis advisory committee, Gunnar Schotta and Zuzana Storchova, for always taking the time to come and discuss my projects.

Collaborations are a big part of our lab and are something I am grateful to Sandra for encouraging us to participate in. Not only have I benefitted scientifically from such partnerships, but it has also been fun to work with so many like-minded people and I thank those involved.

Although I haven't seen him since 2006, I would like to give a special mention to Dr. Alessandro Rossi, who supervised me during a one year scholarship in Salt Lake City. The patience he had in teaching me played a key role in my decision to do a PhD and set the foundation for my scientific career. In addition, crazy Sofia Robb whose love of epigenetics inspired me to do my graduate studies on this wonderful topic.

Finally, I would like to thank Clemens Bönisch, who although didn't talk to me much in the beginning is now probably stuck with me for life!